

# An evaluation of the regional distribution and wet deposition of secondary inorganic aerosols and their gaseous precursors in IFS-COMPO preparatory to cycle 49R1.

Jason E. Williams<sup>1</sup>, Swen Metzger<sup>2</sup>, Samuel Rémy<sup>3</sup>, Vincent Huijnen<sup>1</sup> and Johannes Flemming<sup>4</sup>

<sup>1</sup> R&D Weather and Climate Modeling, Royal Netherlands Meteorological Institute, De Bilt, the Netherlands

<sup>2</sup> ResearchConcepts Io, Freiburg, Germany

<sup>3</sup> HYGEOS, Lille, France

<sup>4</sup> European Centre for Medium-Range Weather Forecasts, Bonn, Germany

## Abstract

Secondary Inorganic Aerosol (SIA) makes up a considerable fraction of the total particulate matter exposure and, thus, is an important product from any forecasting system of atmospheric composition and air quality. The subsequent loss to the surface of SIA via dry and wet deposition determines the duration of the exposure time for humans and the extent of acidification imposed on sensitive ecosystems. Here we provide a description and evaluation of the most recent updates made towards aerosol production, aerosol scavenging and wet deposition components of the global [Integrated Forecast System-COMPO](#) chemical forecasting system, which is used as part of the Copernicus Atmosphere Monitoring Service. The [implementation](#) of the EQSAM4Clim simplified thermodynamic module in IFS-COMPO, [for use in](#) cycle 49R1 changes the efficacy of phase transfer of SIA precursor gases (Sulphur dioxide, Nitric Acid and Ammonia) which significantly impacts the [respective](#) SIA particulate concentrations by changing the fraction converted into SIA. Comparisons made against observational composites at the surface for Europe, the U.S. and [Southeast](#) Asia during 2018 show reductions in the global [yearly](#) mean bias statistics for both sulphates and nitrates. Updating the IFS-COMPO model towards cycle 49r1 increases both the burden and lifetime of sulphate and ammonium particles by one third. Coupling EQSAM4Clim into IFS-COMPO provides a better description of the partitioning between state phases involving ammonia and ammonium across regions, whereas changes for sulphate are minimal. For nitric acid and nitrates, the partitioning changes significantly, leading to lower particulate concentrations and a corresponding increase in gas-phase nitric acid with an associated improvement in surface nitrate. There is also a shift in the size of particles towards the fine mode nitrate away from the coarse mode. The impact on the total regional wet deposition values is generally positive, except for sulphates in the U.S. and ammonium particles in [Southeast](#) Asia which are strongly influenced by the precursor emission estimates. This provides confidence that [this update to](#) IFS-COMPO has the ability to provide accurate deposition fluxes of S and N at global scale.

Formatted: Header

**Style Definition:** Heading 1: Font: (Default) Calibri, Font colour: Custom Colour (RGB(47,84,150)), (Asian) Japanese

**Style Definition:** Heading 2: Font: (Default) Calibri, Font colour: Custom Colour (RGB(47,84,150)), (Asian) Japanese

**Style Definition:** Heading 3: (Asian) Japanese, Space Before: 0 pt, After: 8 pt

**Style Definition:** Heading 4: Font colour: Black, (Asian) Japanese, Border: Top: (No border), Bottom: (No border), Left: (No border), Right: (No border), Between : (No border)

**Style Definition:** Heading 5: Font colour: Black, (Asian) Japanese, Border: Top: (No border), Bottom: (No border), Left: (No border), Right: (No border), Between : (No border)

**Style Definition** ... [3]

**Style Definition** ... [2]

**Style Definition:** x\_msonormal

**Style Definition:** List Paragraph: (Asian) Japanese

**Style Definition:** Balloon Text: (Asian) Japanese

**Style Definition:** Comment Reference

**Style Definition:** Comment Text: (Asian) Japanese

**Style Definition** ... [1]

**Formatted** ... [4]

**Formatted:** Normal5, Left

**Deleted:** Cycle

**Formatted** ... [5]

**Formatted:** Font: 16 pt, Pattern: Clear

**Formatted:** Normal5

**Deleted:** IFS-COMPO

**Deleted:** application

**Deleted:** concentrations of the

**Deleted:**

**Deleted:** .

**Deleted:** South-East

**Deleted:** annual

**Deleted:** South-East

**Deleted:** cycle 49r1

**Deleted:**

**Deleted:** 39

**Formatted:** Normal5, Right: 0,63 cm

**Formatted:** Page Number

## 1 Introduction

Secondary Inorganic Aerosol (SIA) is found throughout the troposphere, where resident concentrations are dependent on Temperature (T), Relative Humidity (RH) and the concentrations of inorganic precursor gases, namely water vapour ( $\text{H}_2\text{O}$ ), sulphur dioxide ( $\text{SO}_2$ ), ammonia ( $\text{NH}_3$ ) and nitric acid ( $\text{HNO}_3$ ). High concentrations of SIA contribute to total Particulate Matter that are smaller than using various predefined particle sizes namely:  $1.0\mu\text{m}$  ( $\text{PM}_{1.0}$ ),  $2.5\mu\text{m}$  ( $\text{PM}_{2.5}$ ) and  $10\mu\text{m}$  ( $\text{PM}_{10}$ ) (Liu et al., 2022), and have detrimental effects on both human health and visibility (Sharma et al., 2020; Ting et al., 2021). The main types of SIA are ammonium sulphate ( $(\text{NH}_4)_2\text{SO}_4$ ), ammonium bisulphate ( $\text{NH}_4\text{HSO}_4$ ) and ammonium nitrate ( $\text{NH}_4\text{NO}_3$ ). Once formed, the sulphates are very stable and deposit to the surface, whereas  $\text{NH}_4\text{NO}_3$  is more unstable and can decompose back to the precursor gases (Feick and Hainer, 1954) depending on T and RH. These particles can be transported out of source regions subsequently influencing air quality in neighbouring countries (e.g., Vieno et al., 2014; Chang et al., 2022). Anthropogenic activity makes a significant contribution to SIA formation via the emission of  $\text{NO}_x$  (oxidised nitrogen in the form of  $\text{NO}$  and  $\text{NO}_2$ ),  $\text{NH}_x$  (reduced nitrogen) and  $\text{SO}_2$ , where there has been a general trend of decreasing sulphur (S) and nitrogen (N) emissions in the EU, U.S. and China (Tørseth et al., 2012; Aas et al., 2019; Benish et al., 2022; Jiang et al., 2022) resulting in an increasing fraction of SIA consists of  $\text{NH}_4\text{NO}_3$ . This results in a decrease in the lifetime of SIA, due to the increased instability of  $\text{NH}_4\text{NO}_3$  due to variations in RH and temperature (e.g. Williams et al., 2015; Metzger et al., 2002; 2006), reducing the potential for reduced long-range transport out of the source regions (He et al., 2018).

At RH values above 50%, SIA take up water and exist in a deliquescent state. At high RH values of 80-100%, SIA formation is enhanced (Gao et al., 2020) therefore, under constant or changing emissions, SIA is likely to become more ubiquitous in a warming atmosphere. The hygroscopic growth of SIA alters both the optical properties (in terms of scattering and absorption) and interactions with gas-phase trace species via changes in pH (e.g. Jayne et al., 1990; Shi et al., 2018). The concentrated salt solution produced typically has higher ionic strength than cloud droplets with pH values ranging between -1 to 6 (Ault, 2020). The high solubility of SIA results in the scavenging into aquated aerosols and clouds being a dominant loss term. This has impacts in terms of the acidification of sensitive ecosystems and an increase in eutrophication due to high nitrogen loading in inland water bodies, which can result in the exceedance of critical loads for vegetation (e.g. Sun et al., 2020). The uptake of carbon to land is also enhanced with an increase in N loading (Holland et al., 1997; Reary et al., 2008). Once dissolved in solution, SIA dissociates efficiently into the respective ionic constituents (e.g. nitrate ( $\text{NO}_3^-$ ), ammonium ( $\text{NH}_4^+$ ) and sulphate ( $\text{SO}_4^{2-}$ )) whereas these anions/cations are deposited on land during precipitation events.

A distinct difference exists with respect to the main source terms for the various SIA species. For  $\text{NO}_x$  and  $\text{NH}_x$  species, particle formation is sensitive to the resident gas-phase precursor species, temperature, and RH, in the absence of aqueous phase droplets. For  $\text{SO}_4^{2-}$ , production occurs almost exclusively in the aqueous phase after  $\text{SO}_2$  is scavenged into cloud and fog, whose overall oxidation rate is dependent on the prescribed pH in solution. Recent studies have shown that the correct prescription of cloud pH is necessary to account for changes in  $\text{SO}_4^{2-}$  efficacy over long time scales for the determination of long-term trends with respect to resident concentrations (Thurock et al., 2019; Myriokefalitakis et al., 2022). The representation of acidity in tropospheric aerosols and clouds ranges significantly across large-scale atmospheric models. The most simplistic representation is to use a fixed cloud water pH of between 5.0-5.6, thus effectively representing the impact of dissolved carbon dioxide ( $\text{CO}_2$ ). A more accurate representation includes the influence of other dissolved species which either acidify (e.g.  $\text{HNO}_3$ ,  $\text{H}_2\text{SO}_4$ ) or buffer (e.g.  $\text{NH}_3$ ) the pH of the solution, once scavenged via irreversible uptake. This is the approach adopted in the Integrated Forecasting System with atmospheric composition extension (IFS-COMPO) for both cloud and precipitation. Other  $\text{SO}_4^{2-}$  production terms involving e.g. methyl-hydroperoxide ( $\text{CH}_3\text{OOH}$ ) have been shown to be of secondary importance towards the total  $\text{SO}_4^{2-}$  production (Myriokefalitakis et al., 2022). The more buffering of solution due to the scavenging and dissolution of  $\text{NH}_3$ , the faster the conversion rate as dictated by the rate of reaction of  $\text{HSO}_3^-$  being less than that for  $\text{SO}_3^-$  (Wareck, 1991).

One dominant loss term for SIA is wet deposition in precipitation to the surface. Previous global tropospheric modelling studies have been performed focusing on the temporal accuracy and yearly deposition totals at continental scale for  $\text{NH}_x$  and  $\text{SO}_x$  (Zhang et al., 2012; Kanikadou et al., 2016; Ge et al., 2021), as well as multi-model intercomparison studies to examine the variability across different models and the main assumptions causing such differences (Dentener et al., 2006; Bain et al., 2017; Tan et al., 2018). The accuracy of any model towards capturing the correct wet deposition terms is a balance between the accuracy of the precursor emission inventory, the distribution of the cloud liquid water content (defining the cloud Surface Area Density, SAD), the representation of the formation and distribution of aerosol particles, the extent of phase-transfer and the parametrizations adopted for describing dry/wet deposition to the surface.

Formatted: Header

Deleted: The

Deleted: occurs

Deleted: dependant

Deleted: Sulphur Dioxide

Deleted: Ammonia

Deleted: Nitric Acid

Deleted: concentrations

Deleted: accumulate in

Deleted: size bins of

Deleted:

Deleted: neighboring

Deleted: Sulphur

Deleted: Nitrogen

Deleted: US

Deleted: being from

Deleted: meteorological

Deleted: most

Deleted: cumulative

Deleted: trends

Deleted: pH

Deleted: by

Deleted: annual

Deleted: 39

Formatted: Normal5, Right: 0,63 cm

Formatted: Page Number

Formatted: Header

**Deleted:** Peuch et al., 2022; Williams et al., 2022; ... Rémy et al., 2024) used in the Copernicus Atmosphere Monitoring Service (CAMS; Peuch et al. 2022). This service provides forecasts and reanalysis of trace gases and aerosols for the purpose of informing national service providers and policy makers. It currently provides ...hemical/aerosol forecast products, among them Ozone (O<sub>3</sub>), Nitrogen Dioxide (NO<sub>2</sub>), SO<sub>2</sub>, PM2.5, PM10 and also ...erosol Optical Depth. One main...focus of the recent updates made to IFS-COMPO (... [6])

**Deleted:** Cy48r1...Y48R1 and Cy49r1 ...he version used for developing CY49R1 (hereafter referred to as pre-CY49R1) towards the surface distributions N and S gaseous precursors for SIA and the associated particle concentrations and distributions as evaluated against ground based observation networks, with special focus on the application of latest update of EQSAM4Clim (Metzger et al., 2024) in the global chemical forecasting model IFS-COMPO Cy49r1...re-CY49R1. This work is both parallel and complementary to the recent evaluation of the performance of IFS-COMPO Cy48r1 and Cy49r1...Y48R1 and of the impact of using EQSAM4Clim...re-CY49R1 with respect to regional PM2.5 distributions and Aerosol Optical Depth presented in Rémy et al (2024). The influence on regional wet and dry deposition terms are subsequently evaluated to assess upgrades to...he application of both EQSAM4Clim (Metzger et al., 2024) and the deposition schemes. In Sect. 2 we provide details of the IFS-COMPO simulations used, a brief description of the latest model updates and emissions used. In Sect 3 we describe the observational networks against which the surface evaluations are performed for the precursor gases and resulting SIA particulates. In Sect. 4 we provide details of the changes in regional surface concentrations of precursor (... [7])

**Deleted: 2 Model description of**

**Deleted:** Cy48r1 version of IFS, and uses recently updated chemical and aerosol components for the near-real time simulations of atmospheric composition

**Deleted:** cy48r1...Y48R1-part-viii-atmospheric-composition ; last access: 20 February 2024; Rémy et al., 2022; Williams et al., 2022), but since...), Since end of (... [8])

**Deleted:** For this study we perform simulations with both Cy48r1 and a version of IFS-COMPO pertaining to Cy49r1, which is now operational. These ...everal updates were (... [9])

Formatted: Font: Bold

Formatted: Font: 10 pt, Bold

Formatted: Normal5, Left

**Deleted:** Cy49r1

Formatted: Normal5

**Deleted:** Cy49r1...re-CY49R1 is built on the previous operational cycle (Cy48r1...Y48R1) and contains 8 distinct aerosol types with multiple bins for size segregation, r (... [10])

**Deleted:** Cy49r1...re-CY49R1 there has been an integration of the aerosol and chemistry components in the code to make them more consistent, where both the sulfur (... [11])

**Deleted:** 39

Formatted: Normal5, Right: 0,63 cm

Formatted: Page Number

particulate species) and the chemistry module (for gaseous species and aqueous  $\text{SO}_4^{2-}$  production). The aerosol module also provides additional input to the chemistry module to better represent heterogeneous reactions (via Surface Area Density (SAD)) and the effects of aerosols on photolysis rates. The extent of gas-particle partitioning and conversion via heterogeneous reactions on dust and sea-salt particles, are outlined in Rémy et al. (2019), as based on the work of Hauglustaine et al. (2014). In [CY48R1](#), the first version of the Equilibrium Simplified Aerosol Model (EQSAM; Metzger et al., 2002) was implemented for the calculation of e.g.  $\text{NH}_4\text{NO}_3$  concentrations. These parameterizations rely on meteorological data provided by IFS, as well as gaseous precursors such as  $\text{HNO}_3$  and  $\text{NH}_3$  from the chemistry module. The gas-particle partitioning scheme estimates compound production through the neutralization of  $\text{HNO}_3$  by  $\text{NH}_3$  left over after the neutralization of  $\text{H}_2\text{SO}_4$ . It also accounts for the formation of specific compounds from heterogeneous reactions of  $\text{HNO}_3$  with calcite (found in dust aerosol) and sea-salt particles.

In IFS-COMPO [pre-CY49R1](#), EQSAM4Clim is used to estimate the gas/particle partitioning of the  $\text{HNO}_3$ - $\text{NO}_3^-$  and  $\text{NH}_3$ - $\text{NH}_4^+$  couples and to provide an estimate of the aerosol pH. The pH of aqueous solutions, aquated aerosols and precipitation is now updated each time-step using the EQSAM4Clim approach accounting for additional cations ( $\text{Ca}^{2+}$ ,  $\text{Mg}^{2+}$ ,  $\text{Na}^+$ ,  $\text{K}^+$ ), anions ( $\text{SO}_4^{2-}$ ,  $\text{HSO}_4^-$ ,  $\text{NO}_3^-$ ,  $\text{Cl}^-$ ) and their solute interactions, whose methodology is comprehensively described in Metzger et al. (2012, 2016, 2024). This replaces the original estimate of the pH of the solution determined by summing the contributions from dissolved  $\text{CO}_2$  and strong acids ( $\text{HNO}_3$ ,  $\text{HSO}_3^-$ ,  $\text{H}_2\text{SO}_4$ ,  $\text{NO}_3^-$  and Methane Sulfonic Acid) which is buffered by dissolved  $\text{NH}_3$ . The contribution towards the pH of the solution of dissolved Formic and Acetic acid ( $\text{HCOOH}$  and  $\text{CH}_3\text{COOH}$ , respectively) are also now accounted for in [pre-CY49R1](#), which has been shown to contribute to the pH in cloud droplets (Shah et al., 2020). This impacts the phase-transfer, speciation, and subsequent aqueous-phase oxidation of  $\text{SO}_2$  in cloud droplets (thus impacting  $\text{SO}_4^{2-}$ ). Also, the loss of gas-phase species such as e.g.  $\text{H}_2\text{O}_2$  and the corresponding formation of SIA particles is affected. Note that both the original ([CY48R1](#)) and updated ([pre-CY49R1](#)) approaches account for the most dominant gaseous contributions towards the pH of the solution, namely  $\text{SO}_2$ ,  $\text{HNO}_3$  and  $\text{NH}_3$ . This means that differences imposed in cloud pH are naturally less than the associated changes in aerosol pH. The aqueous phase oxidation of  $\text{SO}_2$  by transition metal ions ( $\text{Fe}^{2+}$ ,  $\text{Mg}^{2+}$ ) is not currently accounted for but considered a minor pathway.

Below cloud scavenging of gaseous precursors is also affected by the pH of solution (e.g. Seinfeld and Pandis, 2006). In [CY48R1](#) fixed values for cloud pH are used over land (pH=5.0) and ocean (pH=5.6), thus only providing limited variability with respect to regions affected by both high and low emissions. In [pre-CY49R1](#) this has been updated such that the calculator of the pH is coupled to resident trace gas and aerosol concentrations to improve consistency within IFS-COMPO and to provide variable scavenging rates dependent on tropospheric composition.

In [CY48R1](#), the wet deposition routines for aerosols and chemistry in IFS-COMPO are distinct, though both utilise a scheme adapted from Luo et al. (2019), which is used operationally. To ensure a consistent approach between aerosol and trace gases wet deposition, and to simplify code maintenance, these separate implementations have been merged into a unified routine. This new routine now represents the wet deposition processes for both aerosols and chemical species and is called with either chemical or aerosol tracers as input. As with [CY48R1](#) and previous versions, the wet deposition routine in [pre-CY49R1](#) is executed twice: once for large-scale precipitation and once for convective precipitation. In the case of convective precipitation, the assumed precipitation fraction has been standardised to 0.05 (whereas in [CY48R1](#) a value of 0.1 was used for chemistry scavenging and 0.05 for aerosol scavenging).

Additional upgrades have been made for aerosol wet deposition as follows: (i) The aerosol activation parameterization of Verheggen et al. (2007) has been implemented. This parameterization estimates the fraction of aerosols that can be scavenged through in-cloud processes as a function of temperature. It is applied to mixed clouds, specifically for temperatures between the freezing point and 233K. For temperatures above 0°C, the consistency of the parameters determining the fraction of aerosols subject to in-cloud wet deposition with the results of the Verheggen parameterization has been verified. (ii) For below-cloud scavenging of aerosol species, the scavenging rates have been updated to reflect the particle size dependency more accurately as described by Croft et al. (2009). This update includes adjustments to the below-cloud scavenging parameters, which describe the efficiency with which aerosols are removed by rain and snow, depending on the species and the assumed size distribution. Additionally, a below-cloud scavenging model has been implemented.

## 2.2 Setup of model simulations

The IFS-COMPO simulations used for evaluating the impact of IFS-COMPO atmospheric composition upgrades proposed for [pre-CY49R1](#) on tropospheric composition, precursor gases, particle distributions and wet deposition terms employ both the IFS cycles [CY48R1](#) and [pre-CY49R1](#). Here, [pre-CY49R1](#) denotes the IFS-

Formatted: Header

Deleted:

Deleted: Cy48r1

Deleted: nitric

Deleted: sulfuric acid

Deleted: Cy49r1

Deleted: pH

Deleted: pH

Deleted: Cy49r1

Deleted: Cy48r1

Deleted: Cy49r1

Deleted: pH

Formatted: Not Superscript/ Subscript

Deleted:

Deleted: Cy48r1

Deleted: Cy49r1

Deleted: Cy48r1

Deleted: Similar to Cy48r1

Deleted: Cy49r1

Deleted: Cy48r1

Deleted: more accurately

Deleted: ¶

... [12]

Deleted: Cy49r1

Deleted: Cy48r1

Deleted: Cy49r1

Deleted: Cy49r1

Deleted: 39

Formatted: Normal5, Right: 0,63 cm

Formatted: Page Number



COMPO, ~~CY48R1~~ including updates of aerosol/chemistry modules which are now applied in IFS ~~pre-CY49R1~~. The meteorological component is the same between simulations and corresponds to ~~CY48R1~~. The simulations presented here are for the year 2018, with a one-month spin-up period. The vertical resolution uses 137 individual model levels and a horizontal resolution of T<sub>1</sub>511, corresponding to approx. 0.4° x 0.4° (with further details being given at <https://confluence.ecmwf.int/display/UDOC/L137+model+level+definitions>). The experiments do not include the data assimilation of observations, meaning that although the changes shown will not be directly visible in the final operational forecast, they will influence the resulting skill scores for e.g. PM<sub>2.5</sub>. Meteorology is initialised every 24 hours based on ERA5 reanalysis data, i.e. IFS-COMPO is run in a cyclic forecast mode. A 15-minute chemical time-step is used for solving a modified version of CB05 tropospheric chemistry (Williams et al., 2022), excluding active stratospheric chemistry for efficiency (with this study being focused on changes at the surface). Three-hourly 3D global output is used for the analysis and aggregated into weekly, monthly, and yearly mean values.

The details of the sensitivity experiments are summarised in Table 1. The ~~CY48R1~~ reference simulation pertains to the 48R1 version of IFS-COMPO while the ~~pre-CY49R1~~ simulation is based on the version described in Rémy et al (2024), which is ~~CY48R1~~ updated with new components for use in future versions of IFS-COMPO. The ~~pre-CY49R1~~ NOEQ4C simulation is identical to the ~~pre-CY49R1~~ simulation, except the EQSAM4Clim module (Metzger et al., 2024) is deactivated. For future reference, the experiment identities on the ECMWF Multiversion Asynchronous Replicated Storage system (MARS) are hylm (~~CY48R1~~), i3bw (~~pre-CY49R1~~ NOEQ4C) and i3ad (~~pre-CY49R1~~). These three simulations use a configuration, and emissions as those used for the simulations presented in Rémy et al. (2024) for evaluating PM. We select the year 2018 to provide further evaluation which is complimentary to the results presented for 2019 in Rémy et al. (2024)

**Table 1:** Definitions of the IFS-COMPO simulations used in this study. The experiment ID's can be used to retrieve the original data from the MARS archiving system hosted at ECMWF.

Simulation	Experiment ID	Comments
<del>CY48R1</del>	rd.hylm	Reference <del>CY48R1</del> model version
<del>pre-CY49R1</del> NOEQ4C	rd.i3bw	As <del>CY48R1</del> but with all composition modeling updates for <del>pre-CY49R1</del> , except EQSAM4Clim.
<del>pre-CY49R1</del>	rd.i3ad	As <del>CY48R1</del> , but with all composition modeling updates for <del>pre-CY49R1</del> , particularly activating EQSAM4Clim in both aerosols and cloud droplets

The emissions adopted in these configurations are taken from CAMS\_GLOB\_ANT v5.3 (Soulie et al., 2024), with biogenic emissions taken from the CAMS\_GLOB\_BIO v3.1 dataset (Sindelarova et al., 2022; <http://eccad.aeris-data.fr/>) and biomass burning emissions taken from GFAS v1.2 (Kaiser et al., 2012), all applied using the methodology as described in Ye et al. (2021), provided at 0.1 x 0.1 resolution on a monthly basis. For biomass burning and SO<sub>2</sub> emissions vertical profiles are used representing pyrogenic convection or industrial stack heights, with other emissions being applied in the lowest model level. A diurnal cycle is imposed for isoprene and biomass burning emissions to capture either photolytic activity or the tropical burning cycle. Volcanic outgassing of SO<sub>2</sub> is also included based on Andres and Kasgnoc (1998). For di-methyl sulphide (DMS) oceanic emissions are based on Kloster et al. (2006) i.e. not coupled to sea surface temperature which controls biogenic activity (Deschaseaux et al., 2019). Moreover, direct production of SO<sub>4</sub><sup>-</sup> and HNO<sub>3</sub> in hot shipping exhausts is not accounted for (e.g. von Glasow et al., 2003).

### 3 Observations

For SO<sub>2</sub>(g)/SO<sub>4</sub><sup>2-</sup>, NH<sub>3</sub>(g)/NH<sub>4</sub><sup>+</sup> and HNO<sub>3</sub>(g)/NO<sub>3</sub><sup>-</sup> evaluation in Europe we compare IFS-COMPO model output against data taken from the EMEP measurement network as stored on the EBAS data archive (EMEP, Torseth et al., 2012; <https://ebas.nilu.no/>; last access 6 June 2025) using a composite of 49 individual stations located in 10 different countries, as shown in the top panel of Fig A1 in the Appendix. We chose sites which monitor both the pre-cursor gases and associated SIA simultaneously to ensure valid comparisons. The sampling sites are located mostly in Northern and Eastern Europe, but co-location of model output means the comparison is still valid, albeit

Formatted: Header

Deleted: Cy48r1

Deleted: Cy49r1

Deleted: Cy48r1

Deleted:

Deleted: annual

Deleted: Cy48r1

Formatted: Normal5, Right: 0 cm

Deleted: Cy49r1

Deleted:

Deleted: ).

Deleted: Cy49r1

Deleted: Cy49r1

Deleted: Cy48r1

Deleted: Cy49r1

Deleted: Cy49r1

Deleted: similar to

Deleted: Remy

Deleted:

Formatted: Normal5

Formatted Table

Deleted: Cy48r1

Deleted: Cy48r1

Formatted: Normal5

Deleted: Cy49r1

Deleted: Cy48r1

Formatted: Normal5

Deleted: Cy49r1

Deleted: Cy49r1

Deleted: Cy48r1

Formatted: Normal5

Deleted: Cy49r1

Formatted: Normal5

Deleted: Apart from Biomass Burning (BB)

Deleted: ,

Formatted: Subscript

Deleted: . Currently the emission of Di-Methyl Sulphide

Deleted: is taken from a climatology,

Deleted: The sampling locations are

Deleted: .

Deleted: 39

Formatted: Normal5, Right: 0,63 cm

Formatted: Page Number

541 having less representation for southern Europe. For the U.S. we compare model output aggregated on a weekly  
 542 basis against data provided at locations included in the Clean Air Status and Trends Network (CASTNET;  
 543 <https://www.epa.gov/castnet>, last access: 6 June 2025) using a composite of 92 individual stations distributed  
 544 across the U.S. The distribution of the U. S. measurement sites is shown in the middle panel of Fig. A1 in the  
 545 Appendix. For NH<sub>3</sub>(g) not direct measurements are available from the CASTNET database, therefore we compare  
 546 against both weekly and yearly mean values as derived from sites located near CASTNET stations (within 0.5  
 547 degrees radius) i.e. 92 of the current 106 sites in the Ammonia Monitoring Network (AMoN,  
 548 <https://nadp.slh.wisc.edu/networks/ammonia-monitoring-network/>, last access on 6 June 2025). No filtering has  
 549 been applied to any of the observational data used in this study. Unfortunately for S. E. Asia measurements of both  
 550 precursors and SIA at a weekly time frequency are not readily available which hinders analysis and evaluation for  
 551 this region.

552 For evaluating the SIA particle concentrations, we use available data from the EMEP (Europe), CASTNET (US)  
 553 and the Acid Deposition Monitoring Network in East Asia (EANET, <https://www.eanet.asia/>, last access: 6 June  
 554 2025; S. E. Asia), for SO<sub>4</sub><sup>2-</sup>, NH<sub>4</sub><sup>+</sup> and NO<sub>3</sub><sup>-</sup>. The EANET network includes 41 individual stations covering a wide  
 555 region, whose location is shown in the bottom panel of Fig A1 in the Appendix. Although we use all the  
 556 observations provided in each database, the distribution is non-homogeneous, with those in EMEP being clustered  
 557 towards Northern Europe and those in Southeast Asia spanning a large area from Eastern China to Japan. The  
 558 locations of the stations used for evaluation are also shown (black circles) on the corresponding figures associated  
 559 with regional and spatial validation.

560 For the wet deposition totals we use data taken from the same measurement networks and sampling frequency as  
 561 those used for evaluating the gaseous precursors and SIA (EMEP, CASTNET, EANET) thus removing any  
 562 differences potentially introduced by spatial sampling which would complicate the comparisons discussed here.  
 563 Although seasonal variability is of interest, the EANET wet deposition totals are only provided as yearly mean  
 564 values placing constraints on the sampling frequency used for the analysis. Therefore, the averaging period chosen  
 565 for the evaluation is constrained by the frequency and availability of the data from Southeast Asia. All statistical  
 566 metrics represent spatio-temporal averages unless otherwise noted, combining all station-time pairings into a single  
 567 evaluation vector per region and species. No filtering of the data was performed before making the comparisons.

#### 568 4 The influence of pH on SIA chemical precursors and particulates

569 The efficacy of SIA formation is strongly governed by the resident concentrations of the gaseous precursors.  
 570 Therefore, changes imposed with respect to the parameterizations used for simulating particle formation also have  
 571 an associated feedback effect on the precursors, due to changes in the fractional uptake governed by the solute pH.  
 572 In this section, we evaluate the temporal and regional distribution and biases of both gaseous precursors (SO<sub>2</sub>,  
 573 NH<sub>3</sub>, HNO<sub>3</sub>) and associated SIA (namely SO<sub>4</sub><sup>2-</sup>, NH<sub>4</sub><sup>+</sup>, NO<sub>3</sub><sup>-</sup>) simulated by IFS-COMPO for Europe, the U.S. and  
 574 Southeast Asia. Mixing ratios and particle concentrations are strongly influenced by the description and  
 575 distribution of the primary emission sources, meteorology, dry/wet deposition, aerosol pH (for NH<sub>3</sub> and NO<sub>3</sub>) and  
 576 atmospheric transport. To investigate the ability of IFS-COMPO towards capturing the observed distributions, we  
 577 compare both weekly and yearly mean composites for CY48R1 and pre-CY49R1 against the corresponding values  
 578 derived from in-situ measurements. A direct link exists between [NH<sub>4</sub><sup>+</sup>] and [NO<sub>3</sub><sup>-</sup>] in that fine mode NO<sub>3</sub><sup>-</sup>  
 579 predominantly takes the form of NH<sub>4</sub>NO<sub>3</sub>.

#### 581 4.1 SO<sub>2</sub> and SO<sub>4</sub><sup>2-</sup>

582 Figure 1 shows the regional monthly mean distributions in surface SO<sub>2</sub> mixing ratios for July and December 2018  
 583 for CY48R1, along with the relative percentage differences between CY48R1, pre-CY49R1, NOEQ4C and pre-  
 584 CY49R1. When comparing the spatial distributions across regions, Europe exhibits the lowest SO<sub>2</sub> mixing ratios  
 585 in CY48R1, where the region has undergone strong mitigation practices over the last decades (e.g. Vestreng et al.  
 586 2007). The maps for December show higher mixing ratios towards the East, with a significant contribution from  
 587 shipping. For the US, a stark East-West gradient exists as governed by the continental distribution in  
 588 anthropogenic emissions, with higher emissions towards the East Coast, again with a seasonal signature. Maximal  
 589 surface mixing ratios are 5-10 times higher than those simulated for Europe distributed over a much larger area.  
 590 As expected, China exhibits the highest regional mixing ratios of between 10-20 ppb over the entire country,  
 591 which is approximately 20 times higher than those simulated for Europe for both months shown.

Formatted

[13]

Deleted: US

Deleted: against

Deleted: as derived from the in-situ measurements

Deleted: S., whose locations are

Deleted: the in-situ measurements taken from

Deleted: station locations (

Deleted: ), with measurements being at the location ( [16]

Deleted: these measurements due to the quality contr [17]

Deleted: does not allow the same

Deleted: in

Deleted: networks

Deleted:

Deleted: of

Deleted: South-East

Deleted: ,

Deleted: potentially

Deleted: Specifically, these are: the EMEP network [18]

Deleted: annual

Deleted: The

Deleted: predominantly

Deleted: South-East

Deleted: , which only provides annual mean values. [19]

Deleted: the

Deleted: the

Deleted: the

Deleted: component

Deleted: show

Deleted: annual

Deleted: comparisons

Deleted: Cy48r1

Deleted: Cy49r1 as compared

Deleted: measurement composites. In that the differe [20]

Deleted: the budget analysis of the gaseous precurs [21]

Deleted: nitrate

Deleted: All observational data is used for the calcul [22]

Deleted: To investigate the scale of such feedbacks w [23]

Deleted: Cy48r1

Deleted: Cy48r1, Cy49r1

Deleted: Cy49r1

Deleted: Cy48r1

Deleted: 39

Formatted

[15]

Formatted

[14]

When comparing [CY48R1](#) against [pre-CY49R1](#) NOE4C there are reductions in  $[\text{SO}_2(\text{g})]$  at the surface for all regions of between 0-10%, resulting in limited increases in  $\text{SO}_4^{2-}$  production of a few percent due to changes other than those related to [the application of EQSAM4Clim](#). This small increase in the  $\text{SO}_4^{2-}$  production is reversed when applying the EQSAM4Clim pH methodology (Metzger et al., 2024), where the conversion efficacy of  $\text{SO}_2$  is faster at a more alkaline pH. [Table 2 provides the global budget terms for  \$\text{SO}\_2\(\text{g}\)\$](#) , which shows that in addition to primary emission, approximately one third of  $\text{SO}_2$  in the troposphere comes from the oxidation of DMS by the hydroxyl radical (OH), with DMS originating from biogenic activity in the oceans.

In [CY48R1](#), approximately 20% of  $\text{SO}_2$  is oxidised in the gas-phase and 43% in the aqueous phase, with the remaining 37% being lost to surface via dry and wet deposition. This increase in gas-phase production via OH is linked to changes imposed by differences in  $\text{O}_3$ - $\text{NO}_x$  reaction cycles near anthropogenic source regions which results in a small increase in  $\text{O}_3$  of a few percent (not shown). The corresponding values for [pre-CY49R1](#) NOE4C show changes in the order of a few percent across terms, increasing the global burden by [of  \$\text{SO}\_2\(\text{g}\)\$  by 1.5%](#) mostly in the lower troposphere. For [pre-CY49R1](#) the application of EQSAM4Clim pH in cloud droplets reduces both the uptake and oxidation of  $\text{SO}_2$  by reducing aquated sulphite ( $[\text{SO}_3^{2-}]_{\text{aq}}$ ,  $\text{pKa}(\text{HSO}_3^-)=7.2$ ) and an enhancement of the gas-phase oxidation due to increased OH, resulting in more gas-phase production of  $\text{H}_2\text{SO}_4$ . This is subsequently scavenged into solution further increasing solution acidity ([lowering pH values](#)) in case of excess  $\text{SO}_4^{2-}$  (insufficient cations to completely neutralise all  $\text{SO}_4^{2-}$ ).

Figure 2 shows a comparison of weekly  $[\text{SO}_2(\text{g})]$  and  $[\text{SO}_4^{2-}]$  surface composites as simulated in IFS-COMPO against weekly composites of measurements taken from the EMEP measurement network (top left panel). For  $\text{SO}_2(\text{g})$  a consistent positive bias exists for the entire year across all IFS-COMPO simulations suggesting emission estimates which are high. [Surface](#) concentrations exhibit around 100% positive bias, increasing to almost 200% during wintertime. The variability in the observational means (grey shaded area) does indicate that the simulated increase in surface  $[\text{SO}_2(\text{g})]$  during wintertime does occur at some of the measurement sites. The corresponding observational means of  $[\text{SO}_4^{2-}]$  show that there is higher weekly variability during wintertime than summertime, with concentrations ranging typically between 1.0-2.0  $\mu\text{g}/\text{m}^3$ . This significant [wintertime](#) weekly variability is simulated well by IFS-COMPO across all simulations, [where both \[CY48R1\]\(#\) and \[pre-CY49R1\]\(#\) exhibit significant positive biases of 0.5-1.0  \$\mu\text{g}/\text{m}^3\$](#) . Surprisingly, [pre-CY49R1](#) NOE4C has the lowest bias during wintertime of around 0.2-0.5  $\mu\text{g}/\text{m}^3$ . [For \[pre-CY49R1\]\(#\), there is an increase in surface  \$\[\text{SO}\_4^{2-}\]\$  by approximately 10-25%, albeit with a significant negative bias of around 0.8-1.5  \$\mu\text{g}/\text{m}^3\$](#) . During summertime, the weekly variability in the observed weekly means is [insignificant](#). All simulations capture [this limited variability, with differences across simulations being around 0.1-0.2  \$\mu\text{g}/\text{m}^3\$](#) . Due to the primary source term of  $\text{SO}_2$  being direct emissions, [the high  \$\[\text{SO}\_2\(\text{g}\)\]\$  simulated for Eastern Europe suggests a local overestimate \(c.f. Fig. 1\)](#). The [yearly mean bias \(MB\) value decreases by around 25%, with a moderate correlation](#).

Formatted: Header

Deleted: Cy48r1

Deleted: Cy49r1

Deleted: updates to aerosol and solution pH.

Deleted: The

Deleted: show

Deleted: ,

Deleted: Cy48r1

Deleted: Cy49r1

Deleted: Cy49r1

Formatted: Not Superscript/ Subscript

Deleted: which

Deleted: lower

Deleted: Figure 1 shows that the region with the highest surface  $\text{SO}_2$  is the North-East of the U.S., with the other regions moderating the biases. Again little seasonality exists in the weekly observational composites. There is a positive bias for wintertime and a negative bias for summertime around 0.5-1.0  $\mu\text{g}/\text{m}^3$  across all simulations. There is an increase in the annual mean negative bias by around 0.1  $\mu\text{g}/\text{m}^3$  in Cy49r1 with poor correlation with the observations. Finally for China, weekly  $\text{SO}_2$  concentrations are an order of magnitude larger than those observed in the other regions reaching 15-20  $\mu\text{g}/\text{m}^3$  during wintertime. The simulated concentrations exhibit a very large positive bias of between 10-20  $\mu\text{g}/\text{m}^3$ , suggesting that the regional  $\text{SO}_2$  emissions are likely overestimated in the global inventory. Only a (... [24]

Formatted (... [25]

Deleted: , where surface

Deleted: . For wintertime

Deleted: Cy48r1

Deleted: Cy49r1

Deleted: Cy49r1

Deleted: . Comparing Cy49r1 against Cy48r1 shows

Deleted: % during wintertime in Cy49r1,

Deleted: still

Deleted: much lower with monthly gradients being c (... [26]

Deleted: the extent of

Deleted: quite well. Differences

Deleted: is

Deleted: , with Cy49r1 having a slightly higher bias.

Deleted: indicates that estimates

Deleted: could be too high

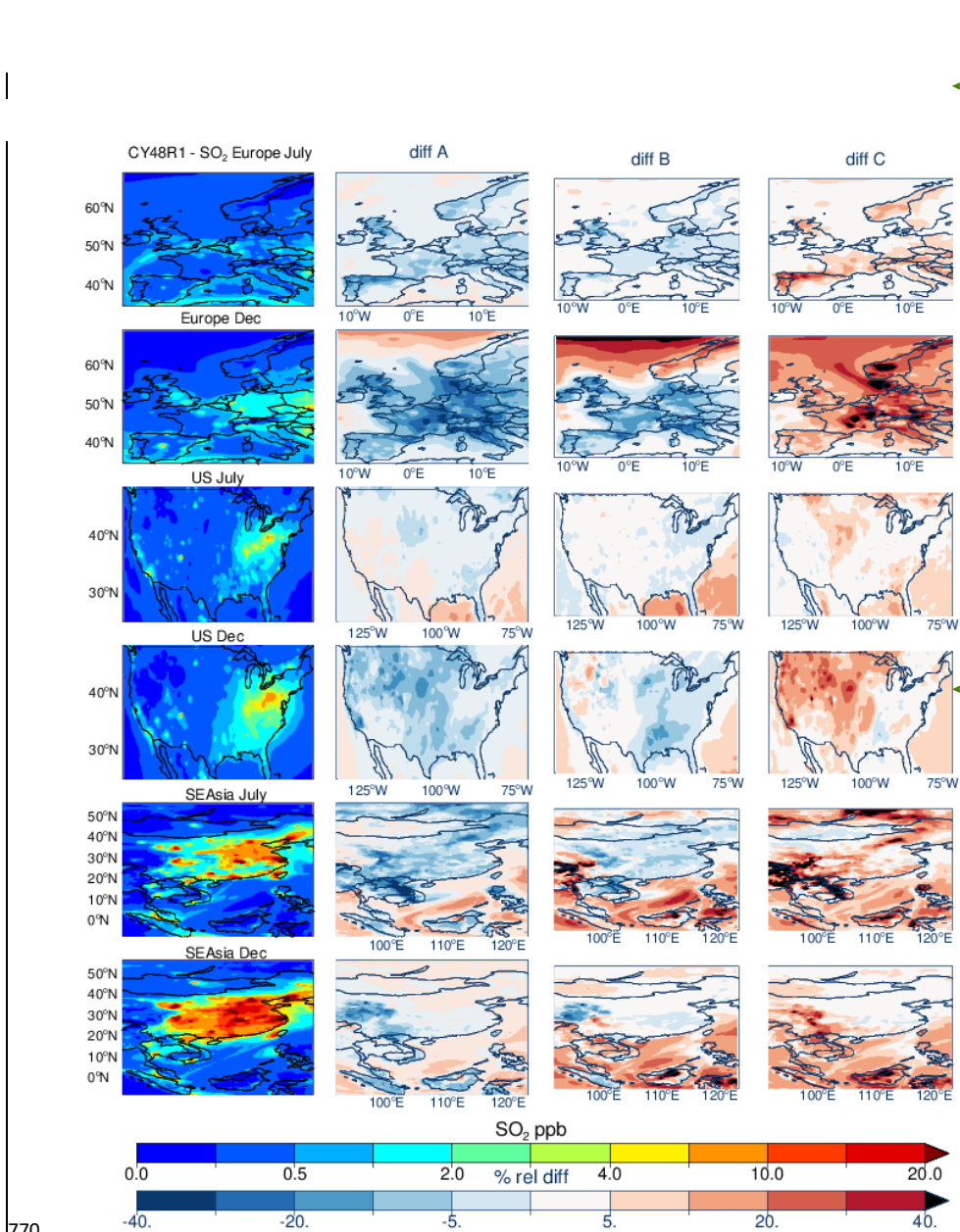
Deleted: annual

Deleted: For the US the weekly mean  $\text{SO}_2$  values in t (... [27]

Deleted: 39

Formatted: Normal5, Right: 0,63 cm

Formatted: Page Number



770  
 771 **Figure 1:** The horizontal monthly mean distribution for surface SO<sub>2</sub> for CY48R1 for July and December 2018 for  
 772 Europe (top), the United States (middle) and Southeast Asia (bottom). The corresponding relative differences  
 773 when compared against the other simulations. Panel definitions: Diff A =  $(\text{pre-CY49R1 NOEQ4C} -$   
 774  $\text{CY48R1})/\text{CY48R1}$ ; Diff B =  $(\text{pre-CY49R1} - \text{CY48R1})/\text{CY48R1}$  and Diff C =  $(\text{pre-CY49R1} - \text{pre-}$   
 775  $\text{CY49R1 NOEQ4C})/\text{CY48R1}$ .

776  
 777

Formatted: Header

Formatted: Normal5, Justified

Deleted: Cy48r1

Formatted: Normal5

Deleted: South-East

Deleted:

Deleted: =(Cy49r1

Deleted: Cy48r1)/Cy48r1

Deleted: Cy49r1-Cy48r1)/Cy48r1

Deleted: Cy49r1-Cy49r1

Deleted: Cy48r1

Formatted: Font: Not Bold

Deleted: 39

Formatted: Normal5, Right: 0,63 cm

Formatted: Page Number



Table 2 The tropospheric SO<sub>2</sub> budget in Tg S/year for 2018 as calculated by CY48R1, pre-CY49R1 NOE4C and pre-CY49R1, with the associated percentage differences being provided in parentheses as e.g. ((pre-CY49R1-CY48R1)/CY48R1)\*100.

Process	CY48R1	pre-CY49R1 NOE4C	pre-CY49R1
Emission	54.0	54.0 (-)	54.0 (-)
DMS + OH → SO <sub>2</sub>	21.8	21.8 (-)	21.5 (-1.6)
SO <sub>2</sub> + OH → H <sub>2</sub> SO <sub>4</sub>	15.1	15.4 (+2.3)	16.5 (+9.3)
SO <sub>2</sub> (aq) → SO <sub>4</sub> (aq)	33.7	33.9 (+1.2)	33.0 (-2.2)
Dry Deposition	21.6	21.3 (-3.0)	22.2 (+3.0)
Wet Deposition	8.2	8.0 (-3.0)	6.9 (-15.8)
Burden	0.70	0.71 (+1.4)	0.75 (+7.1)
Lifetime (days)	3.25	3.29 (+1.2)	3.48 (+7.1)

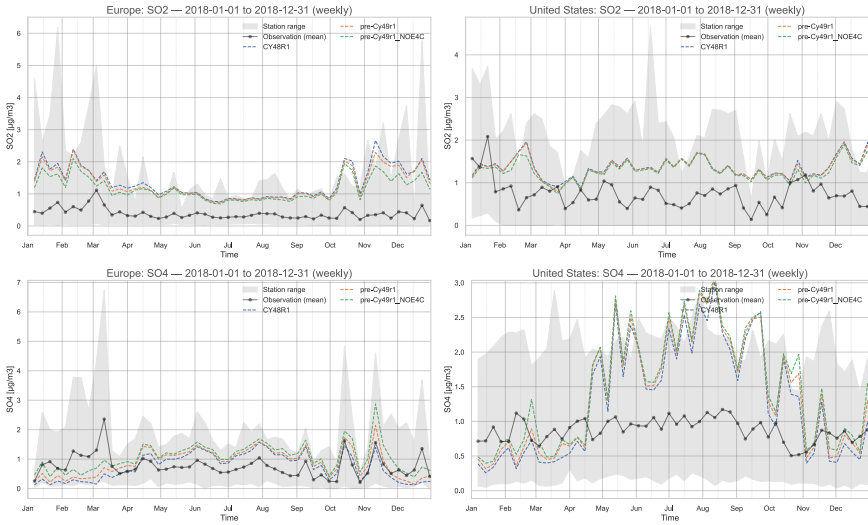


Figure 2: A comparison of weekly mean SO<sub>2</sub> and SO<sub>4</sub><sup>2-</sup> for Europe (left panels; µg/m<sup>3</sup>) and the U.S. (right panels) simulated in IFS-COMPO as compared against EMEP and CASTNET observational networks, respectively, for 2018. The sampling frequency of the data for SE-Asia does not allow a corresponding weekly plot for this region.

In the right-hand panels of Fig. 2 a similar comparison is made against weekly observational composites of surface [SO<sub>2</sub>(g)] and [SO<sub>4</sub><sup>2-</sup>] from the CASTNET measurement network. As for Europe, no seasonal cycle exists in the observations of either surface [SO<sub>2</sub>(g)] or [SO<sub>4</sub><sup>2-</sup>] with typical weekly mean values of around 0.7-1.0 µg/m<sup>3</sup>, even though the latitudinal range is large for the CASTNET measurement stations. For the wintertime lower weekly MB occur for both pre-CY49R1 NOE4C and pre-CY49R1 as compared with CY48R1, where the weekly variability is inverse of that seen in the observations. During the summertime much larger positive biases occur reaching between 200-300% across all IFS-COMPO simulations which exhibit a strong seasonal cycle despite no such increase in the simulated [SO<sub>2</sub>(g)]. Although some smaller differences occur between simulations, there is no improvement in pre-

Formatted: Header

Deleted: Cy48r1, Cy49r1...Y48R1, pre-CY49R1\_NOE4C and Cy49r1...re-CY49R1, with the associated percentage differences being provided in parentheses as e.g. ((Cy49r1-Cy48r1)/Cy48r1)\*

Formatted: Normal5

Deleted: Cy48r1

Deleted: Cy49r1

Deleted: Cy49r1

Formatted Table

Formatted: Normal5

Formatted: Normal5

Formatted: Normal5

Formatted: Normal5

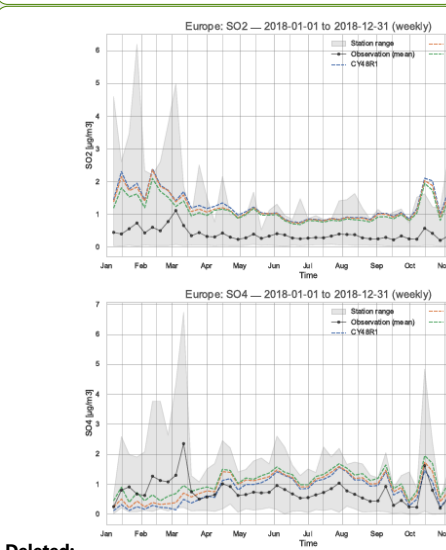
Formatted: Normal5

Formatted: Normal5

Formatted: Normal5

Formatted: Normal5

Formatted: Normal5



Deleted:

Deleted: US...S. (right panels) simulated in IFS-COMPO as compared against EMEP and CASTNET observations (... [29]

Deleted: ...hand panels of Fig. 2 a similar comparison is made against weekly observational composites of surf (... [30]

Deleted: 39

Formatted: Normal5, Right: 0,63 cm

Formatted: Page Number

852 CY49R1 with respect to the weekly MB. Considering the corresponding high summertime MB for SO<sub>2</sub> shows either a  
853 significant fraction is transported in IFS-COMPO, where a slower oxidation rate of SO<sub>2</sub> by OH and/or aqueous phase  
854 processing would be required to improve the performance of IFS-COMPO which would then lower the negative bias  
855 seen for [SO<sub>2</sub>(g)].

856 Figure 3 shows the yearly means of surface [SO<sub>2</sub>(g)] and [SO<sub>4</sub><sup>2-</sup>] for CY48R1 and pre-CY49R1 for Europe (top panels),  
857 the U.S. (middle panels) and Southeast Asia (bottom panels). The changes in surface [SO<sub>4</sub><sup>2-</sup>] here are somewhat  
858 unaffected by the changes in PM<sub>2.5</sub> due to EQSAM4Clim that are shown in Rémy et al. (2024) for 2019, due to the  
859 dominant aqueous-phase production term (albeit with small increases due to the additional contribution from organic  
860 acids). One main difference for SO<sub>x</sub> than either NH<sub>x</sub> or NO<sub>x</sub>, is that the gas-particle partitioning is dependent on cloud  
861 pH, dissolved O<sub>3</sub> and hydrogen peroxide (H<sub>2</sub>O<sub>2</sub>), where SO<sub>4</sub><sup>2-</sup> production is irreversible.

862 For Europe, a sharp North-South gradient exists imposed by the variability in H<sub>2</sub>SO<sub>4</sub> production between seasons,  
863 cloud cover for the wet production term and the distribution of the primary point sources for SO<sub>2</sub> emissions, although  
864 mitigation measures remove the increase in the emitted flux during the cold winter months associated with domestic  
865 heating (Versteeg et al., 2007). Simulated concentrations in CY48R1 are lower in Scandinavia as compared with e.g.  
866 France, which results in a low bias of around 1 µg/m<sup>3</sup> in e.g. Finland and around the Baltic, here related to missing  
867 shipping emissions of SO<sub>2</sub>, which quickly converts to SO<sub>4</sub><sup>2-</sup> in the plume (Celik, et al., 2020). For the other sites in  
868 Europe agreement is better with the low bias decreasing to approx. 0.5 µg/m<sup>3</sup>. One outlier exists for the most easterly  
869 station, which exhibits a significant high bias of 1.5 µg/m<sup>3</sup>. Comparing pre-CY49R1 shows increases in the simulated  
870 surface [SO<sub>4</sub><sup>2-</sup>] of between 0.2-0.4 µg/m<sup>3</sup>, which leads to an improved bias. Only small improvements are made to the  
871 correlation coefficient due to identical emission estimates being used and EQSAM4Clim affecting SO<sub>x</sub> the least, i.e.,  
872 only indirectly through changes in pH.

873 For the U.S., the CASTNET observations show an East-West continental gradient in surface [SO<sub>4</sub><sup>2-</sup>] exists as  
874 determined by the distribution in the primary SO<sub>2</sub> emissions and transport (c.f. Figure 1). A significant transport  
875 component exists for SO<sub>4</sub><sup>2-</sup>, resulting in surface [SO<sub>4</sub><sup>2-</sup>] in the Marine Boundary Layer between 1.0-2.5 µg/m<sup>3</sup>, where  
876 transport dominates local surface [SO<sub>4</sub><sup>2-</sup>] produced from DMS oxidation (Simpson et al., 2014). For pre-CY49R1 there  
877 is a reduction in surface [SO<sub>4</sub><sup>2-</sup>] at continental scale, with a decrease in the yearly MB from 0.67 to 0.20 µg/m<sup>3</sup>, with a  
878 corresponding increase in the correlation coefficient to 0.43, albeit remaining only rather weakly correlated. For the  
879 West of the U.S. a positive MB is introduced for the rural background in pre-CY49R1 of 0.5-0.7 µg/m<sup>3</sup>, with a  
880 contribution being transported from the East. Hence, reductions in the yearly MB primarily stem from improved  
881 agreement at Eastern U.S. monitoring sites. That a positive MB of approx. 1-1.5 µg/m<sup>3</sup> exists in the yearly mean values  
882 around Kentucky/Tennessee suggests that the local SO<sub>2</sub> emission estimates are too high (see Discussion in Sect. 5).

883 For Southeast Asia, the scarcity of sampling sites in the EANET network results in a less robust evaluation. Many  
884 sampling sites are located at coasts rather than inland, thus the influence of changes at coastal regions has an influence  
885 on the regional statistics. Higher primary SO<sub>2</sub> emissions occur on the land. Therefore, any positive MB near source  
886 regions is not included in the statistics; the results shown here for surface SO<sub>4</sub><sup>2-</sup> should be considered lower limits.  
887 The long-range transport of SO<sub>4</sub><sup>2-</sup> in Asia has been shown to somewhat neutralise national SO<sub>2</sub> mitigation measures  
888 taken in e.g. Taiwan and South Korea. This originates from changing trends in SO<sub>2</sub> emission from mainland China as  
889 captured by EANET measurement sites (Chang et al, 2022). For CY48R1 the yearly mean statistics show an  
890 exceptionally low MB and a good correlation coefficient of 0.75. For pre-CY49R1 there is a significant degradation,  
891 where the MB increases to 0.48 µg/m<sup>3</sup> showing a trend in the performance for SO<sub>x</sub> that is like the U.S. Notably, the  
892 more remote sampling stations (e.g. oceanic) exhibit regional negative biases (approx. -0.7 µg/m<sup>3</sup>) whereas those  
893 situated near Mongolia and South Korea agree well with low MB values. For Thailand and Vietnam there are typically  
894 large MB values, suggesting regional SO<sub>2</sub> emission estimates are too high. Unfortunately, there are no in-situ  
895 measurements available for better quantification. The correlation coefficient degrades in pre-CY49R1 compared to  
896 CY48R1 towards 0.66. Overall, the improvements are mixed for the SO<sub>2</sub> - SO<sub>4</sub><sup>2-</sup> couple and much less pronounced  
897 compared to the other SIA.

Formatted: Header

Deleted: annual

Deleted: Cy48r1

Deleted: Cy49r1

Deleted: the US.

Deleted: aerosol pH

Deleted: For Europe the sampling sites for this aerosol species in the EMEP network are located such that comparisons for southern european countries are not included in the regional mean statistics or discussed further. A

Deleted: Cy48r1

Deleted: ) .

Deleted: Cy49r1

Deleted: .

Deleted: Cy49r1

Deleted: annual

Deleted: Cy49r1

Deleted: annual

Deleted: annual

Deleted: South-East

Deleted: Also many

Deleted: have a large

Deleted: are

Deleted: Cy48r1

Deleted: annual

Deleted: a very

Deleted: Cy49r1

Deleted: similar to

Deleted: . .

Deleted: Cy49r1

Deleted: Cy48r1

Deleted: 39

Formatted: Normal5, Right: 0,63 cm

Formatted: Page Number

Formatted: Header

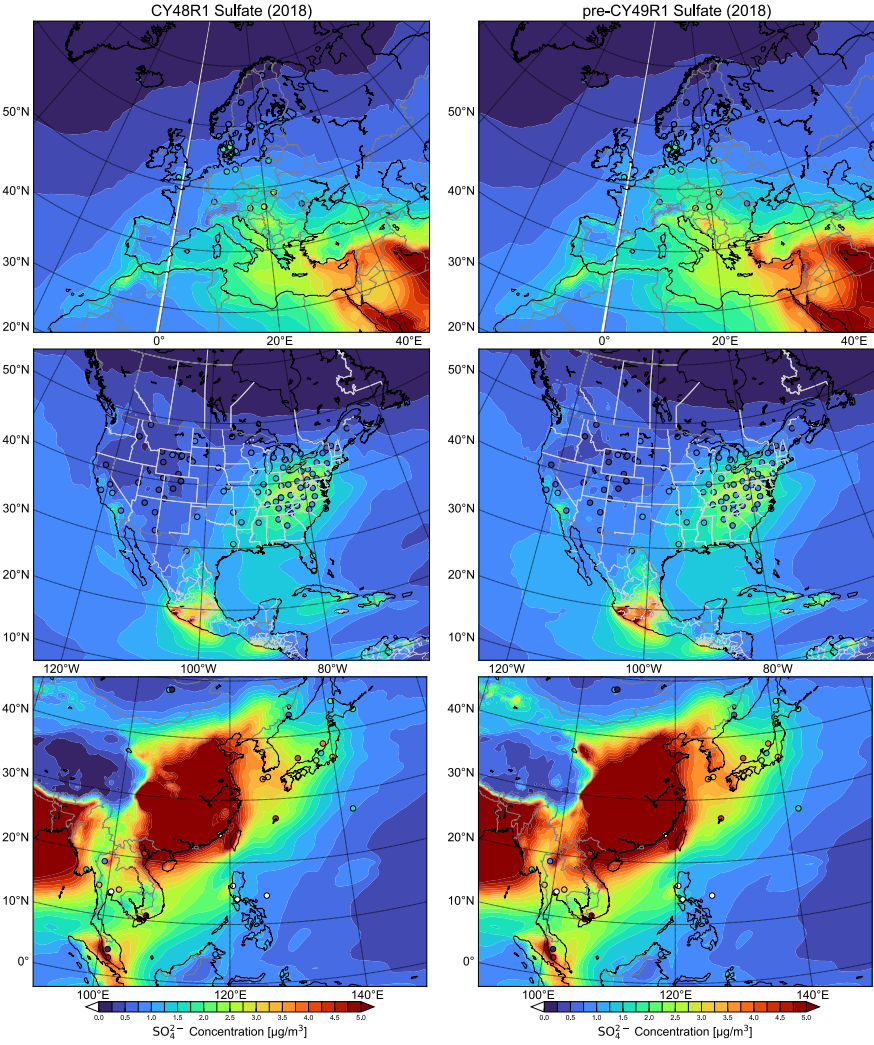
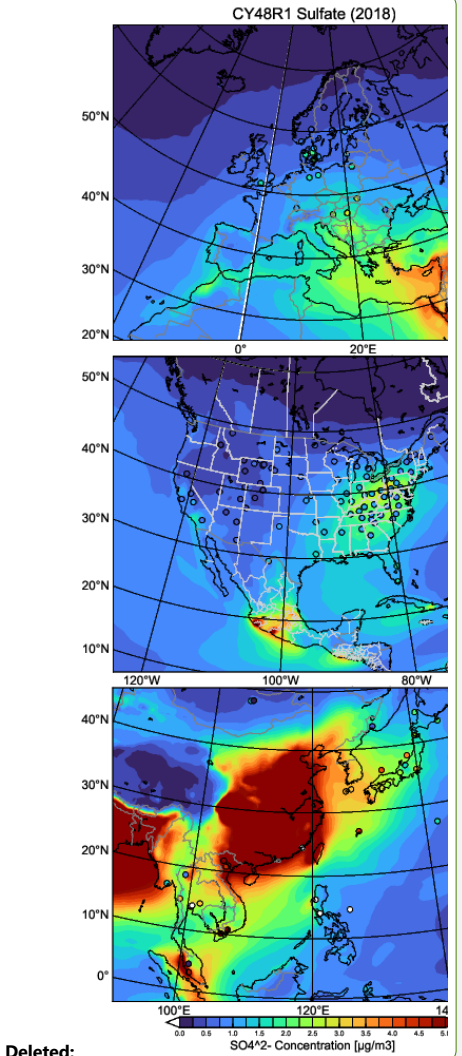


**Figure 3:** Comparisons of yearly mean  $[SO_4^{2-}]$  simulated at the surface in CY48R1 and pre-CY49R1 when compared against measurements for the three selected regions during 2018 ( $\mu g/m^3$ ). The corresponding regional statistics are provided in Table 3. The site locations used are shown in each pane and taken from the EMEP, CASTNET and EANET networks, respectively.



Deleted:

Deleted:

Deleted: annual

Deleted: Cy48r1

Deleted: Cy49r1

Formatted: Normal5

Formatted: Normal5, Space After: 10 pt

Deleted: 39

Formatted: Normal5, Right: 0,63 cm

Formatted: Page Number

Table 3: The yearly MB, RMSE and Pearsons R values for the comparisons of the daily (EMEP, Europe), weekly (CASTNET, US) and yearly (EANET, Southeast Asia) mean regional distributions and concentrations of surface SO<sub>4</sub><sup>2-</sup> as compared against composites assembled from the observations for 2018 shown in Fig. 4 for Europe, the U.S. and Southeast Asia. Percentage differences are calculated as ((pre-CY49R1-CY48R1)/CY48R1)\*100 and given in parentheses.

	Europe (EMEP)		US (CASTNET)		SE Asia (EANET)	
SO <sub>4</sub> <sup>2-</sup>	CY48R1	pre-CY49R1	CY48R1	pre-CY49R1	CY48R1	pre-CY49R1
MB (µg/m <sup>3</sup> )	-0.49	-0.32 (-35)	0.67	0.20 (-70)	-0.02	0.48 (+96)
RMSE	1.35	1.31 (-3)	0.93	0.46 (-50)	1.64	2.28 (+39)
Pearsons R	0.45	0.47 (+4)	0.33	0.43 (+23)	0.75	0.66 (-12)

4.2 NH<sub>3</sub> and NH<sub>4</sub><sup>+</sup>

The regional distribution of surface NH<sub>3</sub> for 2018 in the three chosen global regions and the resulting changes for pre-CY49R1 NOE4C and pre-CY49R1 are shown in Figure 4. Although there is a declining trend in European regional NH<sub>3</sub> emissions (Tichý et al, 2023), a strong seasonal cycle exists in CY48R1. Maximal mixing ratios are situated around Benelux and Northern Italy, with local differences of 8-20 ppb between July and December across regions. The CAMS\_GLOB\_ANT v5.3 (Soulie et al, 2024) emission inventory has recently been validated for NH<sub>3</sub> against top-down estimates providing confidence in the quality of the estimates for Europe (Ding et al., 2024). For the U.S., a similar seasonal signature exists especially for the Northwest and Southeast associated with agricultural emissions (Wang et al, 2020), with background mixing ratios of between 0.5-2.0 ppb remaining constant. For China, whose NH<sub>3</sub> emissions have increased over the last decades (Liu et al., 2019; Chen et al. 2023), surface mixing ratios of between 5-20 ppb occur for July for large areas, again associated with agricultural practices. Likewise, high mixing ratios are found around Bangladesh (> 20 ppb). For December, mixing ratios are typically an order of magnitude lower, except for the Southwest, which again exhibits high mixing ratios (> 20 ppb). Measurements of NH<sub>3</sub> over the ocean are rare, thus the substantial increase which is simulated in pre-CY49R1 cannot be evaluated. Nevertheless, estimates range from 0.1-4.2 ppb depending on season and location (Sharma et al., 2012) indicating that CY48R1 has a significant negative bias which is somewhat improved in pre-CY49R1.

Table 4 provides the global budget terms for all three simulations, showing the significant increase in deposition terms and tropospheric burden for NH<sub>3</sub>(g). For pre-CY49R1, the improved gas/particle partitioning from EQSAM4Clim reduces the particle phase concentrations of the semi-volatile aerosol species which leads to an increase in the respective gas phase concentrations, also affecting aerosol pH. This determines the solubility of NH<sub>3</sub>(g), also contributing to its reduced conversion into NH<sub>4</sub><sup>+</sup> (see Table 4, approx. 44% reduction), which is an effect amplified by the inclusion of mineral cations (i.e. Ca<sup>2+</sup>, Na<sup>+</sup>, K<sup>+</sup>, Mg<sup>2+</sup>). The tropospheric lifetime of NH<sub>3</sub>(g) more than doubles in pre-CY49R1, allowing more transport from strong source regions, in line with changes in the tropospheric burden. Both the associated loss due to dry and wet deposition increases (37% and 51%, respectively), due to lower NH<sub>3</sub> particle production (see Sect. 4.2).

Formatted: Header

Deleted:

Deleted: annual

Formatted: Normal5

Deleted: annual

Deleted: South-East

Deleted: US

Deleted: South-East

Deleted: Cy49r1-Cy48r1)/Cy48r1

Formatted Table

Deleted: Cy48r1

Formatted: Normal5

Deleted: Cy49r1

Deleted: Cy48r1

Deleted: Cy49r1

Deleted: Cy48r1

Deleted: Cy49r1

Formatted: Normal5

Formatted: Normal5

Deleted: which occur due to both the IFS cycle upgrades

Deleted: the application of EQSAM4Clim

Deleted: Cy48r1

Deleted: US

Deleted: North West

Deleted: South East

Deleted: relatively

Deleted: with

Deleted: exception of the South-West

Deleted: large

Deleted: shown

Deleted: verified

Deleted: Cy48r1

Moved (insertion) [1]

Formatted: Normal5

Deleted: 39

Formatted: Normal5, Right: 0,63 cm

Formatted: Page Number



**Table 4.** The tropospheric NH<sub>3</sub> budget in Tg N/year for 2018 as calculated by CY48R1, pre-CY49R1 NOE4C and pre-CY49R1, with the associated percentage differences being provided in parentheses as e.g. ((pre-CY49R1-CY48R1)/CY48R1)\*100.

Process	CY48R1	pre-CY49R1 NOE4C	pre-CY49R1
<b>Emission</b>	51.1	51.1 (-)	51.1 (-)
NH <sub>3</sub> + OH	0.82	0.99 (+20)	1.98 (+240)
NH <sub>3</sub> → NH <sub>4</sub> <sup>+</sup>	30.6	30.3 (-1)	17.3 (-44)
Dry Deposition	16.3	16.6 (+2)	22.4 (+37)
Wet Deposition	7.0	6.2 (-13)	10.6 (+51)
Burden	0.13	0.16 (+19)	0.29 (+118)
Lifetime (days)	0.9	1.1 (+22.0)	2.0 (+133)

Figure 5 shows comparisons between weekly observational composites from EMEP of [NH<sub>3</sub>(g)] against those extracted from the various IFS-COMPO simulations for 2018. The observational composite shows that there is a skewed seasonal cycle exhibiting a maximum in April/May from agricultural activity, with wintertime values being around 0.4-0.5 µg/m<sup>3</sup> increasing to 0.8-1.5 µg/m<sup>3</sup> during spring and summertime. This seasonal variability is captured across all simulations with a high correlation with a Pearson's R value between 0.71-0.73. For wintertime there is limited variability and an associated low weekly bias of around 0.1 µg/m<sup>3</sup>. For summertime, there is a weekly bias of between 0.5-1.0 µg/m<sup>3</sup> in CY48R1 (yearly MB of approximately 0.5 µg/m<sup>3</sup>), with the MB almost doubling for pre-CY49R1 (with a yearly MB of approximately 0.7 µg/m<sup>3</sup>).

Formatted: Header

Deleted: Cy49r1.

Formatted: Normal5

Deleted: maxima

Deleted: .

Deleted: a

Deleted: and a positive

Deleted: 2

Deleted: Cy48r1 (annual

Deleted: 1.04

Deleted: where a 20% increase in

Deleted: bias is simulated

Deleted: Cy49r1 (annual MB 1.21

Deleted: There is a high correlation across simulations resulting in values from 0.71-0.73, where the occurrence of weekly increases in the observed values are typically captured in IFS-COMPO.

Deleted: 39

Formatted: Normal5, Right: 0,63 cm

Formatted: Page Number

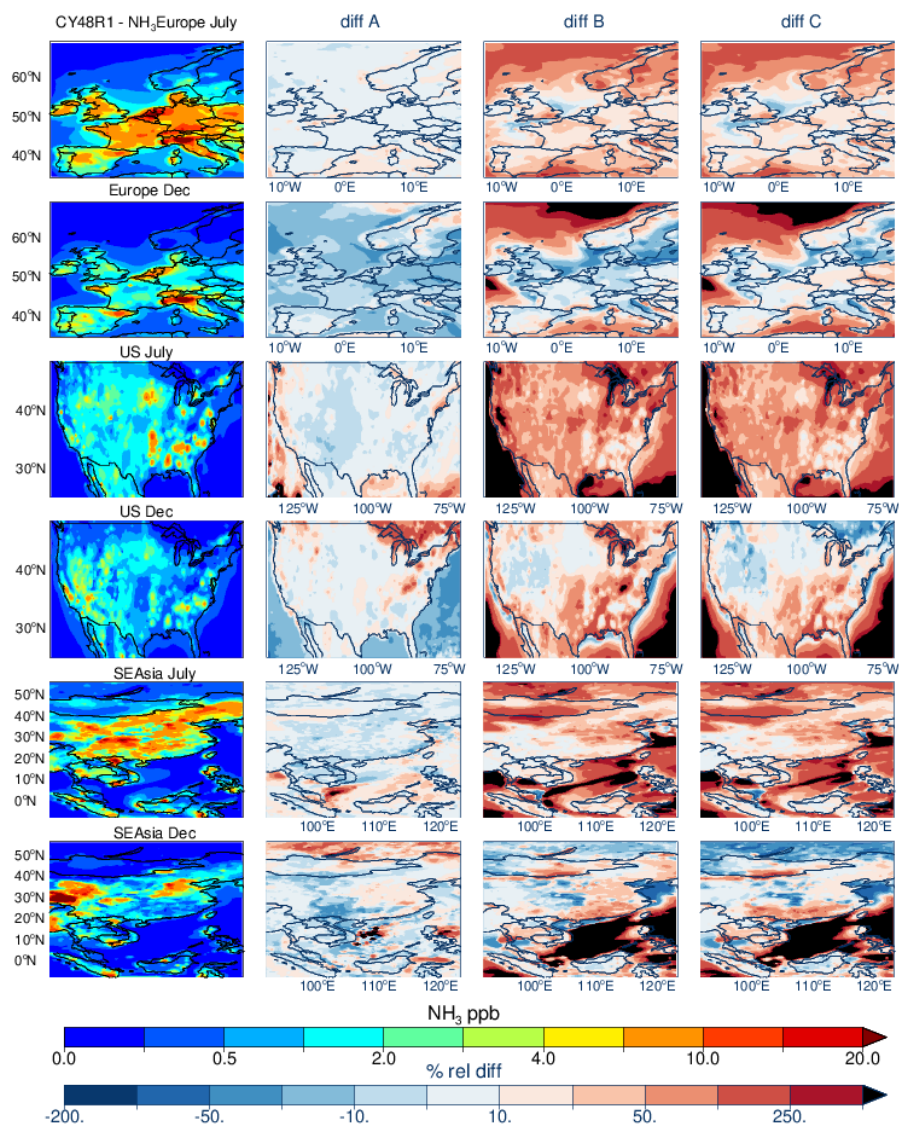


**Figure 4:** As for Fig. 1 except for  $\text{NH}_3$ . Panel definitions: Diff A=(pre-CY49R1\_NOEQ4C - CY48R1)/CY48R1; Diff B=(pre-CY49R1-CY48R1)/CY48R1 and Diff C=(pre-CY49R1-pre-CY49R1\_NOEQ4C)/CY48R1.

The bottom left panel of Fig. 5 shows the corresponding comparisons of  $[\text{NH}_4^+]$  in Europe using the weekly observational means from the EMEP network. There is a reversed seasonality for  $[\text{NH}_4^+]$  with higher  $[\text{NH}_4^+]$  during wintertime due to the colder temperatures decreasing the volatility of the particles (e.g. Tang et al., 2021). Moreover, for CY48R1 there is clearly a large positive bias of  $[\text{NH}_4^+]$  with only minor changes introduced due to the wet scavenging in pre-CY49R1\_NOEQ4C. Wintertime biases are reduced in pre-CY49R1 especially for weeks which exhibit peaks in the observational means which JFS-COMPO can capture.

Formatted: Header

Formatted: Normal5, Justified

Deleted: that there

Formatted: Normal5

Deleted: in

Deleted: in the observational means,

Formatted: Not Superscript/ Subscript

Deleted: Cy48r1

Deleted: little change in Cy49r1

Deleted: Table 4 provides the global budget terms for all three simulations, showing the large increase

**Moved up [1]:** allowing more transport from strong source regions, in line with changes in the tropospheric burden. Both the associated loss due to dry and wet deposition increases (37% and 51%, respectively), due to lower  $\text{NH}_4^+$  particle production (see Sect. 4.2).

Deleted: deposition terms and tropospheric burden for  $\text{NH}_3(\text{g})$ . For Cy49r1, the improved gas/particle partitioning from EQSAM4Clim reduces

Deleted: particle phase concentrations of the semi-volatile aerosol species which leads to an increase in the respective gas phase concentrations, also affecting aerosol pH. This determines the solubility of  $\text{NH}_3(\text{g})$ , also contributing to its reduced conversion into  $\text{NH}_4^+$  (see Table 4, approx. 44% reduction),...

Deleted: is an effect amplified by the inclusion of mineral cations (i.e.  $\text{Ca}^{2+}$ ,  $\text{Na}^+$ ,  $\text{K}^+$ ,  $\text{Mg}^{2+}$ ). The tropospheric lifetime of  $\text{NH}_3(\text{g})$  more than doubles in Cy49r1

Deleted: 39

Formatted: Normal5, Right: 0,63 cm

Formatted: Page Number

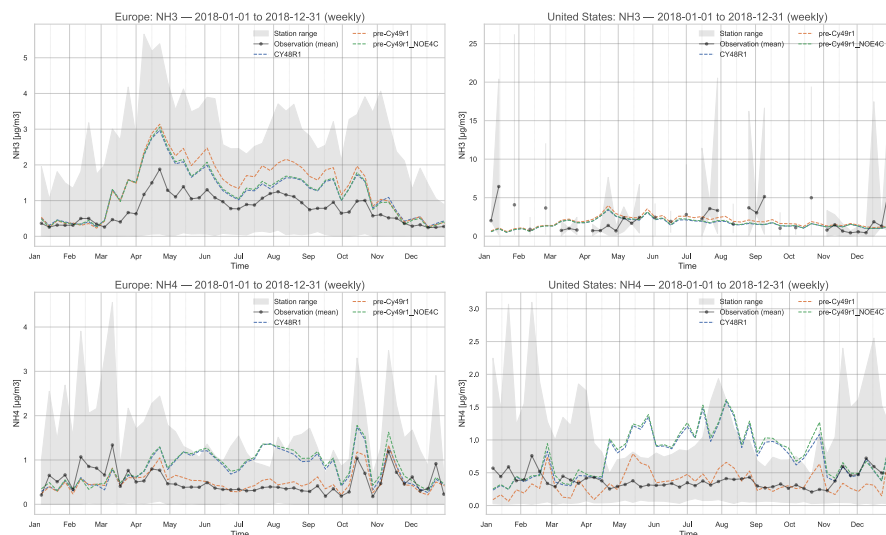


**Figure 5:** A comparison of weekly mean  $[\text{NH}_3(\text{g})]$  and  $[\text{NH}_4^+]$  at the surface for Europe (left panels;  $\mu\text{g}/\text{m}^3$ ) and the U.S. (right panels) as simulated in IFS-COMPO as compared against the composites of measurements taken from EMEP and CASTNET for 2018. For the U.S., the data for  $\text{NH}_3(\text{g})$  is taken from the AMoN measurement network in the top right panel. The data frequency provided for the Southeast Asia region does not allow a corresponding plot, although yearly statistics are provided in Table 5.

Similar comparisons are shown for the U.S. in the bottom right panel of Fig. 5 using weekly composites assembled from the CASTNET data. In contrast to the seasonal cycle for  $[\text{NH}_3(\text{g})]$ , which peaks during April/May, there is no corresponding seasonal cycle in the weekly  $[\text{NH}_4^+]$  values peaks, being consistent between  $0.4\text{--}0.5 \mu\text{g}/\text{m}^3$  during summertime. This indicates that a saturation occurs with respect to  $\text{NH}_4^+$  particle formation which is linked to availability of  $\text{HNO}_3(\text{g})$  (c.f. See sect 4.3. below). Again, significant biases exist in CY48R1 and pre-CY49R1 NOE4C, reaching around  $1.0 \mu\text{g}/\text{m}^3$  during summertime (which is 200% of the summertime observational values). Applying EQSAM4Clim essentially removes this positive MB in pre-CY49R1, resulting in good agreement for the entire year.

**Table 5:** As for Table 3 except for  $\text{NH}_4^+$ .

	Europe (EMEP)		US (CASTNET)		SE Asia (EANET)	
$\text{NH}_4^+$	Cy48r1	Cy49r1	Cy48r1	Cy49r1	Cy48r1	Cy49r1
MB ( $\mu\text{g}/\text{m}^3$ )	0.26	-0.05 (-81)	0.95	0.23 (-48)	0.96	0.55 (-43)
RMSE	0.94	0.72 (-23)	1.71	0.46 (-73)	1.73	1.30 (-25)
Pearsons R	0.46	0.62 (+29)	0.59	0.43 (-27)	0.59	0.44 (-25)

Figure 6 shows the distribution of the corresponding yearly mean  $[\text{NH}_4^+]$  for the three chosen regions for both CY48R1 and pre-CY49R1 during 2018, with the associated regional yearly mean statistics being given in Table 5. The location of the measurement sites is shown in each panel, with the respective yearly mean values within each circle. Significant decrease in the conversion rate of  $\text{NH}_3$  in pre-CY49R1 results in lower  $[\text{NH}_4^+]$ . This is a result of the improved

Formatted

... [31]

Moved up [2]: ¶

Deleted: Panel definitions : Diff A=(Cy49r1\_NOEQ ... [35]

Deleted: The tropospheric  $\text{NH}_3$  budget in Tg N/year ... [36]

Formatted ... [34]

Deleted: Also shown in Fig. 5 are weekly comparison ... [37]

Deleted: in Fig. 5

Deleted: US

Deleted: in the bottom right panel.

Deleted: the

Deleted: during July

Deleted: fairly

Deleted: 1

Deleted: -1.75

Deleted: most likely

Deleted: Cy48r1

Deleted: Cy49r1

Deleted: 5

Deleted: 600

Deleted: halves

Deleted: bias

Deleted: Cy49r1

Deleted: fairly

Deleted: during

Deleted: winter and summer months

Deleted: :

Formatted ... [38]

Formatted Table ... [39]

Formatted ... [40]

Formatted ... [41]

Formatted ... [42]

Deleted: annual

Deleted: Cy48r1

Deleted: Cy49r1

Deleted: annual

Deleted: are

Deleted: annual

Deleted: decreases

Deleted: Cy49r1

Deleted: 39

Formatted ... [33]

Formatted ... [32]

1236 gas/aerosol partitioning and the subsequent increase in aerosol pH when applying EQSAM4Clim (see Table 4; Rémy  
1237 et al., 2024). More direct depositional loss to the surface for  $\text{NH}_3(\text{g})$  occurs in pre-CY49R1 due to increased residence  
1238 time. There is a wide variability in the simulated aerosol pH between regions, with Europe exhibiting aerosol pH  
1239 values of around 3-4, whereas the Southern U.S. and Northern China exhibit aerosol pH values in the range 2-3 (Pan  
1240 et al, 2024; Rémy et al, 2024) which indirectly affects the temporal variability in  $\text{NH}_4^+$  production. Once formed,  
1241 regional transport contributes to the continental distribution of  $\text{NH}_4^+$  away from strong source regions (e.g. Simpson  
1242 et al., 2010; Renner and Wolke, 2010; Du et al, 2020).

1243 For Europe (top panels), most observational yearly mean values are between 0.2-1.2  $\mu\text{g}/\text{m}^3$  which are exceeded by >  
1244 50% in CY48R1. In pre-CY49R1 the reductions in the yearly mean  $[\text{NH}_4^+]$  are of the order of 0.5-1.0  $\mu\text{g}/\text{m}^3$  and result  
1245 in low yearly mean  $[\text{NH}_4^+]$  values for e.g. Spain/UK, whilst reducing maximal concentrations by approx. 50% in  
1246 Northern Italy. This subsequently contributes to a reduction in the cumulative PM2.5 biases for this region as shown  
1247 in Rémy et al. (2024) for 2019. The associated MB values in Table 5 show a significant reduction in the bias (> 80%)  
1248 along with an increase in the correlation coefficient, although the simulated  $\text{NH}_4^+$  distribution is still only moderately  
1249 correlated ( $r=0.62$ ). Unfortunately, the lack of available measurements means no quantification of the performance  
1250 of IFS-COMPO around the mediterranean can be shown. It should be noted that with a more realistic distribution and  
1251 seasonal variability in  $\text{NH}_3(\text{g})$  emissions (e.g. Shepard et al, 2011; Dammers et al, 2019), the  $[\text{NH}_4^+]$  distributions  
1252 shown here will not be affected as other SIA species determine the  $\text{NH}_3 - \text{NH}_4^+$  gas/aerosol partitioning.

1253 For the U.S. (middle panels) similar decreases in yearly mean  $[\text{NH}_4^+]$  values occur in pre-CY49R1 as compared to  
1254 CY48R1, with very low concentrations of between 0.1-0.4  $\mu\text{g}/\text{m}^3$  for the West of the U.S., which shows less bias  
1255 when compared against the observational mean values. This causes a reduction in the yearly mean regional bias of  
1256 around 0.7  $\mu\text{g}/\text{m}^3$  as shown in Table 5. A gradient exists in the aerosol pH from EQSAM4Clim ranging from yearly  
1257 mean values of pH=3.0 towards the northwest of the U. S. and becoming more acidic towards the southwest U.S. with  
1258 yearly mean values of pH=2.0 (Rémy et al., 2024). This reduces the transfer of  $\text{NH}_3(\text{g})$ , thus moderating  $\text{NH}_4^+$   
1259 production (c.f. Table 5). For the northeast of the U.S. with high  $\text{NO}_x$  emissions, there are reductions of between 0.5-  
1260 1.0  $\mu\text{g}/\text{m}^3$ . For the South-West U.S., with high  $[\text{NH}_3(\text{g})]$  from agriculture (c.f. Fig. 5) there are reductions of between  
1261 0.3-1.0  $\mu\text{g}/\text{m}^3$ . There is a degradation in the correlation coefficient exhibiting a moderate yearly mean correlation with  
1262 significant overestimates for the South-West U.S. as shown for the comparisons of  $[\text{NH}_3(\text{g})]$  at selected sites in Figure  
1263 5.

Formatted: Header

Deleted: Cy49r1

Deleted:

Deleted: annual

Deleted: Cy48r1

Deleted: Cy49r1

Deleted: annual

Deleted: annual

Deleted: most likely

Deleted: annual

Deleted: Cy49r1

Deleted: Cy48r1

Deleted: annual

Deleted: annual

Deleted: North-West

Deleted: South West

Deleted: annual

Deleted: North-East

Deleted: annual

Deleted: 39

Formatted: Normal5, Right: 0,63 cm

Formatted: Page Number



Formatted: Header

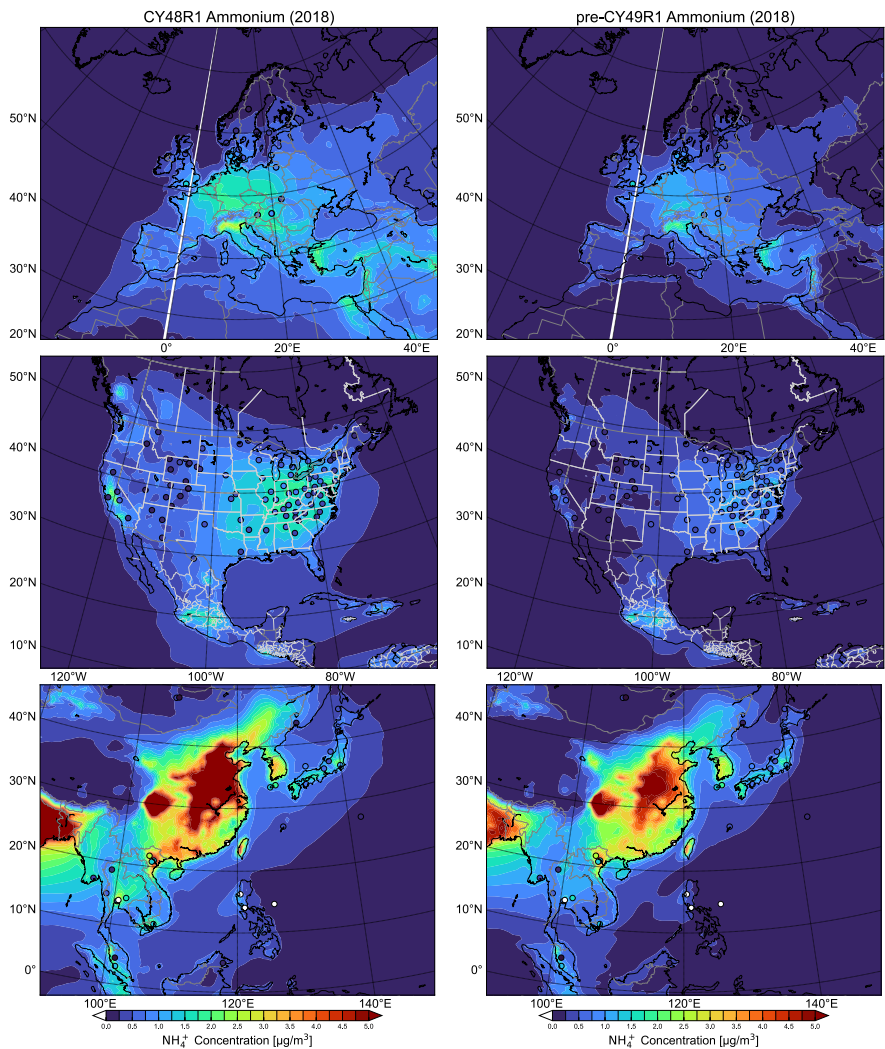
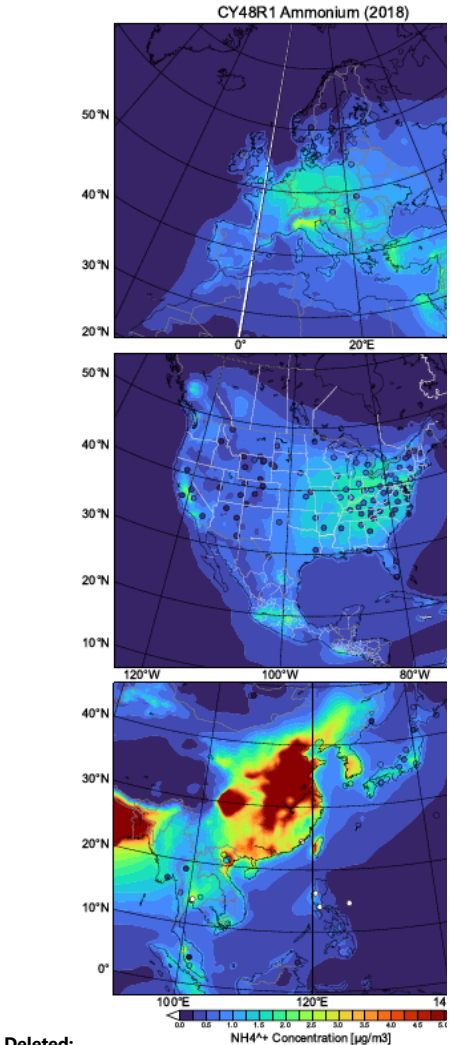


**Figure 6:** Comparisons of yearly mean  $[NH_4^+]$  simulated at the surface in CY48R1 and pre-CY49R1 when compared against measurements for the three selected regions during 2018 ( $\mu g/m^3$ ). The corresponding regional statistics are provided in Table 5. The site locations used are shown in each pane and taken from the EMEP, CASTNET and EANET networks, respectively.

For Southeast Asia (bottom panels), the simulated yearly mean  $[NH_4^+]$  over land are typically much higher than those simulated for either Europe or the U.S., with maximal values of between 7.0-9.0  $\mu g/m^3$  for eastern China, in spite of the similar surface mixing ratios in  $NH_3(g)$  between Europe and China as shown in Fig. 5. This difference is predominantly driven by the relatively high  $HNO_3(g)$  in China due to the more polluted chemical regime (the availability of  $O_3(g)$ ,  $NO_2(g)$  and  $OH(g)$  determining gas-phase  $HNO_3(g)$  production). Applying EQSAM4Clim in pre-CY49R1 results in significant decreases of between 1-2  $\mu g/m^3$   $[NH_4^+]$  as associated with the highest yearly mean  $[NH_4^+] > 6.0 \mu g/m^3$ . This reduces the associated yearly mean regional bias by 0.4  $\mu g/m^3$ , with a corresponding reduction in the correlation, due to less transport. Again, the lack of sampling sites in the region with high primary



Deleted:

Deleted: ... Comparisons of annual...early mean  $[NH_4^+]$  simulated at the surface in Cy48r1...Y48R1 and Cy4... [43]

Formatted: Normal5

Deleted: South-East...outheast Asia (bottom panels), the simulated annual...early mean  $[NH_4^+]$  over land are typically much higher than those simulated for either Europe or the U.S., with maximal values of between 7.0-9.0  $\mu g/m^3$  for Eastern...astern China, in spite of the similar surface mixing ratios in  $NH_3(g)$  between Europe and China as shown in Fig. 5. This difference is predominantly driven by the relat... [44]

Deleted: 39

Formatted: Normal5, Right: 0,63 cm

Formatted: Page Number

1331 NH<sub>3</sub>(g) emissions skews the associated yearly mean biases. For the more remote locations (e.g. Mongolia/South China  
1332 Sea) low values of < 0.5 µg/m<sup>3</sup> are captured well in both CY48R1 and pre-CY49R1.

### 1333 4.3 HNO<sub>3</sub> and NO<sub>3</sub><sup>-</sup>

1334 Figure 7 shows the monthly mean distributions and mixing ratios of HNO<sub>3</sub>(g) for July and December 2018 for the  
1335 three chosen global regions for CY48R1, along with the relative differences when compared with pre-  
1336 CY49R1 NOE4C and pre-CY49R1. The corresponding global chemical budget terms for HNO<sub>3</sub>(g) during 2018 are  
1337 provided in Table 6. No direct emission of HNO<sub>3</sub> occurs in IFS-COMPO, which is often prescribed in global  
1338 chemistry transport models to represent e.g. chemistry in the plumes of ships (e.g. Vinken et al., 2011), with the  
1339 main source being the oxidation of NO<sub>2</sub> by OH in the gas-phase as shown in Table 6. This production term increases  
1340 in pre-CY49R1 by approx. 14% because of the enhancements in OH via changes in O<sub>3</sub> (not shown). For  
1341 heterogeneous conversion, the cumulative HNO<sub>3</sub> production term is approximately 50% that of the gas-phase  
1342 production term, remaining relatively constant between simulations. There is a shift between fine mode NO<sub>3</sub><sup>-</sup>  
1343 (NH<sub>4</sub>NO<sub>3</sub>) and coarse mode NO<sub>3</sub><sup>-</sup> (CaNO<sub>3</sub>/NaNO<sub>3</sub>), strengthening the link between NH<sub>4</sub><sup>+</sup> and NO<sub>3</sub><sup>-</sup> in pre-CY49R1.  
1344 Both dry and wet loss terms increase significantly due to the increase in the availability of HNO<sub>3</sub>(g), which reduces  
1345 the fraction converted to NO<sub>3</sub><sup>-</sup>. The temporal variability of HNO<sub>3</sub>(g) is influenced by the magnitude and extent of  
1346 regional NO<sub>x</sub> emissions, photochemical activity (via OH formation), gas/aerosol partitioning (where particles with  
1347 high SO<sub>4</sub><sup>=</sup> content having an associated low NO<sub>3</sub><sup>-</sup> content) and scavenging in clouds and aerosols.

1348 For Europe very low surface mixing ratios occur over land for both months shown in CY48R1 (< 0.1 ppb), which  
1349 is surprising considering that the Benelux has been shown to have high NO<sub>x</sub> levels (van der A, 2024) therefore likely  
1350 to have correspondingly high HNO<sub>3</sub>(g) mixing ratios. Higher mixing ratios of between 0.25-0.5 ppb occur around  
1351 the Coasts and the Mediterranean originating from direct shipping emissions of NO<sub>2</sub>. This can lead to elevated NO<sub>3</sub><sup>-</sup>  
1352 concentration due to uptake of HNO<sub>3</sub>(g) on sea salt, which might be too high as the current formulation of  
1353 EQSAM4Clim only assumes thermodynamic equilibrium which is not dynamically limited. A coupling with a  
1354 dynamical aerosol model is foreseen for future versions of IFS-COMPO. In contrast, the application of  
1355 EQSAM4Clim in pre-CY49R1 results in large increases in surface HNO<sub>3</sub>(g) at continental scale during July. For  
1356 December, a strong latitudinal variability in the relative differences imposed in pre-CY49R1 occurs, with decreases  
1357 of between 25-75% in HNO<sub>3</sub>(g) at latitudes higher than 60°N due to lower temperatures and lower RH under a  
1358 relatively low NO<sub>x</sub> environment.

1359 For the U.S., the highest HNO<sub>3</sub>(g) mixing ratios in CY48R1 occur for the eastern states and California (1-2 ppb),  
1360 with much lower values in the more remote central U.S. (0.1-0.2 ppb), with a strong seasonal cycle in maximal  
1361 values peaking in July. Comparing relative differences between simulations shows a significant increase of surface  
1362 HNO<sub>3</sub>(g) in pre-CY49R1 (between 0.1-6 ppb) at continental scale for both months, with the largest increases  
1363 occurring in the northern States. In contrast to Europe no seasonal decreases occur for any location.

1364 Finally for Southeast Asia, the surface mixing ratios are the high across all regions, with maximal values being of  
1365 the order of 4-5 ppb towards the eastern coast (July) and central regions (c.f. December). Comparing the relative  
1366 differences between simulations shows significant increases of between 50-5000%, apart from the more remote  
1367 regions to the north where NO<sub>x</sub> emissions are lower. As for Europe, a strong seasonality can be seen with decreases  
1368 above 30°N occurring regardless of the NO<sub>x</sub> regime. As shown for NH<sub>3</sub> (c.f. Fig. 4), there are significant increases  
1369 in HNO<sub>3</sub> over the ocean for both months shown, associated with lower [NO<sub>3</sub><sup>-</sup>] (as shown by the cumulative reduction  
1370 in global conversion by 50%).

Formatted: Header

Deleted: annual

Deleted: Cy48r1

Deleted: Cy49r1

Deleted: regional distribution

Deleted: Cy48r1

Deleted: Cy49r1

Deleted: Cy49r1

Deleted: Cy49r1

Deleted: as a result

Deleted: approx

Deleted: IFS-COMPO

Deleted:

Deleted: Cy48r1

Deleted: .

Deleted: Cy49r1

Deleted: Cy49r1

Deleted: Cy48r1

Deleted: Eastern

Deleted: Central

Deleted: Cy49r1

Deleted: Northern

Deleted: South-East

Deleted: highest

Deleted: Eastern Coast

Deleted: Central

Deleted: with the exception of

Deleted: North

Deleted: 39

Formatted: Normal5, Right: 0,63 cm

Formatted: Page Number

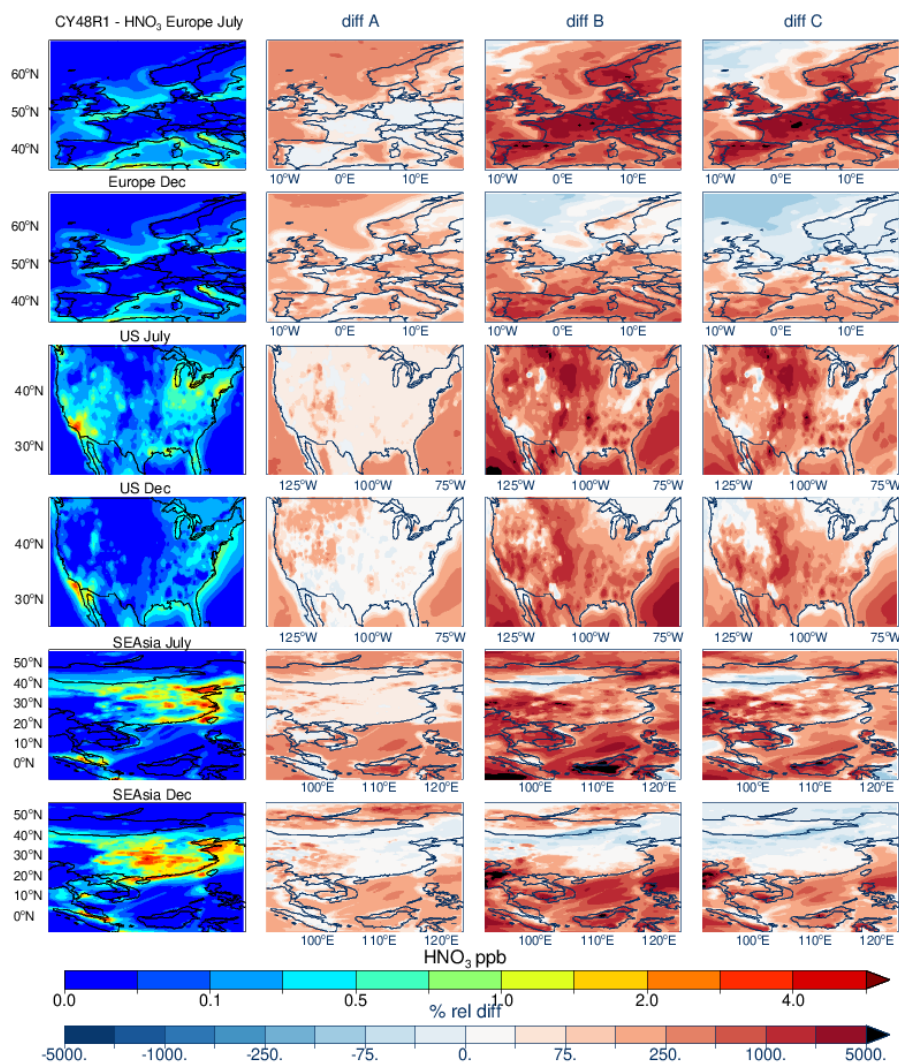


**Figure 7:** As for Fig. 1 except for HNO<sub>3</sub>. Panel definitions; Diff A = (pre-CY49R1\_NOEQ4C - CY48R1)/CY48R1; Diff B = (pre-CY49R1-CY48R1)/CY48R1 and Diff C = (pre-CY49R1-pre-CY49R1\_NOEQ4C)/CY48R1.

Figure 8 shows the resulting changes in surface [HNO<sub>3</sub>(g)] across simulations for Europe when compared against weekly means from the EMEP measurement sites (top left panel). The location of these sites is shown in Figure A1 in the Appendix, where the location of the sampling sites results in a significant bias in the evaluation towards northern Europe. No obvious seasonal cycle is evident in the observational weekly means, with concentrations in the range of 0.3-0.7 µg/m<sup>3</sup>, although many sites are located away from strong NO<sub>x</sub> sources. Both CY48R1 and pre-CY49R1\_NOEQ4C exhibit negative weekly biases resulting in under-estimations of around 100% in concentrations during the summertime, although the weekly variability is captured to a degree. There is a reduction in the bias of around 0.2-0.4 µg/m<sup>3</sup> in pre-CY49R1\_NOEQ4C due to changes in the gas-phase production term (c.f. Table 8). For

Deleted:

Deleted: Cy49r1

Deleted: - Cy48r1)/Cy48r1

Deleted: Cy49r1-Cy48r1)/Cy48r1

Deleted: Cy49r1-Cy49r1

Deleted: Cy48r1

Deleted: composites assembled

Deleted: Northern

Deleted: Cy48r1

Deleted: Cy49r1

Deleted: 1

Deleted: Cy49r1

Deleted: showing that the other changes made between IFS cycles cause

Deleted: in addition to the changes in NH<sub>4</sub>NO<sub>3</sub> from EQSAM4Clim

Deleted: 39

Formatted: Normal5, Right: 0,63 cm

Formatted: Page Number



pre-CY49R1 there is a significant excess of [HNO<sub>3</sub>(g)] due to enhanced production and less transfer into the particulate phase, despite an increase in the cumulative deposition terms. Such changes are associated with relatively low [HNO<sub>3</sub>(g)] IFS-COMPO values of around < 0.1 ppb.

**Table 6:** The tropospheric HNO<sub>3</sub> budget in Tg N/year for 2018 as calculated by CY48R1, pre-CY49R1 NOE4C and pre-CY49R1, with the associated percentage differences being provided in parentheses as e.g. ((pre-CY49R1-CY48R1)/CY48R1)\*100.

Process	CY48R1	pre-CY49R1 NOE4C	pre-CY49R1
NO <sub>2</sub> + OH → HNO <sub>3</sub>	11.0	11.6 (+5)	12.6 (+14)
N <sub>2</sub> O <sub>5</sub> + Liq → HNO <sub>3</sub>	2.2	2.5 (+12)	2.6 (+17)
N <sub>2</sub> O <sub>5</sub> + Aer → HNO <sub>3</sub>	3.2	2.3 (-28)	2.3 (-27)
NO <sub>3</sub> + Aer → HNO <sub>3</sub>	0.8	0.4 (-47)	0.5 (-42)
HNO <sub>3</sub> → Fine NO <sub>3</sub> -	1.4	1.2 (-18)	2.0 (+41)
HNO <sub>3</sub> → Coarse NO <sub>3</sub> -	9.3	5.9 (-36)	3.6 (-61)
Dry Deposition	2.0	2.4 (+17)	5.1 (+150)
Wet Deposition	6.8	5.9 (-13)	9.3 (+38)
Trop. Burden	0.31	0.30 (-3)	0.32 (+3)

Figure 8 also shows comparisons of weekly [HNO<sub>3</sub>(g)] from the CASTNET measurement network in the U.S. (op right panel). As for Europe, both the concentrations and seasonal variability in the observations is low, with typical weekly concentrations being approximately 0.5 µg/m<sup>3</sup>. The homogeneous distribution of measurement sites in the U.S. means the evaluation presented does not have any significant regional bias. That the observed weekly mean concentrations are rather constant is surprising considering that variability in the gas-phase chemical production term involves OH. However, changes in RH, temperature and NH<sub>3</sub>(g) across seasons also contribute to the seasonal lifetime. In contrast to Europe, both CY48R1 and pre-CY49R1 NOE4C show good agreement against the measurements with weekly biases of the order of 0.2-0.25 µg/m<sup>3</sup>. However, for pre-CY49R1 a large positive bias is introduced directly from the use of EQSAM4Clim due to a limitation in the ability for HNO<sub>3</sub> to condense on particle surfaces. This means that condensed HNO<sub>3</sub> does not contribute to NH<sub>4</sub>NO<sub>3</sub> formation (which requires a coupling of EQSAM4Clim with an aerosol dynamical model as e.g., described in Metzger et al., 2018), which is proposed for future cycles of IFS-COMPO. It also shows that although the cumulative global dry and wet deposition terms in pre-CY49R1 have increased markedly compared to CY48R1 (c.f. Table 6), fluxes are not large enough to compensate for the reduced aerosol formation.

Figure 8 also shows the corresponding changes in surface [NO<sub>3</sub>·] for Europe (bottom left panel). The observational composites show that [NO<sub>3</sub>·] has concentrations almost twice those of the corresponding [HNO<sub>3</sub>(g)] during wintertime. For summertime there is almost an equal split in the phase partitioning between precursor and SIA. Unlike for HNO<sub>3</sub>(g), a shallow concave seasonal cycle exists in the weekly observational composites, related to seasonal differences in temperatures and lifetime (Tang et al., 2021). Both CY48R1 and pre-CY49R1 NOE4C fail to capture the correct seasonality and exhibit higher concentrations during summertime, resulting in substantial positive biases of 1-2 µg/m<sup>3</sup>. Considering the associated biases in [HNO<sub>3</sub>(g)] shows that the HNO<sub>3</sub>-NO<sub>3</sub>· partitioning is not captured well. For pre-CY49R1 the description of the seasonal cycle is significantly improved due to the inclusion of EQSAM4Clim, resulting in much lower biases of < 0.5 µg/m<sup>3</sup> throughout the year, also pointing to the importance of a better representation of gas/particle partitioning. The corresponding changes in [NO<sub>3</sub>·] in the simulations are evaluated against weekly composites from the CASTNET measurement network, are shown in the bottom right panel of Fig. 8. A similar seasonal cycle exists as for Europe with similar concentrations. For CY48R1 and pre-CY49R1 NOE4C an inverse seasonal variability occurs in [NO<sub>3</sub>·] as compared with the observational weekly means, resulting in significant positive biases of around 1.0-1.5 µg/m<sup>3</sup>. For pre-CY49R1

Formatted: Header

Deleted: Cy49r1...re-CY49R1 there is a significant excess of [HNO<sub>3</sub>(g)] due to enhanced production and less transfer into the particulate phase, in spite of ... [45]

Deleted: ...udget in Tg N/year for 2018 as calculated by Cy48r1, Cy49r1...Y48R1, pre-CY49R1 NOE4C and Cy49r1...re-CY49R1, with the associated percentage differences being provided in parentheses as e.g. ((Cy49r1-Cy48r1)/Cy48r1)\*100. ... [46]

Formatted: Subscript

Deleted: Cy48r1

Deleted: Cy49r1\_NOEQ4Clim

Deleted: Cy49r1

Formatted Table

Formatted: Normal5

Formatted: Normal5

Formatted: Normal5

Formatted: Normal5

Formatted: Normal5

Formatted: Normal5

Formatted: Normal5

Formatted: Normal5

Formatted: Normal5

Formatted: Normal5

Deleted: US are shown in the top....S. (op right panel.... As for Europe, both the concentrations and seasonal variability in the observations is low, with typical weekly concentrations being around ±0...approximately 0.5 µg/m<sup>3</sup>. The rather equal...omogeneous distribution of measurement sites in the U.S....S. means the evaluation presented does not have any significant regional bias. That the measured...bserved weekly mean concentrations are rather constant is surprising considering that variability in the gas-phase chemical production term involves OH, which has strong seasonality from the differences... However, changes day length...H, temperature and NH<sub>3</sub>(g) across seasons also contribute to the seasonal lifetime. In contrast to Europe, both Cy48r1...Y48R1 and Cy49r1...re-CY49R1\_NOE4C show good agreement against the measurements with weekly biases of the order of 0.2-0.25 µg/m<sup>3</sup>. However, for Cy49r1...re-CY49R1 a large positive bias is introduced by...irectly from the use of EQSAM4Clim due to a limitation in the ability for HNO<sub>3</sub> to condense on particle surfaces, such... This means that condensed HNO<sub>3</sub> does not contribute to NH<sub>4</sub>NO<sub>3</sub> formation (which requires a coupling of EQSAM4Clim with an aerosol dynamical model as e.g., described in Metzger et al., 2018)...., which is proposed for future cycles of IF... [47]

Deleted: The bottom left panel of ...figure 8 also shows the corresponding changes in surface [NO<sub>3</sub>·] as shown for ... [48]

Deleted: 39

Formatted: Normal5, Right: 0,63 cm

Formatted: Page Number



biases decrease by an order of magnitude and the seasonal variability is improved markedly, again showing improved particle distribution when using EQSAM4Clim.

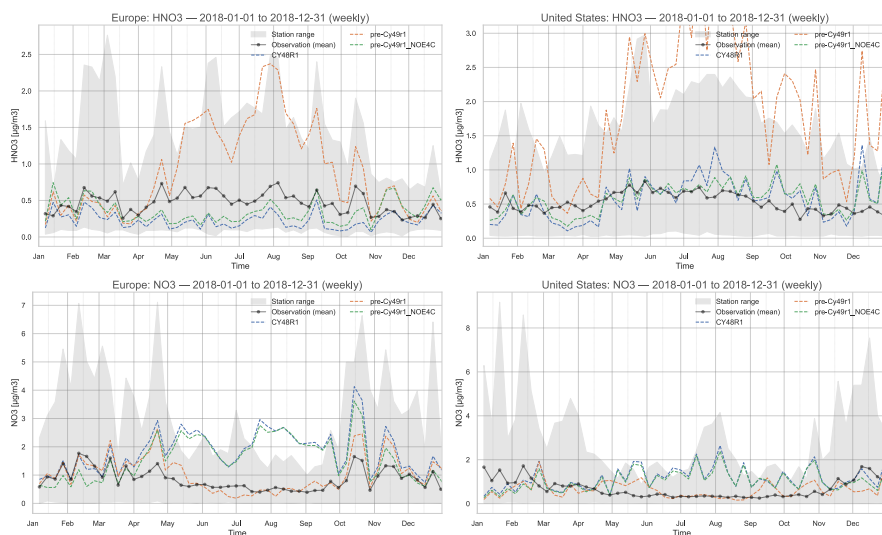
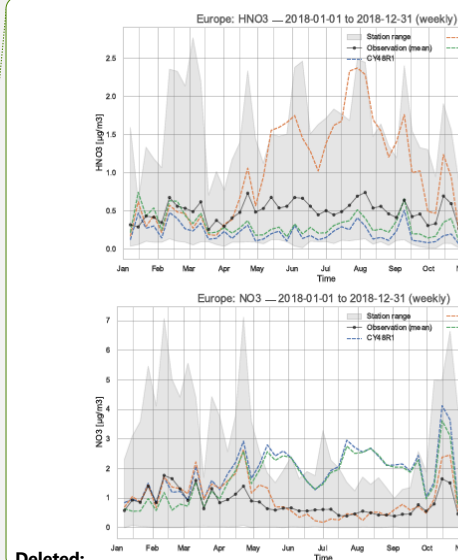


**Figure 8:** A comparison of weekly mean  $[\text{HNO}_3(\text{g})]$  and  $[\text{NO}_3^-]$  for Europe (left panels;  $\mu\text{g}/\text{m}^3$ ) and the U.S. (right panels) at the surface as simulated in IFS-COMPO as compared against measurement composites from EBAS (left) and CASTNET (right) stations for 2018. The various simulations are defined within the panels, and the grey band represents the variability in the measurement values across stations.

In Figure 9 we show the corresponding regional distributions of the yearly mean  $[\text{NO}_3^-]$  for CY48R1 and pre-CY49R1 during 2018 for the three chosen global regions, where the associated changes in the regional yearly mean statistics are provided in Table 7. Some commonality exists between the changes shown for yearly mean  $[\text{NH}_4^+]$  and yearly mean  $[\text{NO}_3^-]$ , due to the speciation of the SIA involved. The cumulative sums of the smaller  $\text{NO}_3^-$  particle (fine mode  $\text{NO}_3^-$  in Table 6 with the form  $\text{NH}_4(\text{NO}_3)$ ) and the larger  $\text{NO}_3^-$  particle (coarse mode  $\text{NO}_3^-$  in Table 6 with the form of  $\text{CaNO}_3$  and  $\text{NaNO}_3$ ) are both included in the plots. Therefore, the changes evaluated here are a combination of changes to both the fine and coarse mode  $\text{NO}_3^-$ , rather than the changes associated with individual particle sizes. In contrast to the reduced N analysis provided above, which is impacted more directly due to changes in the fine mode  $\text{NO}_3^-$ , with  $[\text{NO}_3^-]$  also indirectly affected by the coarse mode assumptions through the effect of cations on the neutralisation level that subsequently controls the gas/aerosol equilibrium partitioning. The change in the partitioning for  $\text{HNO}_3$  shown above results in an associated reduction in the fraction of  $\text{NO}_3^-$  held in particulate form due to e.g. a higher dry deposition component.

For Europe, the simulated yearly mean  $[\text{NO}_3^-]$  in CY48R1 generally ranges between  $0.2\text{--}2.0 \mu\text{g}/\text{m}^3$  over Scandinavia/Spain and the surrounding seas and between  $2.0\text{--}6.3 \mu\text{g}/\text{m}^3$  over North-Western/Central Europe and the Mediterranean, becoming lower towards the northeast and southwest. The highest European  $\text{NO}_x$  emissions occur around the southeast of the UK, Benelux, the Ruhr, and Po valleys (e.g. Liu et al., 2021; van der A., 2024). This, and the rather homogeneous distribution within central Europe shows that a significant degree of transport occurs once  $\text{NO}_3^-$  particles are formed. No such continental gradient in the yearly mean  $[\text{NO}_3^-]$  exists in the observational mean values indicating an overestimate in IFS-COMPO. Nevertheless, in pre-CY49R1 decreases in  $[\text{NO}_3^-]$  of between  $2\text{--}4 \mu\text{g}/\text{m}^3$  occur for the Baltic states/France/Germany and over the Mediterranean Sea (from relatively high shipping  $\text{NO}_x$  emissions) compared to CY48R1. This results in much better agreement with the yearly mean observed values for the individual measurement stations. The yearly regional MB is reduced by  $\approx 90\%$ , decreasing to  $0.1 \mu\text{g}/\text{m}^3$  in pre-CY49R1 with an associated increase in the correlation coefficient due to lower transport of  $[\text{NO}_3^-]$  out of the main source region. A large impact occurs due to the acidification of sea salt

Formatted: Header



Deleted:

Deleted:

Deleted: ... $\text{NO}_3^-$  ...or Europe (left panels;  $\mu\text{g}/\text{m}^3$ ) and the US... [49]

Formatted: Font: Bold

Formatted: Normal5

Deleted: annual...early mean  $[\text{NO}_3^-]$  for Cy48r1...Y48R1 and Cy49r1...re-CY49R1 during 2018 for the three ch... [50]

Deleted: annual...early mean  $[\text{NO}_3^-]$  in Cy48r1...Y48R1 generally ranges between  $0.2\text{--}2.0 \mu\text{g}/\text{m}^3$  over... [51]

Deleted:

Deleted: Cy48r1

Formatted: Font: Times New Roman

Formatted: Font: Times New Roman

Formatted: Font: Times New Roman

Deleted: annual

Deleted: annual

Formatted: Font: Times New Roman

Formatted: Font: Times New Roman

Deleted:

Deleted: Cy49r1

Formatted: Font: Times New Roman

Deleted: 39

Formatted: Normal5, Right: 0,63 cm

Formatted: Page Number

aerosols under high  $\text{NO}_x$  emission from dense shipping lanes, which can be seen by similar  $[\text{NO}_3^-]$  reductions over the sea, though difficult to evaluate due to the lack of sufficient *in-situ* measurements.

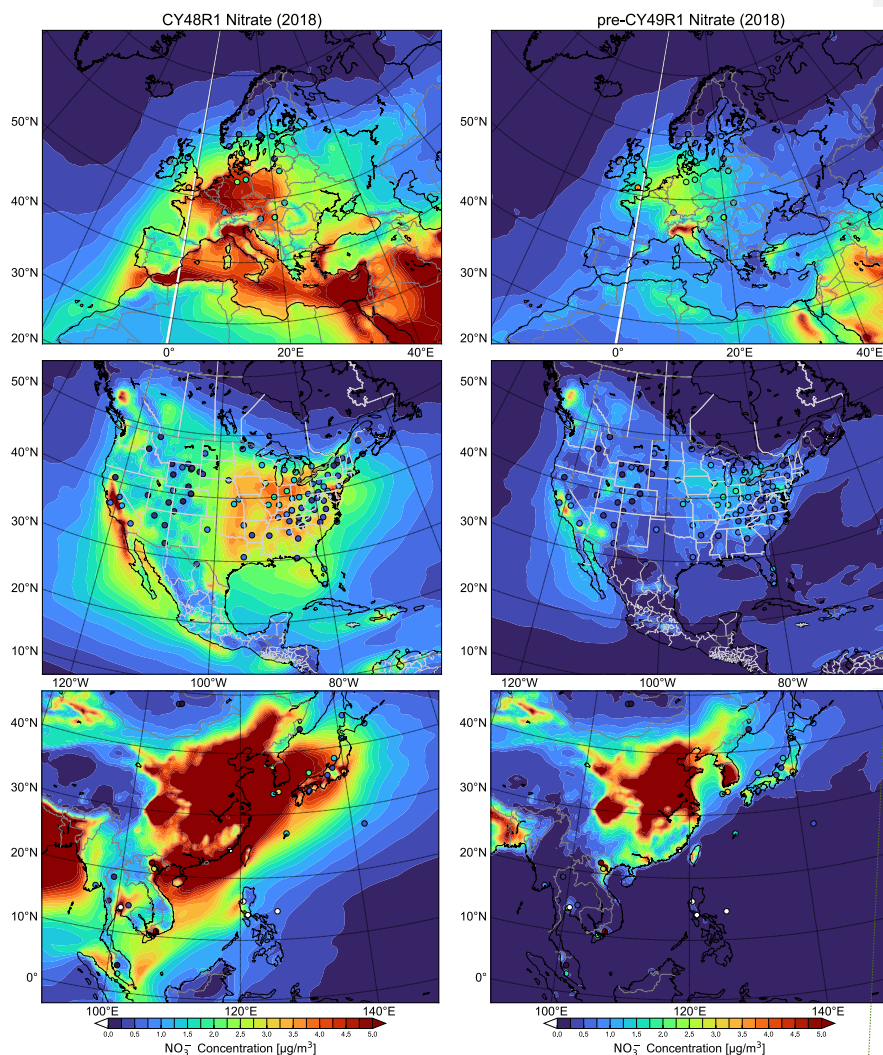
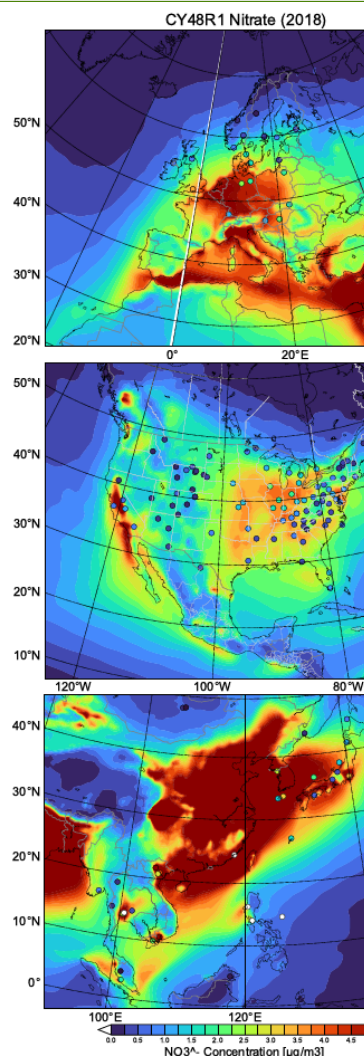


**Figure 9:** Comparisons surface comparisons of  $[\text{NO}_3^-]$  simulated in CY48R1 and pre-CY49R1 as compared against measurements for the three selected regions given in  $\mu\text{g}/\text{m}^3$ . The corresponding regional statistics are provided in Table 7. The site locations used are shown in each pane and taken from the EMEP, CASTNET and EANET networks, respectively.

For the U.S., there is a similar impact on  $[\text{NO}_3^-]$  as shown for Europe, where the high yearly MB in  $[\text{NO}_3^-]$  decreases significantly (94%) from CY48R1 to pre-CY49R1 (bottom right panel of Fig. 8). For CY48R1,  $[\text{NO}_3^-]$  typically ranges between 2-4  $\mu\text{g}/\text{m}^3$  with medium-range transport resulting in appreciable concentrations over the surrounding oceans. There is surprisingly little variability in the observed yearly mean  $[\text{NO}_3^-]$  despite the large difference in the resident  $[\text{HNO}_3(\text{g})]$  across different states of the U.S. related to the distribution of the  $\text{NO}_x$

Formatted: Header

Deleted: relatively



Deleted:

Deleted: Cy48r1...Y48R1 and Cy49r1...re-CY49R1 as compared against measurements for the three selected regions given in  $\mu\text{g}/\text{m}^3$ . The corresponding ... [52]

Formatted: Normal5

Deleted: annual...early MB in  $[\text{NO}_3^-]$  decreases significantly (94%) from Cy48r1...Y48R1 to Cy49r1...re-CY49R1 (bottom right panel of Fig. 8). For Cy48r1...Y48R1,  $[\text{NO}_3^-]$  typically ranges between 2-4  $\mu\text{g}/\text{m}^3$  with medium-range transport resulting in appreciable concentrations over the surrounding oceans. Considering the precursors, ... [53]

Deleted: 39

Formatted: Normal5, Right: 0,63 cm

Formatted: Page Number

emissions (Figure 7; Goldberg et al., 2021). Only in the southwest, around California, the yearly mean  $[\text{NO}_3^-] > 2.0 \mu\text{g}/\text{m}^3$ , shows typical yearly mean  $[\text{NO}_3^-]$  being  $\leq 1.0 \mu\text{g}/\text{m}^3$  in pre-CY49R1 for most of the U.S. This implies that the cations used as input for EQSAM4Clim imposes a limit concerning the phase-transfer of  $\text{HNO}_3(\text{g})$  into more acidic aerosols via neutralisation of the anions by cations in the particle phase.

**Table 7:** As for Table 3 except for  $\text{NO}_3^-$ .

	Europe (EMEP)		US (CASTNET)		SE Asia (EANET)	
$\text{NO}_3^-$	CY48R1	pre-CY49R1	CY48R1	pre-CY49R1	CY48R1	pre-CY49R1
MB ( $\mu\text{g}/\text{m}^3$ )	0.95	0.10 (-90)	1.71	0.10 (-94)	2.68	-0.16 (-94)
RMSE	2.37	1.60 (-32)	2.20	0.83 (-62)	3.62	1.41 (-61)
Pearsons R	0.41	0.58 (+29)	0.31	0.57 (+46)	0.65	0.52 (-20)

## 5 The changes in regional wet deposition

In this section, we evaluate the temporal distribution and biases associated with the yearly wet deposition terms of soluble trace gas species and particulates. All three SIA are lost to the surface by both dry and wet deposition processes. Over the last decades the main source of acidification has shifted from  $\text{SO}_x$  based to  $\text{NO}_x$  based in line with the reduction measures imposed for  $\text{SO}_x$  and the increase and associated emission changes from e.g. road transport. Here we evaluate whether pre-CY49R1 captures the correct wet scavenging and improves on the performance of CY48R1 for the various dissolved precursors and SIA. Evaluations are made using comparisons of model output against yearly wet deposition totals as taken from the observational networks introduced in Sect. 3. The concentrations of the dissolved precursors (i.e.  $\text{SO}_2(\text{aq})$ ,  $\text{NH}_3(\text{aq})$  and  $\text{HNO}_3(\text{aq})$ ) also undergo wet deposition (in IFS-COMPO) and cannot be differentiated well in the observational networks and are therefore included in the measured totals. The wet deposition term is also influenced by meteorological parameters such as the simulated large-scale and convective mixing, liquid and solid precipitation droplet size, SAD, and the frequency and intensity of precipitation as provided by the IFS model.

The changes in the global tropospheric burden, lifetime, dry and wet deposition totals for  $\text{SO}_4^{2-}$ ,  $\text{NH}_4^+$ ,  $\text{NO}_3^-$  (fine) and  $\text{NO}_3^-$  (coarse) during 2018 are given in Table 8. The corresponding statistics for the changes in wet deposition between CY48R1 and pre-CY49R1 as compared against yearly observational means yearly for  $\text{SO}_x$ , reduced N and oxidised N are provided for the three chosen global regions in Table 9.

**Table 8:** The global budget values for the burden, tropospheric lifetime, wet and dry deposition terms for  $\text{SO}_4^{2-}$ ,  $\text{NH}_4^+$  and  $\text{NO}_3^-$  for 2018. Totals are provided in Tg S/year and Tg N/year. Percentage difference changes are calculated as  $((\text{pre-CY49R1}-\text{CY48R1})/\text{CY48R1}) * 100$  and given in parentheses.

	CY48R1	pre-CY49R1 NOE4C	pre-CY49R1
$\text{SO}_4^{2-}$			
Burden	0.4	0.6 (+30)	0.6 (+30)
Lifetime (days)	3.4	4.4 (+29)	4.4 (+29)
Dry dep	5.8	5.4 (-7)	5.4 (-7)
Wet dep	43.1	43.9 (+2)	44.2 (+3)
$\text{NH}_4^+$			
Burden	0.3	0.4 (+32)	0.2 (-33)
Lifetime (days)	3.5	4.6 (+34)	4.1 (+18)
Dry dep	5.1	5.1 (-)	1.8 (-64)
Wet dep	27.5	27.1 (-2)	20.1 (-40)

Formatted: Header

Deleted: annual

Deleted: annual

Deleted: Cy49r1

Deleted: the majority

Formatted: Font: Times New Roman

Deleted:

Formatted Table

Deleted: Cy48r1

Deleted: Cy49r1

Deleted: Cy48r1

Deleted: Cy49r1

Deleted: Cy48r1

Formatted: Normal5

Deleted: Cy49r1

Formatted: Normal5

Formatted: Normal5

Deleted: ¶

In Table 8, the

In Table 8, the

In Table 8, the

In Table 8, the

Deleted: In Table 8, the

Deleted: across all simulations

Deleted: comparison with observations for the

Deleted: annual

Deleted: of

Deleted: ..

Deleted: are

Deleted: Cy49r1-Cy48r1/Cy48r1)\*

Deleted: Cy48r1

Deleted: Cy49r1

Deleted: Cy49r1

Formatted Table

Formatted: Normal5

Formatted: Normal5

Formatted: Normal5

Formatted: Normal5

Deleted: 39

Formatted: Normal5, Right: 0,63 cm

Formatted: Page Number

	<a href="#">CY48R1</a>	<a href="#">pre-CY49R1</a> NOE4C	<a href="#">pre-CY49R1</a>
NO <sub>3</sub> <sup>-</sup> (fine)			
Burden	0.01	0.01 (-)	0.02 (+86)
Lifetime (days)	4.9	5.4 (+12)	6.1 (+25)
Dry dep	0.2	0.2 (-21)	0.1 (-32)
Wet dep	0.6	0.5 (-13)	1.0 (+64)
NO <sub>3</sub> <sup>-</sup> (coarse)			
Burden	0.01	0.01 (-)	0.01 (-)
Lifetime (days)	3.4	3.8 (+11)	2.4 (-29)
Dry dep	1.5	2.5 (+73)	1.2 (-18)
Wet dep	3.5	2.8 (-20)	0.7 (-79)

**Table 9:** The [yearly](#) MB, RMSE and Pearson's R values for the comparisons of the [yearly](#) mean regional wet deposition totals of dissolved SO<sub>2</sub>+SO<sub>4</sub><sup>2-</sup>, NH<sub>3</sub>+NH<sub>4</sub><sup>+</sup> and HNO<sub>3</sub>+NO<sub>3</sub><sup>-</sup> as compared against composites assembled from the regional observation networks for 2018 shown in Figures 9-11 for Europe, the U.S. and [Southeast Asia](#). Percentage difference changes are calculated as  $((\text{pre-CY49R1}-\text{CY48R1})/\text{CY48R1}) * 100$  and given in parentheses.

	Europe (EMEP)		US (CASTNET)		SE Asia (EANET)	
	<a href="#">CY48R1</a>	<a href="#">pre-CY49R1</a>	<a href="#">CY48R1</a>	<a href="#">pre-CY49R1</a>	<a href="#">CY48R1</a>	<a href="#">pre-CY49R1</a>
SO <sub>x</sub>						
MB (mgS/m <sup>2</sup> /yr)	-42	-38 (-9)	137	190 (+39)	-44.2	8.7 (-80)
RMSE	88.2	85 (-3)	203	270 (+33)	447	500.3 (+12)
Pearsons R	0.55	0.58 (+6)	0.68	0.66 (-3)	0.72	0.65 (-10)
Reduced N						
MB (mgN/m <sup>2</sup> /yr)	61	25.9 (-58)	8.4	6.8 (-21)	12	-44 (+260)
RMSE	114	93.4 (-18)	76.0	81.3 (+7)	318	302 (-5)
Pearsons R	0.69	0.68 (-1.4)	0.77	0.72 (-16)	0.75	0.71 (-1)
Oxidised N						
MB (mgN/m <sup>2</sup> /yr)	9.7	-1.4 (-86)	130	99.7 (-23)	142	98.3 (-31)
RMSE	69	72 (+4)	153	122.6 (-20)	324	274.3 (-15)
Pearsons R	0.50	0.47 (-6)	0.86	0.85 (-1)	0.67	0.68 (+2)

## 5.1 Total [yearly](#) wet S deposition

Figure 10 shows the regional distribution and values of [yearly](#) wet S deposition for Europe, the U.S., and [Southeast Asia](#) in both [CY48R1](#) and [pre-CY49R1](#) during 2018. To allow a direct comparison across regions we use a colour scale which covers values larger than 500 mgS/m<sup>2</sup>/year in [Southeast Asia](#). The global budget terms for SO<sub>4</sub><sup>2-</sup> are presented in Table 8 and show that, [despite](#) the global burden increasing by one third, only very small increases of a few percent occur in the [yearly](#) wet SO<sub>4</sub><sup>2-</sup> totals (Rémy et al., 2024), [with associated decreases in the dry deposition term](#). The significant increase in the tropospheric SO<sub>4</sub><sup>2-</sup> lifetime means more remains in the aerosol phase and will [increase both AOD and](#) the degree of scattering in IFS-COMPO as shown for AOD comparisons in [Rémy et al. \(2024\)](#). The most significant change is in the direct gas-phase production term of H<sub>2</sub>SO<sub>4</sub>(g), where increases in [SO<sub>2</sub>(g)] subsequently increase the total mass scavenged into aqueous cloud droplets. This results in

Formatted [54]

Deleted: Cy48r1

Deleted: Cy49r1

Deleted: Cy49r1

Formatted Table [57]

Formatted [58]

Formatted [59]

Formatted [60]

Formatted [61]

Formatted [62]

Deleted: annual

Deleted: weekly

Deleted: South-East

Deleted: Cy49r1-Cy48r1)/Cy48r1)\*

Formatted Table [63]

Deleted: Cy48r1

Deleted: Cy49r1

Formatted [64]

Deleted: Cy48r1

Deleted: Cy49r1

Deleted: Cy48r1

Deleted: Cy49r1

Formatted [65]

Formatted [66]

Formatted [67]

Formatted [68]

Formatted [69]

Formatted [70]

Deleted: annual

Deleted: annual

Deleted: .

Deleted: South-East

Deleted: Cy48r1

Deleted: Cy49r1

Deleted: South-East

Deleted: in spite of

Deleted: annual

Deleted: ). However, the

Deleted: impact

Deleted: Remy

Deleted: 39

Formatted [56]

Formatted [55]



Formatted: Header

an extent of acidification (slowing in-situ oxidation; c.f. Table 2), which is buffered by the increased phase transfer of  $\text{NH}_3(\text{g})$  (c.f. Table 4). These changes are the result of updates to the scavenging approach rather than the application of EQSAM4Clim. Although there is a 16% reduction in the total global  $\text{SO}_2(\text{aq})$  wet deposition (c.f. Table 2), this is compensated for by increases in  $[\text{SO}_4^{2-}(\text{aq})]$  which results in an increase in the cumulative wet S deposition yearly totals.

For Europe (top panels), the changes between model simulations are like the changes in the  $\text{SO}_2(\text{g})$  and  $\text{SO}_4^{2-}$  particle concentrations discussed in Sect. 4. Compared against the yearly mean observational values from EMEP, which range from 100–500  $\text{mgS/m}^2/\text{year}$ , there is an underestimation in CY48R1 of approximately 100  $\text{mgS/m}^2/\text{year}$  for northwest Europe. For the observational means in Ireland, Poland, northern Spain and on the Iberian Peninsula negative MB are enhanced to around 300  $\text{mgS/m}^2/\text{year}$ . This indicates missing local source terms in the global emission inventory provided as monthly mean fluxes. For other regions, the agreement is satisfactory capturing the observed deposition gradient from Germany into Austria/northern Italy. For pre-CY49R1, strong similarity exists for Benelux, Denmark, and Italy, where negative biases of around 50–100  $\text{mgS/m}^2/\text{year}$  occur. A significant negative yearly MB exists in Europe, which decreases by around 10% in pre-CY49R1 (c.f. Table 9) with a marginal increase in the correlation. Considering the associated positive MB for aerosol  $\text{SO}_4^{2-}$  shown during summertime (c.f. Figure 2), there is an indication that not enough phase transfer occurs, thus negative MB values for the yearly deposition totals, and the large observational means at selected stations influencing the regional yearly mean.

For the U.S. (middle panels) there is a stark contrast to the changes shown for Europe. Analysis of the yearly observational yearly mean values from CASTNET shows that a gradient exists in the wet deposition yearly totals from east to west, similar to that for  $\text{SO}_2(\text{g})$  and the location of primary  $\text{SO}_2$  emission sources (c.f. Fig. 1). Maximal values of 300–400  $\text{mgS/m}^2/\text{year}$  occur towards the east coast where a positive MB occurs for  $[\text{SO}_4^{2-}]$  (c.f. Fig. 3). For CY48R1, this gradient in yearly wet deposition is captured to a large degree, albeit with significant positive biases of > 100  $\text{mgS/m}^2/\text{year}$  with a maximal range of 700–900  $\text{mgS/m}^2/\text{year}$ . There is a significant yearly wet deposition of  $\text{SO}_x$  in the Atlantic (250–400  $\text{mgS/m}^2/\text{year}$ ) due to the local oxidation of DMS (released from the ocean) and the long-range transport of  $\text{SO}_2(\text{g})/\text{SO}_4^{2-}$  from the anthropogenic source regions. In pre-CY49R1 the area of maximal wet S deposition increases around, e.g., New York State extending south to Texas resulting in an increase in the positive yearly MB for the U. S. by nearly 40% (to 190  $\text{mgS/m}^2/\text{year}$ ). This contrasts with the significant improvement in the yearly MB for  $[\text{SO}_4^{2-}]$  given in Table 3, which provides the continental mean rather than statistics for the east coast. The changes are determined by changes in the scavenging of  $\text{SO}_4^{2-}$  particles into the aqueous phase, with the application of EQSAM4Clim having a minor influence (Table 8).

Finally for Southeast Asia (bottom panels), the magnitude of EANET yearly wet depositional totals show that more than twice the amount of S deposition occurs as measured in either Europe or the U.S. over an identical period and a much wider area, reaching 1200–1300  $\text{mgS/m}^2/\text{year}$  in central and eastern China (not shown). The spatial distribution of stations shows that a negative gradient exists between deposition totals in China and those extending towards Myanmar (west) and Japan (east) (2000–2200  $\text{mgS/m}^2/\text{year}$ ; not shown). This indicates the importance of the transport component of  $\text{SO}_4^{2-}$  when considering the low regional  $\text{SO}_2(\text{g})$  precursor mixing ratios around the equator (c.f. Fig. 1), and that the primary sources are typically infrequent volcanic eruptions for the region between 5°N–5°S (Fioletov et al., 2020) that typically inject the  $\text{SO}_2$  above the boundary layer (thus with a limited impact on the surface values). Towards the coast of eastern China and Japan, the observations show yearly totals of 250–350  $\text{mgS/m}^2/\text{year}$ , in contrast to high values near the middle of China. Such local scale variability is not captured using the current emission inventory that is employed, where the positive MB increases significantly in pre-CY49R1 using the same observational stations and emission estimates (c.f. Table 3). The extent of high wet deposition values reaches hundreds of kilometres from the coast far away from prescribed emission sources. The regional yearly MB improves markedly to 8.7  $\text{mgS/m}^2/\text{year}$  in pre-CY49R1 despite increases in the MB and decreases in the Pearson's R value for  $[\text{SO}_4^{2-}]$  (Table 3).

**Deleted:** somewhat ...ffered by the increased phase transfer of  $\text{NH}_3(\text{g})$  (c.f. Table 4). These changes are the result of updates to the scavenging approach rather than the application of EQSAM4Clim. Although there is a 15...6% reduction in the total global  $\text{SO}_2(\text{aq})$  wet deposition, the (c.f. Table 2), this is compensated for by increases in  $[\text{SO}_4^{2-}(\text{aq})]$  which results in an increase in the cumulative wet S deposition annual

**Deleted:** similar to...like the changes in the  $\text{SO}_2(\text{g})$  and  $\text{SO}_4^{2-}$  particle concentrations discussed in Sect. 4 ... Compared against the annual EMEP...early mean observational values from EMEP, which range from 100–900...00  $\text{mgS/m}^2/\text{year}$ , there is generally ...n underestimation in Cy48r1...Y48R1 of approx...pproximately 100–150... $\text{mgS/m}^2/\text{year}$  for North-West...orthwest Europe, ... For the observational means in Ireland, Poland, northern Spain and on the Iberian Peninsular...eninsula negative MB are enhanced to around 300  $\text{mgS/m}^2/\text{year}$ . This indicates missing local source terms in the global emission inventory provided as monthly mean fluxes. For other regions, the agreement is quite good...atisfactory capturing the observed deposition gradient from Germany into Austria/Northern...orthern Italy. A limited number of measurement stations exhibit very high localised values (e.g. South-West Ireland, Palma), indicating missing primary emission sources in the global inventory. For Cy49r1...re-CY49R1, strong similarity exists for Denmark, and Italy, where negative biases of around 50–100  $\text{mgS/m}^2/\text{year}$  occur. A significant negative annual...early MB exists in Europe, which decreases by around 10% in Cy49r1...re-CY49R1 (c.f. Table 9) with a marginal increase in the correlation. This is impacted by...onsidering the associated negative...ositive MB for  $\text{SO}_2(\text{g})$  ...erosol  $\text{SO}_4^{2-}$  shown during summertime (c.f. Figure 2) ..., there is an indication that not enough phase transfer occurs, thus negative MB values for the yearly deposition totals, and the large values observed

**Deleted:** Assessing...analysis of the annual...early observational yearly mean ...values from CASTNET shows that an observational ... gradient exists in the wet deposition annual...early totals from east to west, similar as...o that for  $\text{SO}_2(\text{g})$  and the location of primary  $\text{SO}_2$  emission sources (c.f. Fig. 1), with maximal... Maximal values reaching...f 300–400  $\text{mgS/m}^2/\text{year}$  occur towards the East Coast. For Cy48r1...ast coast where a positive MB occurs for  $[\text{SO}_4^{2-}]$  (c.f. Fig. 3). For CY48R1, this gradient in yearly wet deposition is captured well...o a large degree, albeit with large...significant positive biases of > 100  $\text{mgS/m}^2/\text{year}$ , resulting in ...with a maximal range of 700–900  $\text{mgS/m}^2/\text{year}$ . There is a significant annual...early wet deposition of  $\text{SO}_x$  in the Atlantic (250–300...00  $\text{mgS/m}^2/\text{year}$ ) due to the local oxidation of DMS (released from the ocean) and the l...

**Deleted:** South-East...outheast Asia (bottom panels), the magnitude of EANET annual...early wet depositional totals show that more than twice the amount of S deposition occurs as measured in either Europe or the U.S. over an identical timeframe...eriod and a much wider area, reaching 1200–1300  $\text{mgS/m}^2/\text{year}$  in Central...entral and eastern Chir...

Formatted: Normal5, Space After: 10 pt

Deleted: 39

Formatted: Normal5, Right: 0,63 cm

Formatted: Page Number

Formatted: Header

**Deleted:** Towards the Coast of Eastern China the observations show annual totals of 250-350 mgS/m<sup>2</sup>/year, in contrast to high values near the middle of China. This is surprising, considering that high SO<sub>2</sub> emissions are defined in IFS-COMPO around South Korea rather than Central China. The implication is that the regional SO<sub>2</sub> emissions employed for this region are likely too high, considering the low regional deposition values. The regional annual MB improves markedly to 8.7 mgS/m<sup>2</sup>/year, which is very low considering the high values in the measurements. This is accompa... [75]

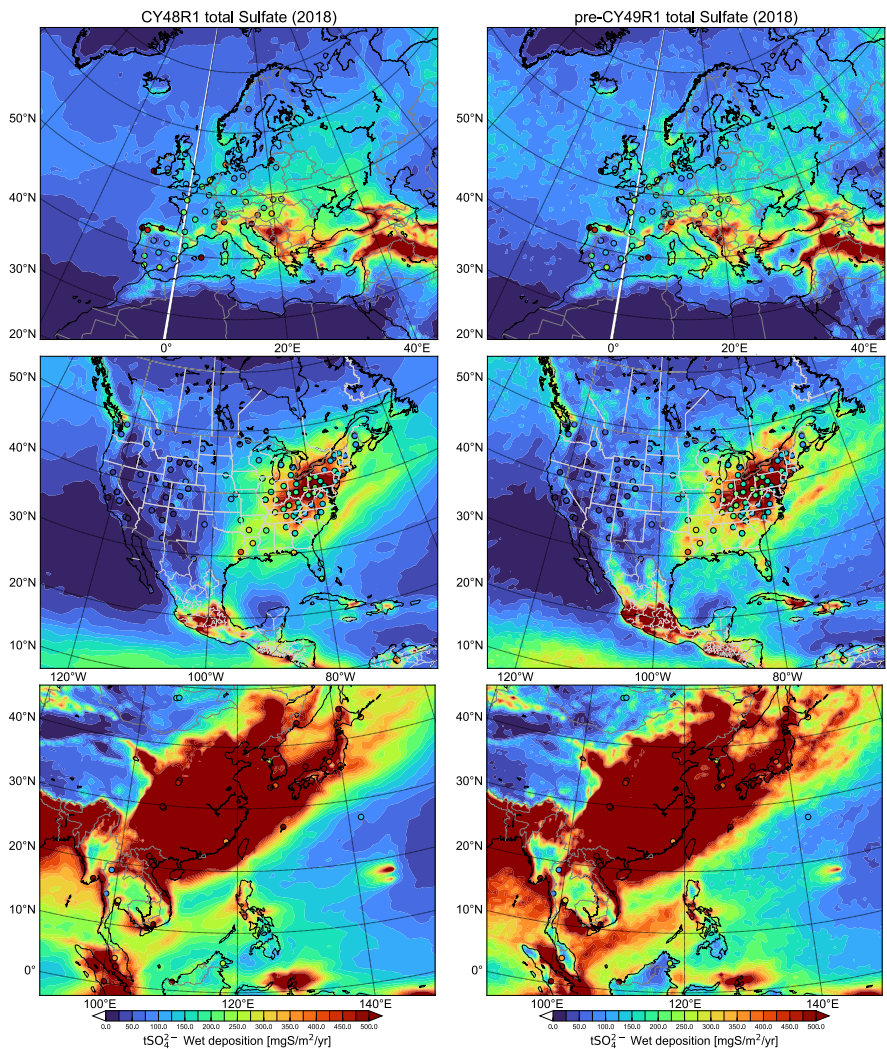


**Figure 10:** Yearly comparisons of the cumulative wet deposition totals of dissolved SO<sub>2</sub> and SO<sub>4</sub><sup>2-</sup> aerosol (mgS/m<sup>2</sup>/year) for 2018 as simulated in CY48R1 (left column) and pre-CY49R1 (right column) shown for Europe (top), the U.S. (middle) and SE Asia (bottom). The corresponding statistics are provided in Table 9. The site locations used are shown in each pane and taken from the EMEP, CASTNET and EANET networks, respectively.

**Deleted:** : Annual

**Formatted:** Normal5

**Deleted:**

**Deleted:** Cy48r1

**Deleted:** Cy49r1

**Deleted:** 39

**Formatted:** Normal5, Right: 0,63 cm

**Formatted:** Page Number

Formatted: Header

Deleted: annual

Deleted: annual...early mean wet deposition of reduced N for both Cy48r1...Y48R1 and Cy49r1...re-CY49R1 during 2018 for the three global regions. The location of the sampling stations is identical to those shown above for the wet S deposition evaluation. In Table 8, the global chemical budget terms for  $\text{NH}_4^+$  show that the cumulative updates to IFS-COMPO...or pre-CY49R1\_NOE4C there is an increase the tropospheric burden by one third (similar to...s for  $\text{SO}_4^{2-}$ , with  $(\text{NH}_4)_2\text{SO}_4$  being a dominant SIA, Seinfeld and Pandis, 2006). This is subsequently reversed when applying EQSAM4Clim for the description of aerosol and cloud pH, as seen when comparing Cy48r1 and Cy49r1...n pre-CY49R1. This results in significant decreases in both the total annual...early global dry and wet deposition terms, as illustrated for the three select regions ... [76]

Deleted: Figure 6...ig. 4 in Sect. 4), the EMEP observational annual...early wet deposition totals show that peak values exist in the Balkans, Germany, Austria and Northern...orthern Italy (Po valley), and that local regional variability exists in e.g. France (ranging between 250-350  $\text{mgN/m}^2/\text{year}$ ). For regions with low  $\text{NH}_3$  emissions, such as Scandinavia and the Iberian Peninsula, wet deposition totals generally have a lower range, of between 50-200  $\text{mgN/m}^2/\text{year}$ . For Cy48r1...Y48R1, the high resident surface mixing ratios of  $\text{NH}_3(\text{g})$  (5-15 ppb; Fig. 1) results in a relatively high  $\text{NH}_x$  annual...early total wet deposition values of between 350-500  $\text{mgN/m}^2/\text{year}$  for North-West...orthwest and Central...entral Europe at a country-wide scale (e.g. Benelux, Austria)...he Netherlands and Belgium). Measured annual...early mean values from EMEP are typically exceeded, which ...results in an annual...early MB of 61  $\text{mgN/m}^2/\text{year}$  in CY48R1, albeit with a high correlation of 0.69 (c.f. Table 8). The continental distribution is therefore represented well, although high values extend too far to both the East and West of Europe..., reflecting the positive local MB shown for  $[\text{NH}_4^+]$  shown in Fig. 6. Comparing the annual...early mean temporal distribution simulated in Cy49r1...re-CY49R1 shows a significant reduction in the area with maximal values ( $> 450 \text{ mgN/m}^2/\text{year}$ )..., being limited to northern Italy only. The reduction in  $[\text{NH}_4^+]$  (c.f. Table 4) reduces the annual...early MB in wet deposition by nearly 60% , ... [77]

Deleted: ....(c.f. Fig. 4 and 6, respectively). The range in observed total wet deposition values is between 30-400  $\text{mgN/m}^2/\text{year}$  showing that, in the absence of local  $\text{NH}_3$  emission sources, that levels of deposition are rather ...ow (lower than that observed for Europe). Comparing the temporal distribution of reduced N wet deposition in Cy48r1...Y48R1 shows that the continental gradient is captured, although maximal values which occur towards Iowa are not seen in the measurements ( $>100\%$  MB) being ... [78]

Deleted: South-East...outeast Asia, the EANET observational annual...early mean wet deposition totals show that, similar to that shown for S deposition, much higher values occur than for the other two regions presented. Similar to that shown for wet S..., This provides values between 200-2400  $\text{mgN/m}^2/\text{year}$  (not shown), with the ... [79]

Deleted: 39

Formatted: Normal5, Right: 0,63 cm

Formatted: Page Number



Formatted: Header

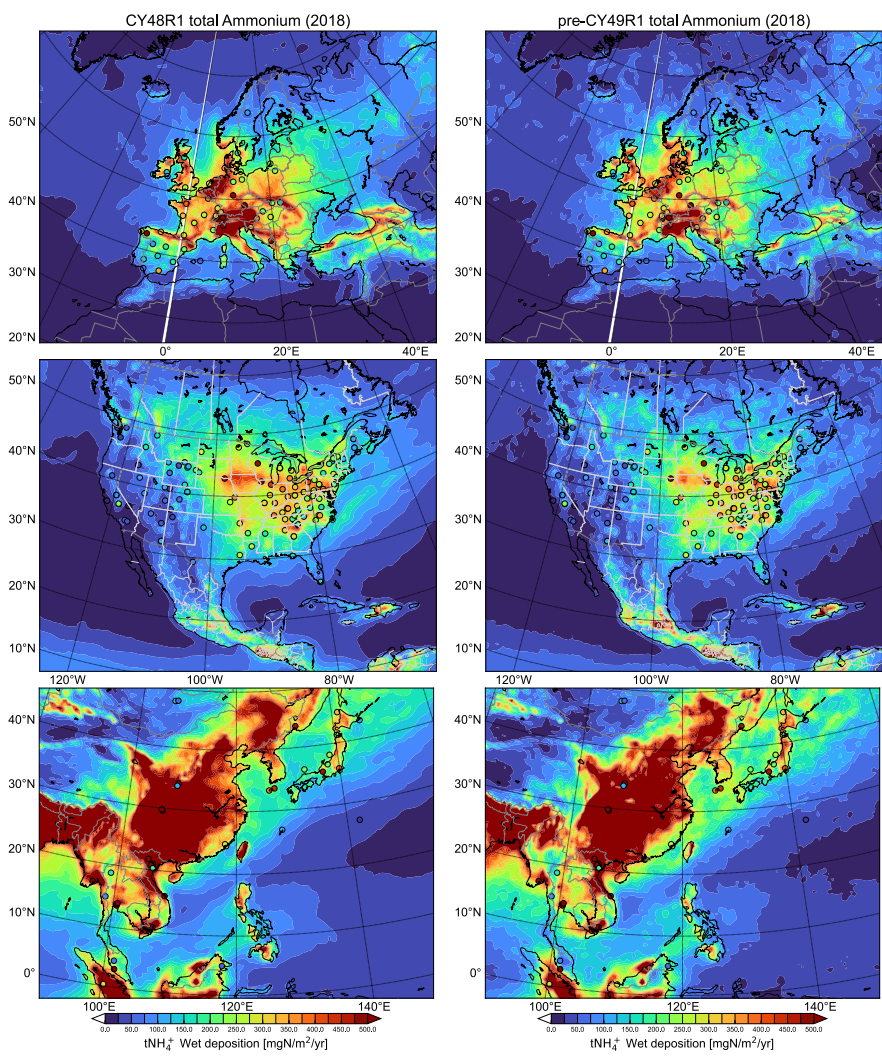
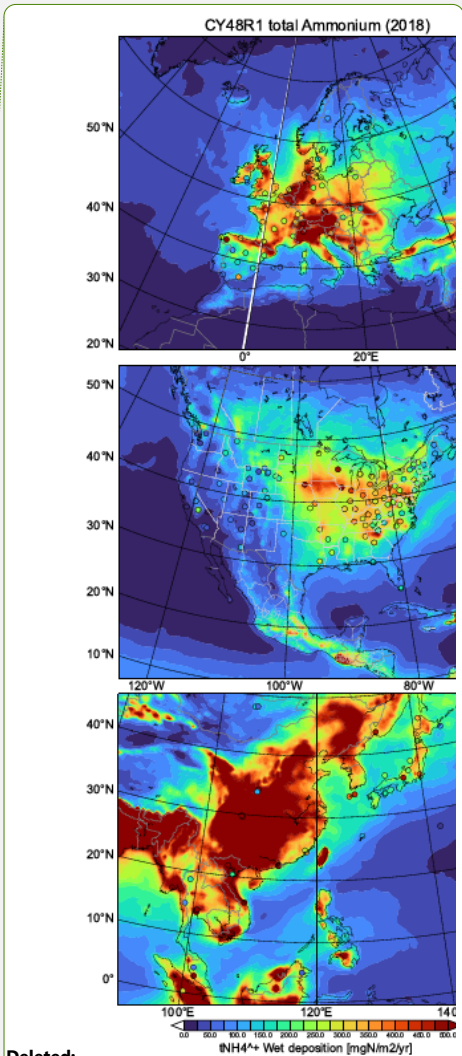


**Figure 11:** Yearly comparisons of the cumulative wet deposition totals of dissolved  $\text{NH}_3$  and  $\text{NH}_4^+$  aerosol ( $\text{mgN}/\text{m}^2/\text{year}$ ) for 2018 as simulated in CY48R1 (left column) and pre-CY49R1 (right column) shown for Europe (top), the U.S. (middle) and SE Asia (bottom). The corresponding statistics are provided in Table 9. The site locations used are shown in each pane and taken from the EMEP, CASTNET and EANET networks, respectively.



Deleted:

Deleted: : Annual... Yearly comparisons of the cumulative wet deposition totals of dissolved  $\text{NH}_3$  and  $\text{NH}_4^+$  aerosol ( $\text{mgN}/\text{m}^2/\text{year}$ ) for 2018 as simulated in Cy48r1... Y48R1 (left column) and Cy49r1 (right column) and Cy49r1

Formatted: Normal5

Formatted: Font: 11 pt

Formatted: Normal5

Deleted: 39

Formatted: Normal5, Right: 0,63 cm

Formatted: Page Number



### 5.3 Total **yearly** wet NOx deposition

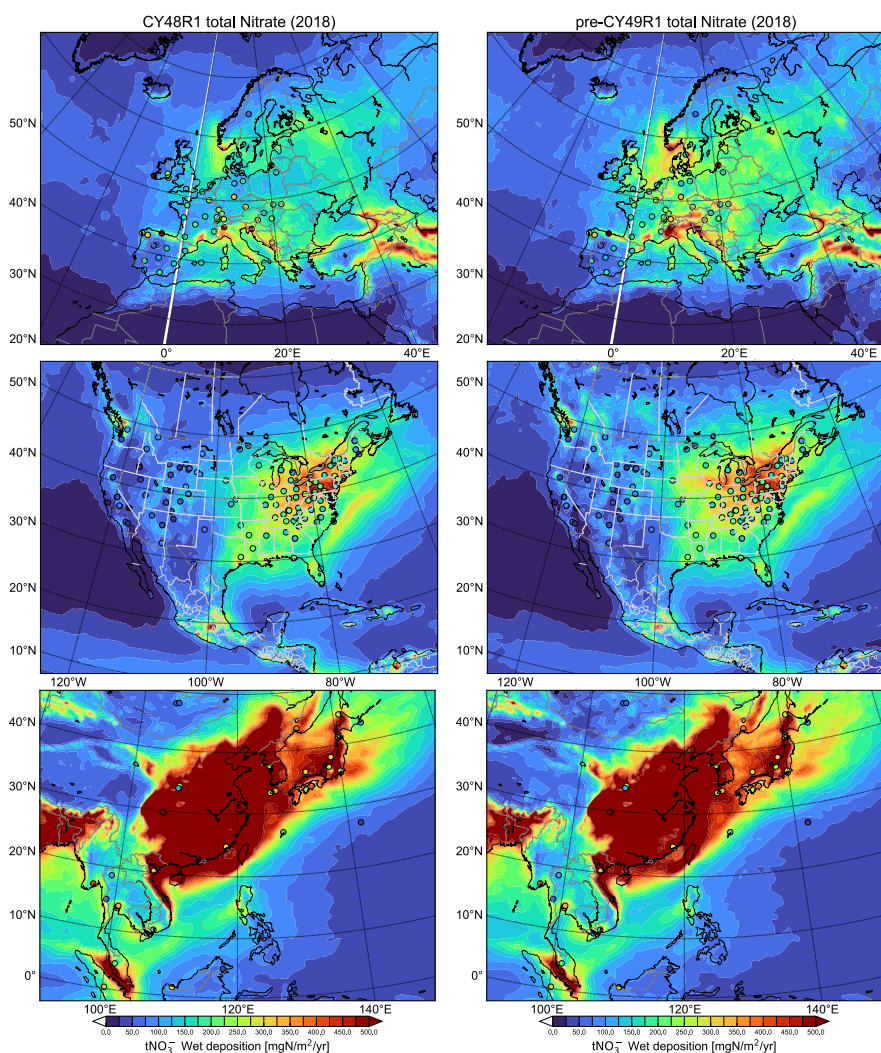
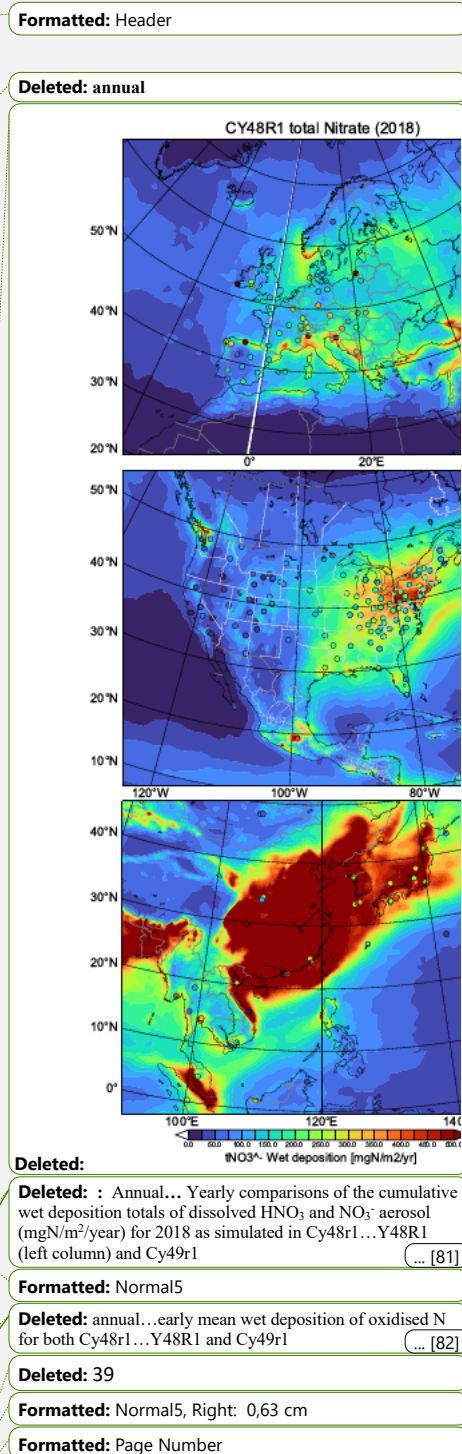


**Figure 12:** Yearly comparisons of the cumulative wet deposition totals of dissolved  $\text{HNO}_3$  and  $\text{NO}_3^-$  aerosol ( $\text{mgN/m}^2/\text{year}$ ) for 2018 as simulated in **CY48R1** (left column) and **pre-CY49R1** (right column) shown for Europe (top), the U.S. (middle) and SE Asia (bottom). The corresponding statistics are provided in Table 9. The site locations used are shown in each pane and taken from the EMEP, CASTNET and EANET networks, respectively.

Finally, in Figure 12 we show the corresponding changes in the total yearly mean wet deposition of oxidised N for both CY48R1 and pre-CY49R1 during 2018. The global chemical budget terms provided in Table 6 shows that there is an increase in the gas-phase production term for  $\text{HNO}_3$ , with a relatively constant heterogeneous conversion term for  $\text{N}_2\text{O}_5$  when summed over the various reactive surfaces. Once formed, a significant fraction of



2697 HNO<sub>3</sub> is directly scavenged into aqueous cloud droplets and deposited to the surface as wet (acidic) deposition  
2698 (c.f. Rémy et al, 2024). However, the large biases shown for HNO<sub>3</sub>(g) does reveal a limit to the loss via wet  
2699 scavenging and deposition, with an excess remaining in the gas phase, which impacts the results shown in this  
2700 section. Note that the particulate NO<sub>3</sub><sup>-</sup> takes various chemical forms in IFS-COMPO (Ca(NO<sub>3</sub>)<sub>2</sub>, NaNO<sub>3</sub>, KNO<sub>3</sub>,  
2701 NH<sub>4</sub>NO<sub>3</sub>), therefore there is only partial commonality between the changes shown for NH<sub>4</sub><sup>+</sup> and NO<sub>3</sub><sup>-</sup>. With the  
2702 application of EQSAM4Clim in pre-CY49R1, the surface concentration and burden of NH<sub>4</sub><sup>+</sup> decreases strongly,  
2703 while the gas phase concentration of HNO<sub>3</sub> increases (c.f Table 4 and 6; Figs. 5 and 8).

2704 For Europe (top panels), the observational yearly total wet deposition values from EMEP show that there is a rather  
2705 constrained range in the deposition of total oxidised N deposition (150-275 mgN/m<sup>2</sup>/year) apart from a few outliers  
2706 such as on the southern coast of Ireland which have values > 500 mgN/ m<sup>2</sup>/year due to missing local emission  
2707 sources not in the global inventories. In general, there are increases in the yearly wet deposition of [NO<sub>3</sub><sup>-</sup>] between  
2708 CY48R1 and pre-CY49R1, which increases the regional background totals improving agreement in e.g. Germany,  
2709 which significantly reduces the yearly MB (c.f. Table 9). In contrast to oxidized S, pre-CY49R1\_NOE4C simulates  
2710 a reduction in the yearly wet deposition totals, for oxidized N which is further decreased for the coarse mode by  
2711 applying EQSAM4Clim. The increase in [HNO<sub>3</sub>(g)] means a larger fraction of oxidized N remains in the gas-  
2712 phase thus reducing [NO<sub>3</sub><sup>-</sup>] and improving the MB against observations as shown in Sect. 4. This subsequently  
2713 leads to an improvement in performance for the regional yearly wet deposition totals. However, the large  
2714 significant MB introduced for [HNO<sub>3</sub>(g)] shows that another loss term is necessary for fully describe the budget  
2715 of oxidized N across phases. For the U.S. (middle panels), higher values of oxidised N deposition occur towards  
2716 the east coast as defined by the distribution of NO<sub>x</sub> emissions (Figs. 12). The range in the observational total wet  
2717 deposition values from CASTNET is between 50-500 mgN/m<sup>2</sup>/year, exhibiting a strong longitudinal gradient.  
2718 Although this gradient is captured rather well, there is typically an overestimation of between 100-200  
2719 mgN/m<sup>2</sup>/year for e.g. New York state and the surrounding regions in CY48R1. For the Western U.S., observations  
2720 provide the range of between 0-100 mgN/m<sup>2</sup>/year, with positive model biases of 100 mgN/m<sup>2</sup>/year for the  
2721 northwestern states in both model versions. For the southern U.S., CY48R1 exhibits overestimates of 50-70  
2722 mgN/m<sup>2</sup>/year, which decreases noticeably in pre-CY49R1. There is a large positive MB in CY48R1 of 130  
2723 mgN/m<sup>2</sup>/year which is improved in pre-CY49R1 decreasing by 23%. Again, the Pearsons R value remains  
2724 relatively unaffected showing the governing influence of the spatial distribution of the main point sources and has  
2725 little effect on the forecasts itself (since IFS-COMPO is not employed here as a fully coupled forecasting system  
2726 using data assimilation).

2727 For Southeast Asia (bottom panels), the range in the EANET observational total wet deposition values is between  
2728 50-800 mgN/m<sup>2</sup>/year (not shown), with the highest values of >2000 mgN/m<sup>2</sup>/year occurring on the Malaysian  
2729 Coast. For northern and central China, total wet deposition values of up to 500 mgN/m<sup>2</sup>/year occur, covering a  
2730 wide area including the similar to oxidised S. For CY48R1, simulated values exceed observed values by 100-  
2731 400%, with a lack of spatial variability across the domain. Much better agreement occurs for Myanmar, Cambodia  
2732 and Thailand related to much lower NO<sub>x</sub> emissions. Comparing CY48R1 and pre-CY49R1 shows that a marked  
2733 decrease in the MB of 31% occurs between cycles, although the MB is at least twice that simulated for the other  
2734 continents.

## 2736 6 Conclusions

2738 In this paper we build on the previous evaluations of the performance of IFS-COMPO pre-CY49R1 presented in  
2739 Rémy et al. (2024), an quantify the impact of applying the EQSAM4Clim module in IFS-COMPO for the revised  
2740 calculation of aerosol and cloud pH (Metzger et al., 2024) on its ability to improve air quality forecasts of SIA. To  
2741 scrutinise its effect on atmospheric composition, we have compared an operational IFS version (CY48R1) with  
2742 the next operational IFS version, which uses EQSAM4Clim in combination with a unified wet scavenging  
2743 approach and other developments (pre-CY49R1). Further improvements are also made with respect to both in-  
2744 cloud and below cloud scavenging of soluble trace gases and aerosols through an implementation of updated  
2745 parameterizations as detailed in Rémy et al. (2024).

2746 EQSAM4Clim significantly influences wet deposition processes through its impact on aerosol loading and gas-  
2747 aerosol partitioning. By altering the aerosol and cloud pH, the scheme modulates the chemical oxidation rates of  
2748 precursor gases such as NH<sub>3</sub>, SO<sub>2</sub> and HNO<sub>3</sub>. This, in turn, affects the formation and partitioning of SIA, their  
2749 hygroscopic growth, and their subsequent removal of both dry and wet deposition pathways - including in-cloud  
2750 and below-cloud scavenging. These changes also influence the aerosol radiative effects, both directly and

Formatted: Header

Deleted: term...nd deposition, with an excess remaining in the gas phase, which impacts the results shown in this section. Note that the particulate NO<sub>3</sub><sup>-</sup> takes various chemical forms in IFS-COMPO (Ca(NO<sub>3</sub>)<sub>2</sub>, NaNO<sub>3</sub>, KNO<sub>3</sub>, NH<sub>4</sub>NO<sub>3</sub>), therefore there is only partial commonality between the changes shown for NH<sub>4</sub><sup>+</sup> and NO<sub>3</sub><sup>-</sup>. With the application of EQSAM4Clim in pre-CY49R1, the surface concentration and burden of NH<sub>4</sub><sup>+</sup> decreases strongly, while the gas phase concentration of HNO<sub>3</sub> increases (c.f Table 6... and F... [83]

Deleted: EMEP...bservational annual...early total wet deposition values from EMEP show that there is a rather constrained range in the deposition of total oxidised N deposition (150-275 mgN/m<sup>2</sup>/year). This correlates with a rather homogeneous distribution of [NO<sub>3</sub><sup>-</sup>] shown in Sect. 4.3; ... apart from a few high ...utliers are most likely affected by strong local NO<sub>x</sub> ...uch as on the southern coast of Ireland which have values > 500 mgN/ m<sup>2</sup>/year due to missing local emission sources. Although...not in the global inventories. In general, there are rather modest differences...ncreases in cumulative...he yearly wet deposition of [NO<sub>3</sub><sup>-</sup>] between Cy48r1...Y48R1 and Cy49r1, there is a marked improvement in ...re-CY49R1, which increases the regional bias...ackground totals improving agreement in e.g. Germany, which significantly reduces the yearly MB (c.f. Table 9). In contrast to oxidized S, pre-CY49R1\_NOE4C simulates a reduction in the oxidised N...early wet deposition term, which decreases by 80% turning from positive to negative, albeit with no...otals, for oxidized N which is further decreased for the coarse mode by applying EQSAM4Clim. The increase in [HNO<sub>3</sub>(g)] means a larger fraction of oxidized N remains in the gas-phase thus reducing [NO<sub>3</sub><sup>-</sup>] and improving the MB against observations as shown in Sect. 4. This subsequently leads to an improvement in performance for the regional yearly wet deposition totals. However, the large significant improvement in the (time-sensitive) correlation. MB introduced for [HNO<sub>3</sub>(g)] shows that another loss term is necessary for fully describe the budget of oxidized N ... [84]

Formatted: Normal5, Right: 0 cm

Deleted: South-East...outeast Asia (bottom panels), the range in the EANET observational total wet deposition values is between 50-800 mgN/m<sup>2</sup>/year....(not shown), with ... [85]

Formatted: Normal5

Deleted: Cy48r1...Y48R1 and Cy49r1...re-CY49R1 shows that a marked decrease in the MB of 31% occurs betw... [86]

Formatted: Not Superscript/ Subscript

Formatted: Normal5

Deleted: Cy49r1...re-CY49R1 presented in Rémy et al. (2024), which evaluates...n quantify the impact of applying EQSAM4Clim and its...odule in IFS-COMPO for the ... [87]

Moved (insertion) [4]

Deleted: We

Formatted

Deleted: 39

Formatted: Normal5, Right: 0,63 cm

Formatted: Page Number

indirectly, underscoring the interconnected role of thermodynamic aerosol modelling in atmospheric composition and deposition simulations.

When applying EQSAM4Clim in a large-scale high resolution global modelling framework, we have shown that the most significant impacts of our IFS-COMPO updates concern the production efficacy of SIA and subsequent phase partitioning of reduced/oxidised nitrogen species. Comparing simulations with and without EQSAM4Clim, shows that changes in SIA are principally caused by altering the gas/aerosol partitioning, as predicted. The verification and analysis that have been presented for the three dominant global source regions (Europe, the U.S., and Southeast Asia), for the gaseous precursors, SIA surface concentrations and wet deposition totals, by comparing against weekly/yearly observational composites for 2018.

For  $\text{SO}_2(\text{g})/\text{SO}_4^{2-}$ , the conversion rate only exhibits moderate changes, with statistics being strong affected by the emission inventory employed. For  $\text{SO}_2(\text{g})$ , an increase in the global tropospheric burden of 7% shows less phase transfer due to limitations in the uptake imposed by the increase in the pH of the solution. An increase in the gas phase production term of  $\text{H}_2\text{SO}_4(\text{g})$ , which is subsequently scavenged, offsets a modest reduction in the aqueous phase production term. For surface  $[\text{SO}_2(\text{g})]$ , no significant impact has occurred with respect to the MB for Europe or the U.S. and with little correlation. For  $[\text{SO}_4^{2-}]$  there is an increase in both the tropospheric burden and lifetime by one third due to the wet scavenging updates made to IFS-COMPO, with an associated reduction in the yearly mean biases for Europe and the U.S. and increases in the corresponding correlation coefficients. However, for China there is a degradation in the performance which is associated with an increase in the positive yearly mean bias and a decrease in the correlation coefficient. For the yearly wet deposition of oxidized S, results are mixed with reductions in the MB for Europe and China but increasing markedly for the U. S.

For  $\text{NH}_3(\text{g})/\text{NH}_4^+$  the changes from applying EQSAM4Clim online are more substantial, resulting in beneficial improvements in the global modelling of reduced nitrogen. For  $\text{NH}_3(\text{g})$  the tropospheric burden almost doubles due to a halving of the conversion rate into  $\text{NH}_4^+$ , where more  $\text{NH}_3(\text{g})$  is directly deposited to the surface. For surface  $[\text{NH}_3(\text{g})]$ , there is some similarity in the increases in the weekly MB between Europe and the U.S. For  $[\text{NH}_4^+]$ , the application of EQSAM4Clim significantly reduces the associated MB against observational yearly means by approximately 45% for all three global regions from a reduction in the efficacy of particle, especially during summertime. For the yearly wet deposition component, the positive MB almost halves for Europe and the U. S., whilst increasing significantly for southeast Asia.

For  $\text{HNO}_3(\text{g})/\text{NO}_3^-$  the changes due to EQSAM4Clim are similar to those simulated for the  $\text{NH}_3(\text{g})/\text{NH}_4^+$  partitioning due to the speciation of the SIA being mainly linked via  $\text{NH}_4\text{NO}_3$ . The gas-phase production of  $\text{HNO}_3(\text{g})$  increases by 15-20% with a limited increase in the global tropospheric burden due to increases in the loss to surface via both dry and wet deposition. The application of EQSAM4Clim increases the fine aerosol component whilst reducing the coarse aerosol component, which reduces the fraction of  $\text{HNO}_3(\text{g})$  held in the particulate phase by 50% and increases transport lifetimes for smaller particles. For  $\text{HNO}_3(\text{g})$  in Europe and the U.S., there is a persistent negative bias which is changed to a significant positive bias. For  $[\text{NO}_3^-]$ , significant improvements in the yearly mean biases occur across the globe as illustrated by the three chosen regions, which comes with improvements in the simulated correlation coefficients. For the yearly wet deposition totals, there are reductions in the MB for all regions, without any significant change in the correlation.

In summary, although the impact on  $\text{SO}_2(\text{g})/\text{SO}_4^{2-}$  are rather small across various global regions, the impact on both particle concentrations and wet deposition totals for both reduced and oxidised N improve markedly for both Europe and the U. S., whereas for southeast Asia changes are rather mixed. Significant improvements could be made by applying more accurate emission inventories and also including additional anions such as chlorine from sea-salt to influence coastal regions and the significant changes simulated over the oceans in this study. Overall, the recent improvements brought by EQSAM4Clim (Metzger et al., 2024) as applied here and in Rémy et al. (2024), shows that the changes shown for pre-CY49R1 are fit-for-purpose with respect to capturing regional particle concentration and the loss terms via wet deposition and improve the forecasting on PM at global scale.

Formatted: Header

Formatted: Normal5

Deleted: .

Deleted: has

Deleted: .

Deleted: South-East

Deleted: where we focus on evaluations of

Deleted: concentration

Deleted: ammal

Deleted: .

Deleted: indicates

Deleted: pH

Deleted: this results in a lower mean annual bias

Deleted: with moderate correlation and a corresponding higher negative bias for

Deleted: No appreciable impact occurs for China, which shows a high positive bias of  $11.5 \mu\text{g}/\text{m}^3$  with respect to CNEC and a correlation coefficient near zero.

Deleted: annual

Deleted: a

Deleted: annual

Deleted: a contrasting change

Deleted: simulated

Deleted: mean bias

Deleted: . For Europe, there is no significant improv... [91]

Deleted: "] in Europe,

Deleted: results in limited changes in the simulated w... [92]

Deleted: , with an associated increase in the annual n... [93]

Deleted: without an associated

Deleted: %.

Deleted:

Deleted: annual

Moved up [4]: EQSAM4Clim significantly influences wet

Deleted: modeling in atmospheric composition and ... [97]

Formatted ... [94]

Formatted ... [95]

Formatted ... [96]

Deleted: Cy49r1 is

Formatted ... [98]

Deleted: ¶ ... [99]

Formatted ... [100]

Deleted: 39

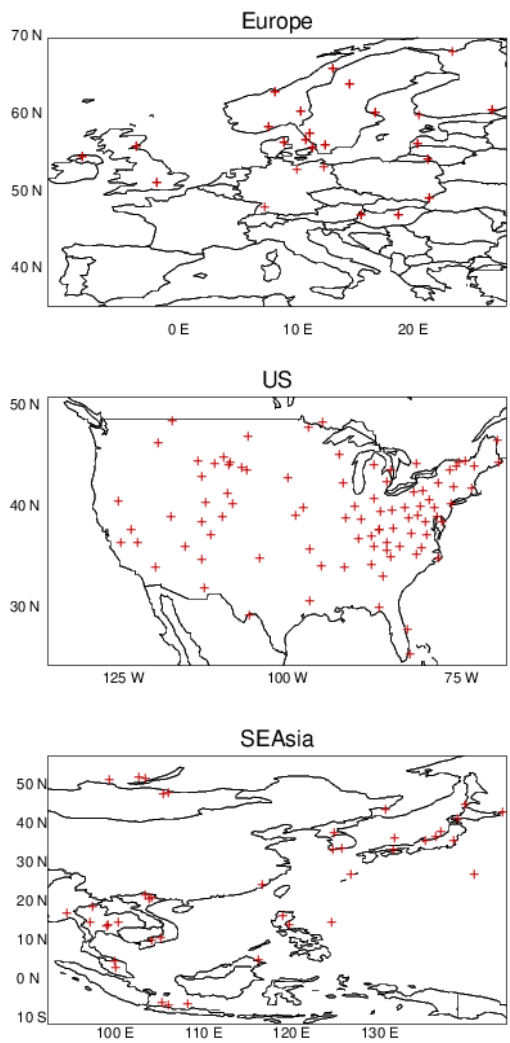
Formatted ... [90]

Formatted ... [89]

3153

3154 Appendix

3155



3156

3157

3158

3159

**Figure A1:** The location of the observational sites used for evaluating the weekly surface concentration of SO<sub>2</sub> for Europe (top panel), the U.S. (middle panel) and SEAsia (lower panel).

Formatted: Header

Deleted:

Formatted: Font: Not Bold

Deleted: US

Deleted: 39

Formatted: Normal5, Right: 0,63 cm

Formatted: Page Number



3162  
3163  
3164  
3165  
3166  
3167  
3168  
3169  
3170  
3171  
3172  
3173  
3174  
3175  
3176  
3177  
3178  
3179  
3180  
3181  
3182  
3183  
3184  
3185  
3186  
3187  
3188  
3189  
3190  
3191  
3192  
3193  
3194  
3195  
3196  
3197  
3198  
3199  
3200

**Author Contributions**

JEW and SM were principal authors of the paper and produced most of the figures. SR conducted the IFS-COMPO simulations and performed the regional comparisons made against observational datasets for evaluating the deposition fluxes and was a co-PI of the CAMS35\_2 development project. SM provided and integrated EQSAM4Clim for the more accurate calculation of pH using aerosols and clouds. VH updated the model towards [pre-CY49R1](#), introduced technical updates with respect to the implementation of EQSAM4Clim and was co-PI of the CAMS35\_2 development project. JF is a representative of the CAMS consortium under which this work was conducted.

**Code availability**

Model codes developed at ECMWF are the intellectual property of ECMWF and its member states, and therefore the IFS code is not publicly available. ECMWF member-state weather services and their approved partners will get access granted. Access to a version of the IFS (OpenIFS) that includes this experimental cycle may be obtained from ECMWF under an OpenIFS licence. More details at <https://confluence.ecmwf.int/display/OIFS/About+OpenIFS>.

**Data availability**

The model codes created by ECMWF are considered intellectual property of ECMWF and its member states, and as such, the IFS code is not available to the public. Access to the IFS code is granted to ECMWF member-state weather services and their authorised partners. However, an open version of the IFS code, known as OpenIFS, which includes cycle CY43R3 IFS(AER) (Huijnen et al., 2022), can be obtained from ECMWF under an OpenIFS license. [More details at https://confluence.ecmwf.int/display/OIFS/About+OpenIFS](https://confluence.ecmwf.int/display/OIFS/About+OpenIFS).

**Competing Interests**

The main author and one of the co-authors [are members](#) of the editorial board of Geoscientific Model Development. The peer-review process was guided by an independent editor, and the authors also have no other competing interests to declare.

**Acknowledgements**

We acknowledge funding from the Copernicus Atmosphere Monitoring Service (CAMS), which is funded by the European Union's Copernicus Programme. We acknowledge the EMEP, EANET, AirNow, CASTNET, AMoN, AQeR and CNEMC monitoring networks for allowing access to surface observational data for [the pre-cursor gases and associated particulates](#).

Formatted: Header

Formatted: Font: Bold, Italic

Formatted: Normal5, Left, Indent: Left: 0 cm, Right: 0 cm, Space Before: 12 pt, Keep with next, Keep lines together, Border: Top: (No border), Bottom: (No border), Left: (No border), Right: (No border), Between : (No border)

Formatted: Normal5

Deleted: Cy49r1

Deleted:

Formatted: Normal5

Formatted: Normal5

Formatted: Font: 10 pt

Deleted: More details at <https://confluence.ecmwf.int/display/OIFS/About+OpenIFS>.

Formatted: Normal5

Deleted: is a member

Formatted: Font: 10 pt

Formatted: Normal5

Deleted: SO<sub>2</sub>, SO<sub>4</sub><sup>2-</sup>, NH<sub>3</sub>, NH<sub>4</sub><sup>+</sup>, HNO<sub>3</sub> and NO<sub>3</sub><sup>-</sup>.  
Page Break

Formatted: Font: Times New Roman, 10 pt

Formatted: Normal5

Deleted: 39

Formatted: Normal5, Right: 0,63 cm

Formatted: Page Number

## References

- van der A, R. J., Ding, J., and Eskes, H.: Monitoring European anthropogenic NO<sub>x</sub> emissions from space, *Atmos. Chem. Phys.*, 24, 7523–7534, <https://doi.org/10.5194/acp-24-7523-2024>, 2024.
- Aas, W., Mortier, A., Bowersox, V. *et al.* Global and regional trends of atmospheric sulfur. *Sci Rep* 9, 953, <https://doi.org/10.1038/s41598-018-37304-0>, 2019.
- Aas, W., Fagerli, H., Alastuey, A., Cavalli, F., Degorska, A., Feigenspan, S., Brenna, H., Gliß, J., Heinesen, D., Hueglin, C., Holubová, A., Jaffrezo, J.L., Mortier, A., Murovec, M., Putaud, J.P., Rüdiger, J., Simpson, D., Solberg, S., Tsyro, S., Tørseth, K. and Yttri, K.E.: Trends in Air Pollution in Europe, 2000–2019. *Aerosol Air Qual. Res.* 24, 230237. <https://doi.org/10.4209/aaqr.230237>, 2024.
- Andres, R. J. and Kasgnoc, A. D.: A time-averaged inventory of subaerial volcanic sulphur emissions, *J. Geophys. Res.*, 103(D19), 25251–25261, <https://doi.org/10.1029/98JD02091>, 1998.
- Ault, A.P.: Aerosol Acidity: Novel Measurements and Implications for Atmospheric Chemistry, *Acc. Chem. Res.*, 53, 9, 1703–1714, <https://doi.org/10.1021/acs.accounts.0c00303>, 2020.
- Benish, S. E., Bash, J. O., Foley, K. M., Appel, K. W., Hogrefe, C., Gilliam, R., and Pouliot, G.: Long-term regional trends of nitrogen and sulfur deposition in the United States from 2002 to 2017, *Atmos. Chem. Phys.*, 22, 12749–12767, <https://doi.org/10.5194/acp-22-12749-2022>, 2022.
- Celik, S., Drewnick, F., Fachinger, F., Brooks, J., Darbyshire, E., Coe, H., Paris, J.-D., Eger, P. G., Schuladen, J., Tadic, I., Friedrich, N., Dienhart, D., Hottmann, B., Fischer, H., Crowley, J. N., Harder, H., and Borrmann, S.: Influence of vessel characteristics and atmospheric processes on the gas and particle phase of ship emission plumes: in situ measurements in the Mediterranean Sea and around the Arabian Peninsula, *Atmos. Chem. Phys.*, 20, 4713–4734, <https://doi.org/10.5194/acp-20-4713-2020>, 2020.
- Chang, C.-T., Wang, L., Wang L.-J, Liu, C.-P, Yang, C.-J, Huang, J.-C., Wang, C.-P, Lin N.-H. and Lin, T.-C.: On the seasonality of long-range transport of acidic pollutants in East Asia, *Environ. Res. Lett.*, 17(9), doi:10.1088/1748-9326/ac8b99, 2022.
- Chen J, Cheng M, Krol M, de Vries W, Zhu Q, Liu X, Zhang F and Xu W (2023), Trends in anthropogenic ammonia emissions in China since 1980: A review of approaches and estimations. *Front. Environ. Sci.* 11:1133753, doi: 10.3389/fenvs.2023.1133753.
- Croft, B., Lohmann, U., Martin, R. V., Stier, P., Wurzler, S., Feichter, J., Posselt, R., and Ferrachat, S.: Aerosol size-dependent below-cloud scavenging by rain and snow in the ECHAM5-HAM, *Atmos. Chem. Phys.*, 9, 4653–4675, 2009.
- de Bruine, M., Krol, M., van Noije, T., Le Sager, P., and Rockmann, T.: The impact of precipitation evaporation on the atmospheric aerosol distribution in EC-Earth v3.2.0, *Geosci. Model Dev.*, 11, 1443–1465, 2018.
- Dentener, F., Drevet, J., Lamarque, J. F., Bey, I., Eickhout, B., Fiore, A. M., Hauglustaine, D., Horowitz, L. W., Krol, M., Kulshrestha, U. C., Lawrence, M., Galy-Lacaux, C., Rast, S., Shindell, D., Stevenson, D., Van Noije, T., Atherton, C., Bell, N., Bergman, D., Butler, T., Cofala, J., Collins, B., Doherty, R., Ellingsen, K., Galloway, J., Gauss, M., Montanaro, V., Müller, J. F., Pitari, G., Rodriguez, J., Sanderson, M., Solomon, F., Strahan, S., Schultz, M., Sudo, K., Szopa, S., and Wild, O.: Nitrogen and sulfur deposition on regional and global scales: A multimodel evaluation, *Global Biogeo. Cycles*, 20, GB4003, doi:10.1029/2005GB002672, 2006.
- Deschaseaux, E., O'Brien, J., Siboni, N., Petrou, K., and Seymour, J. R.: Shifts in dimethylated sulfur concentrations and microbiome composition in the red-tide causing dinoflagellate *Alexandrium minutum* during a simulated marine heatwave, *Biogeosciences*, 16, 4377–4391, <https://doi.org/10.5194/bg-16-4377-2019>, 2019.
- Ding, J., van der A, R., Eskes, H., Dammers, E., Shephard, M., Wichink Kruit, R., Guevara, M., and Tarrason, L.: Ammonia emission estimates using CrIS satellite observations over Europe, *EGU sphere* [preprint], <https://doi.org/10.5194/egusphere-2024-1073>, 2024.
- Du, H., Li, J., Wang, Z., Dao, X., Guo, S., Wang, L., et al.: Effects of regional transport on haze in the North China Plain: Transport of precursors or secondary inorganic aerosols. *Geophysical Research Letters*, 47, e2020GL087461, <https://doi.org/10.1029/2020GL087461>, 2020.

Formatted: Header

Deleted: ¶

Deleted: . :

Formatted: Highlight

Deleted:

Formatted: Normal5

Deleted: 39

Formatted: Normal5, Right: 0,63 cm

Formatted: Page Number

- Feick, G. and Hainer, R. M.: On the Thermal Decomposition of Ammonium Nitrate. Steady-state Reaction Temperatures and Reaction Rate, *J. Am. Chem. Soc.*, 76, 22, 5860–5863, <https://doi.org/10.1021/ja01651a096>, 1954.
- Fioletov, V., McLinden, C. A., Griffin, D., Theys, N., Loyola, D. G., Hedelt, P., Krotkov, N. A., and Li, C.: Anthropogenic and volcanic point source SO<sub>2</sub> emissions derived from TROPOMI on board Sentinel-5 Precursor: first results, *Atmos. Chem. Phys.*, 20, 5591–5607, <https://doi.org/10.5194/acp-20-5591-2020>, 2020.
- Gao, J., Wei, Y., Guoliang, S., Yu, H., Zhang, Z., Song, S., Wang, W., Liang, D. and Feng, Y.: Roles of RH, aerosol pH and sources in concentrations of secondary inorganic aerosols, during different pollution periods, *Atms. Environ.*, 241, 117770, <https://doi.org/10.1016/j.atmosenv.2020.117770>, 2020.
- Ge, Y., Heal, M. R., Stevenson, D. S., Wind, P., and Vieno, M.: Evaluation of global EMEP MSC-W (rv4.34) WRF (v3.9.1.1) model surface concentrations and wet deposition of reactive N and S with measurements, *Geosci. Model Dev.*, 14, 7021–7046, <https://doi.org/10.5194/gmd-14-7021-2021>, 2021.
- Giorgi, F. and Chameides, W. L.: Rainout lifetimes of highly soluble aerosols and gases as inferred from simulations with a general circulation model, *J. Geophys. Res.*, 91, 367–376, 1986.
- Goldberg, D. L., Anenberg, S. C., Kerr, G. H., Mohegh, A., Lu, Z., & Streets, D. G.: TROPOMI NO<sub>2</sub> in the United States: A detailed look at the yearly averages, weekly cycles, effects of temperature, and correlation with surface NO<sub>2</sub> concentrations. *Earth's Future*, 9, e2020EF001665. <https://doi.org/10.1029/2020EF001665>, 2021.
- Gu, B., Ju, X., Chang, J., Ge, Y. and Vitousek, P. M.: Integrated reactive nitrogen budgets and future trends in China, *PNAS*, 112 (28) 8792–8797, <https://doi.org/10.1073/pnas.1510211112>, 2015.
- Hauglustaine, D. A., Balkanski, Y., and Schulz, M.: A global model simulation of present and future nitrate aerosols and their direct radiative forcing of climate, *Atmos. Chem. Phys.*, 14, 11031–11063, <https://doi.org/10.5194/acp-14-11031-2014>, 2014.
- He, H., Liang, X.-Z. and Wuebbles, D. J.: Effects of emissions change, climate change and long-range transport on regional modeling of future U.S. particulate matter pollution and speciation, *Atmos. Environ.*, 179, 166–176, <https://doi.org/10.1016/j.atmosenv.2018.02.020>, 2018.
- Holland, E. A., Braswell, B. H., Lamarque, J.-F., et al.: Variations in the predicted spatial distribution of atmospheric nitrogen deposition and their impact on carbon uptake by terrestrial ecosystems, *J. Geophys. Res.*, 102, 15 849–15 866, 1997.
- Huijnen, V., Flemming, J., Chabrillat, S., Errera, Q., Christophe, Y., Blechschmidt, A.-M., Richter, A., and Eskes, H.: C-IFS-CB05-BASCOE: stratospheric chemistry in the Integrated Forecasting System of ECMWF, *Geosci. Model Dev.*, 9, 3071–3091, <https://doi.org/10.5194/gmd-9-3071-2016>, 2016.
- Huijnen, V., Pozzer, A., Arteta, J., Brasseur, G., Bouarar, I., Chabrillat, S., Christophe, Y., Doumbia, T., Flemming, J., Guth, J., Josse, B., Karydis, V. A., Marécal, V., and Pelletier, S.: Quantifying uncertainties due to chemistry modelling – evaluation of tropospheric composition simulations in the CAMS model (cycle 43R1), *Geosci. Model Dev.*, 12, 1725–1752, <https://doi.org/10.5194/gmd-12-1725-2019>, 2019.
- Huijnen, V., Le Sager, P., Köhler, M. O., Carver, G., Rémy, S., Flemming, J., Chabrillat, S., Errera, Q., and van Noije, T.: OpenIFS/AC: atmospheric chemistry and aerosol in OpenIFS 43r3, *Geosci. Model Dev.*, 15, 6221–6241, <https://doi.org/10.5194/gmd-15-6221-2022>, 2022.
- von Glasow, R., Lawrence, M. G., Sander, R., and Crutzen, P. J.: Modeling the chemical effects of ship exhaust in the cloud-free marine boundary layer, *Atmos. Chem. Phys.*, 3, 233–250, <https://doi.org/10.5194/acp-3-233-2003>, 2003.
- Jayne, J. T., Davidovits, P., Worsnop, D. R., Zahniser, M. S., and Kolb, C. E.: Uptake of SO<sub>2</sub>(g) by Aqueous Surfaces as a Function of pH: The Effect of Chemical Reaction at the Interface, *J. Phys. Chem., J. Phys. Chem.*, 94, 15, 6041–6048, <https://doi.org/10.1021/j100378a076>, 1990.

Formatted: Header

Deleted: . :

Deleted: annual

Deleted: . :

Deleted:

Deleted: 39

Formatted: Normal5, Right: 0,63 cm

Formatted: Page Number

- 3309 Jiang, Z., Zhu, R., Miyazaki, K., McDonald, B. C., Klimont, Z., Zheng, B., et al.: Decadal variabilities in  
3310 tropospheric nitrogen oxides over United States, Europe, and China. *Journal of Geophysical Research:*  
3311 *Atmospheres*, 127, e2021JD035872. <https://doi.org/10.1029/2021JD035872>, 2022.
- 3312 Kanakidou, M., Myriokefalitakis, S., Daskalakis, N., Fanourgakis, G., Nenes, A., Baker, A. R., K. Tsigaridis, K. and  
3313 Mihalopoulos N.: Past, Present and Future Atmospheric Nitrogen Deposition, *J. Atmos. Sci.*, 73(5): 2039–2047,  
3314 doi: 10.1175/JAS-D-15-0278.1, 2016.
- 3315 Liu, L., Zhang, X., Wong, A. Y. H., Xu, W., Liu, X., Li, Y., Mi, H., Lu, X., Zhao, L., Wang, Z., Wu, X., and Wei,  
3316 J.: Estimating global surface ammonia concentrations inferred from satellite retrievals, *Atmos. Chem. Phys.*, 19,  
3317 12051–12066, <https://doi.org/10.5194/acp-19-12051-2019>, 2019.
- 3318 ~~Kloster, S., Feichter, J., Maier-Reimer, E., Six, K. D., Six, K. D., Steir, P. and Wetzel, P.: DMS cycle in the marine~~  
3319 ~~ocean-atmosphere system – a global model study, *Biogeosciences*, 3, 29–51, <https://doi.org/10.5194/bg-3-2006>,~~  
3320 ~~2006.Liu, S., Valks, P., Pinardi, G., Xu, J., Chan, K. L., Argyrouli, A., Lutz, R., Beirle, S., Khorsandi, E., Baier,~~  
3321 ~~F., Huijnen, V., Bais, A., Donner, S., Dörner, S., Gratsea, M., Hendrick, F., Karagkiozidis, D., Lange, K., Piters,~~  
3322 ~~A. J. M., Remmers, J., Richter, A., Van Roozendaal, M., Wagner, T., Wenig, M., and Loyola, D. G.: An improved~~  
3323 ~~TROPOMI tropospheric NO<sub>2</sub> research product over Europe, *Atmos. Meas. Tech.*, 14, 7297–7327,~~  
3324 ~~<https://doi.org/10.5194/amt-14-7297-2021> , 2021.~~
- 3325 Liu, S., Geng, G., Xia, Q., Zheng, Y., Cheng, J., and Zhang, Q.: Tracking Daily Concentrations of PM<sub>2.5</sub>  
3326 Chemical Composition in China since 2000, *Environ. Sci. Technol.*, 56, 16517–16527, 2022.
- 3327 Luo, G., Yu, F., and Schwab, J.: Revised treatment of wet scavenging processes dramatically improves GEOS-  
3328 Chem 12.0.0 simulations of surface nitric acid, nitrate, and ammonium over the United States, *Geosci. Model Dev.*,  
3329 12, 3439–3447, <https://doi.org/10.5194/gmd-12-3439-2019> , 2019.
- 3330 Metzger, S., Dentener, F., Pandis, S., and Lelieveld, J.: Gas/aerosol partitioning: 1. A computationally efficient  
3331 model, *J. Geophys. Res.*, 107, 4312, <https://doi.org/10.1029/2001JD001102>, 2002.
- 3332 Metzger, S., Mihalopoulos, N., and Lelieveld, J.: Importance of mineral cations and organics in gas-aerosol  
3333 partitioning of reactive nitrogen compounds: case study based on MINOS results, *Atmos. Chemistry and Physics*,  
3334 6, 2549–2567, <https://doi.org/10.5194/acp-6-2549-2006>, 2006.
- 3335 Metzger, S., Steil, B., Abdelkader, M., Klingmüller, K., Xu, L., Penner, J. E., Fountoukis, C., Nenes, A., and  
3336 Lelieveld, J.: Aerosol water parameterisation: a single parameter framework, *Atmos. Chem. Phys.*, 16, 7213–7237,  
3337 <https://doi.org/10.5194/acp-16-7213-2016>, 2016.
- 3338 Metzger, S., Abdelkader, M., Steil, B., and Klingmüller, K.: Aerosol water parameterization: long-term evaluation  
3339 and importance for climate studies, *Atmos. Chem. Phys.*, 18, 16747–16774, [https://doi.org/10.5194/acp-18-16747-](https://doi.org/10.5194/acp-18-16747-2018)  
3340 [2018](https://doi.org/10.5194/acp-18-16747-2018), 2018.
- 3341 Metzger, S., Rémy, S., Williams, J. E., Huijnen, V., and Flemming, J.: A computationally efficient  
3342 parameterization of aerosol, cloud, and precipitation pH for application at global and regional scale  
3343 (EQSAM4Clim-v12), *Geosci. Model Dev.*, 17, 5009–5021, <https://doi.org/10.5194/gmd-17-5009-2024>, 2024.
- 3344 Myriokefalitakis, S., Bergas-Massó, E., Gonçalves-Ageitos, M., Pérez García-Pando, C., van Noije, T., Le Sager,  
3345 P., Ito, A., Athanasopoulou, E., Nenes, A., Kanakidou, M., Krol, M. C., and Gerasopoulos, E.: Multiphase  
3346 processes in the EC-Earth model and their relevance to the atmospheric oxalate, sulfate, and iron cycles, *Geosci.*  
3347 *Model Dev.*, 15, 3079–3120, <https://doi.org/10.5194/gmd-15-3079-2022>, 2022.
- 3348 Pan, D., Mauzerall, D.L., Wang, R., Guo, X., Puchalski, M., Guo, Y., Song, S., Tong, D., Sullivan, A. P., Schichtel,  
3349 B. A., Collet Jr, J. L. and Zondlo, M. A.: Regime shift in secondary inorganic aerosol formation and nitrogen  
3350 deposition in the rural United States. *Nat. Geosci.* <https://doi.org/10.1038/s41561-024-01455-9> , 2024.
- 3351 Peuch, V-H., Engelen, R., Rixen, M., Dee, D., Flemming, J., Suttie, M., Ades, M., Agustí-Panareda, A., Ananasso,  
3352 C., Andersson, E., Armstrong, D., Barré, J., Nicolas Bousserez, N., Dominguez, J. J., Garrigues, S., Inness, A.,

Formatted: Header

Deleted: . :

Deleted: Liu, S.,

Deleted: doi:10.1029/2001JD001102,

Deleted: ,

Deleted: ,

Deleted: <https://doi.org/10.5194/acp-18-16747-2018>,

Formatted: Normal5, Pattern: Clear (Background 1)

Formatted: Normal5

Deleted: 39

Formatted: Normal5, Right: 0,63 cm

Formatted: Page Number



- Jones, L., Kipling, Z., Letertre-Danczak, J., Parrington, M., Razinger, M., Ribas, R., Vermoote, S., Yang, X., Simmons, A., Garcés de Marcilla, J., and Thépaut, J.-N.: The Copernicus Atmosphere Monitoring Service: From Research to Operations, BAMS, E2650–E2668, <https://doi.org/10.1175/BAMS-D-21-0314.1>, 2024.
- Reay, D. S., Dentener, F., Smith, P., Grace, J., and Feely, R. A.: Global nitrogen deposition and carbon sinks, Nat. Geosci., 1, 430–437, 2008.
- Renner, E and Wolke, R.: Modelling the formation and atmospheric transport of secondary inorganic aerosols with special attention to regions with high ammonia emissions, Atmos. Environ., 44(15), <https://doi.org/10.1016/j.atmosenv.2010.02.018>, 2010.
- Rémy, S., Kipling, Z., Flemming, J., Boucher, O., Nabat, P., Michou, M., Bozzo, A., Ades, M., Huijnen, V., Benedetti, A., Engelen, R., Peuch, V.-H., and Morcrette, J.-J.: Description and evaluation of the tropospheric aerosol scheme in the European Centre for Medium-Range Weather Forecasts (ECMWF) Integrated Forecasting System (IFS-AER, cycle 45R1), Geosci. Model Dev., 12, 4627–4659, <https://doi.org/10.5194/gmd-12-4627-2019>, 2019.
- Rémy, S., Kipling, Z., Huijnen, V., Flemming, J., Nabat, P., Michou, M., Ades, M., Engelen, R., and Peuch, V.-H.: Description and evaluation of the tropospheric aerosol scheme in the Integrated Forecasting System (IFS-AER, cycle 47R1) of ECMWF, Geosci. Model Dev., 15, 4881–4912, <https://doi.org/10.5194/gmd-15-4881-2022>, 2022.
- Rémy, S., Metzger, S., Huijnen, V., Williams, J. E. and Flemming, J.: An improved representation of aerosol in the ECMWF IFS-COMPO 49R1 through the integration of EQSAM4Climv12 – a first attempt at simulating aerosol acidity, Geosci. Model Dev., 17, 7539–7567, <https://doi.org/10.5194/gmd-17-7539-2024>, 2024.
- Seinfeld, J. and Pandis, S.: Atmospheric Chemistry and Physics: From Air Pollution to Climate Change - second edition, New Jersey: John Wiley and Sons, 2006.
- Shah, V., Jacob, D. J., Moch, J. M., Wang, X., and Zhai, S.: Global modeling of cloud water acidity, precipitation acidity, and acid inputs to ecosystems, Atmos. Chem. Phys., 20, 12 223–12 245, <https://doi.org/10.5194/acp-20-12223-2020>, 2020.
- Sharma, S. K., Singh, A. K., Saud, T., Mandal, T. K., Saxena, M., Singh, S., Ghosh, S. K., and Raha, S.: Measurement of ambient NH<sub>3</sub> over Bay of Bengal during W\_ICARB Campaign, Ann. Geophys., 30, 371–377, <https://doi.org/10.5194/angeo-30-371-2012>, 2012.
- Sharma, S., Chandra, M., and Kota, S.H.: Health Effects Associated with PM<sub>2.5</sub>: a Systematic Review, Curr Pollution Rep 6, 345–367, <https://doi.org/10.1007/s40726-020-00155-3>, 2020.
- Shephard, M. W., Cady-Pereira, K. E., Luo, M., Henze, D. K., Pinder, R. W., Walker, J. T., Rinsland, C. P., Bash, J. O., Zhu, L., Payne, V. H., and Clarisse, L.: TES ammonia retrieval strategy and global observations of the spatial and seasonal variability of ammonia, Atmos. Chem. Phys., 11, 10743–10763, <https://doi.org/10.5194/acp-11-10743-2011>, 2011.
- Shi, G., Xu, J., Shi, X., Liu, B., Bi, X., Xiao, Z., et al: Aerosol pH dynamics during haze periods in an urban environment in China: Use of detailed, hourly, speciated observations to study the role of ammonia availability and secondary aerosol formation and urban environment. Journal of Geophysical Research:Atmospheres, 124, 9730–9742. <https://doi.org/10.1029/2018JD029976>, 2019.
- Sindelarova, K., Markova, J., Simpson, D., Huszar, P., Karlicky, J., Darras, S., and Granier, C.: High-resolution biogenic global emission inventory for the time period 2000–2019 for air quality modelling, Earth Syst. Sci. Data, 14, 251–270, <https://doi.org/10.5194/essd-14-251-2022>, 2022.
- Simpson, D, Aas, W., Bartnicki, J., Berge, H., Bleeker, A., Cuvelier, C., Dentener, F., Dore, A., Erisman, J.-W., Fagerli, H., Flechard, C., Hertel, O., Jaarsveld, H., Jenkin, M.E., Schaap, M. Smeena, V.S., Thunis, P., Vautard, R. and Vieno, M.: Atmospheric transport and deposition of reactive nitrogen in Europe. The European Nitrogen Assessment, 298-316, doi:10.1017/CBO9780511976988.017, 2010.

Formatted: Header

Deleted: . :

Moved (insertion) [5]

Deleted: Rémy, S.,

Formatted: Not Highlight

Moved up [5]: Renner, E and Wolke, R.: Modelling the formation and atmospheric transport of secondary inorganic aerosols with special attention to regions with high ammonia emissions, Atmos. Environ., 44(15), <https://doi.org/10.1016/j.atmosenv.2010.02.018>, 2010.¶ Rémy, S., Rémy, S.,

Deleted: Representation and impact

Formatted: Not Highlight

Formatted

Deleted: acidity

Formatted

Deleted: cycle

Deleted: EQSAM4Clim vXX

Formatted

Formatted: Font: Not Italic

Formatted: Not Highlight

Formatted: Not Highlight

Formatted: Font: Bold,

Formatted: Normal5

Deleted: .

Deleted:

Deleted: 39

Formatted: Normal5, Right: 0,63 cm

Formatted: Page Number

Simpson, R. M. C., S. G. Howell, B. W. Blomquist, A. D. Clarke, and B. J. Huebert, Dimethyl sulfide: ~~Less~~ important than long-range transport as a source of sulfate to the remote tropical Pacific marine boundary layer, *J. Geophys. Res. Atmos.*, 119, 9142–9167, doi:10.1002/2014JD021643, 2014.

Soulie, A., Granier, C., Darras, S., Zilbermann, N., Doumbia, T., Guevara, M., Jalkanen, J.-P., Keita, S., Liousse, C., Crippa, M., Guizzardi, D., Hoesly, R., and Smith, S.: Global Anthropogenic Emissions (CAMS-GLOB-ANT) for the Copernicus Atmosphere Monitoring Service Simulations of Air Quality Forecasts and Reanalyses, *Earth Syst. Sci. Data*, 16, 2261–2279, <https://doi.org/10.5194/essd-16-2261-2024>, 2024.

Sun, Y., Guo, G., Li, Y., Luo, G., Li, L., Yuan, H., Mur, L. A. J. and Guo, S.: Negative effects of the simulated nitrogen deposition on plant phenolic metabolism: A meta-analysis, *Sci. Total Environ.*, 19, 137–142, 2020.

Tan, J., Fu, J. S., Dentener, F., Sun, J., Emmons, L., Tilmes, S., Sudo, K., Flemming, J., Jonson, J. E., Gravel, S., Bian, H., Davila, Y., Henze, D. K., Lund, M. T., Kucsera, T., Takemura, T., and Keating, T.: Multi-model study of HTAP II on sulphur and nitrogen deposition, *Atmos. Chem. Phys.*, 18, 6847–6866, <https://doi.org/10.5194/acp-18-6847-2018>, 2018.

Tang, Y. S., Flechard, C. R., Dämmgen, U., Vidic, S., Djuricic, V., Mitosinkova, M., Uggerud, H. T., Sanz, M. J., Simmons, I., Dragosits, U., Nemitz, E., Twigg, M., van Dijk, N., Fauvel, Y., Sanz, F., Ferm, M., Perrino, C., Catrambone, M., Leaver, D., Braban, C. F., Cape, J. N., Heal, M. R., and Sutton, M. A.: Pan-European rural monitoring network shows dominance of NH<sub>3</sub> gas and NH<sub>4</sub>NO<sub>3</sub> aerosol in inorganic atmospheric pollution load, *Atmos. Chem. Phys.*, 21, 875–914, <https://doi.org/10.5194/acp-21-875-2021>, 2021.

Tichý, O., Eckhardt, S., Balkanski, Y., Hauglustaine, D., and Evangelizou, N.: Decreasing trends of ammonia emissions over Europe seen from remote sensing and inverse modelling, *Atmos. Chem. Phys.*, 23, 15235–15252, <https://doi.org/10.5194/acp-23-15235-2023>, 2023.

Tørseth, K., Aas, W., Breivik, K., Fjæraa, A. M., Fiebig, M., Hjellbrekke, A. G., Lund Myhre, C., Solberg, S., and Yttri, K. E.: Introduction to the European Monitoring and Evaluation Programme (EMEP) and observed atmospheric composition change during 1972–2009, *Atmos. Chem. Phys.*, 12, 5447–5481, <https://doi.org/10.5194/acp-12-5447-2012>, 2012.

Turnock, S. T., Mann, G. W., Woodhouse, M. T., Dalvi, M., O'Connor, F. M., Carslaw, K. S., and Spracklen, D. V.: The impact of changes in cloud water pH on aerosol radiative forcing, *Geophys. Res. Lett.*, 46, 4039–4048, <https://doi.org/10.1029/2019GL082067>, 2019.

Ting, Y. C., Young, L. H., Lin, T. H., Tsay, S. C., Chang, K. E. and Hsiao, T. C.: Quantifying the impacts of PM<sub>2.5</sub> constituents and relative humidity on visibility impairment in a suburban area of eastern Asia using long-term in-situ measurements. *Sci Total Environ.* 2022 Apr 20;818:151759. doi: 10.1016/j.scitotenv.2021.151759. Epub 2021 Nov 22. PMID: 34822889, 2022.

Tørseth, K., Aas, W., Breivik, K., Fjæraa, A. M., Fiebig, M., Hjellbrekke, A. G., Lund-Myrhe, C., Solberg, S. and Yttri, K. E.: Introduction to the European Monitoring and Evaluation Programme (EMEP) and observed atmospheric composition change during 1972–2009, *Atmos. Chem. Phys.*, 12, pp. 5447–5481, 2012.

van Noije, T. P. C., Le Sager, P., Segers, A. J., van Velthoven, P. F. J., Krol, M. C., Hazeleger, W., Williams, A. G., and Chambers, S. D.: Simulation of tropospheric chemistry and aerosols with the climate model EC-Earth, *Geosci. Model Dev.*, 7, 2435–2475, <https://doi.org/10.5194/gmd-7-2435-2014>, 2014.

Verheggen, B., Cozic, J., Weingartner, E., Bower, K., Mertes, S., Connolly, P., Gallagher, M., Flynn, M., Choularton, T., and Baltensperger, U.: Aerosol partitioning between the interstitial and the condensed phase in mixed-phase clouds, *Journal of Geophysical Research: Atmospheres*, 112, <https://doi.org/https://doi.org/10.1029/2007JD008714>, 2007.

Verstraeten, W. W., Boersma, K. F., Douros, J., Williams, J. E., Eskes, H., Liu, F., Beirle, S. and Delcloo, A.: Top-Down NO<sub>x</sub> Emissions of European Cities Based on the Downwind Plume of Modelled and Space-Borne Tropospheric NO<sub>2</sub> Columns, *Sensors*, 18, 2893, <http://dx.doi.org/10.3390/s18092893>, 2018.

Formatted: Header

Deleted: Lessimportant

Deleted:

Deleted: . ,

Deleted: 39

Formatted: Normal5, Right: 0,63 cm

Formatted: Page Number

3468 Vestreng, V., Myhre, G., Fagerli, H., Reis, S., and Tarrasón, L.: Twenty-five years of continuous sulphur dioxide  
 3469 emission reduction in Europe, *Atmos. Chem. Phys.*, 7, 3663–3681, <https://doi.org/10.5194/acp-7-3663-2007>,  
 3470 2007.

3471 Vieno, M., Heal, M. R., Hallsworth, S., Famulari, D., Doherty, R. M., Dore, A. J., Tang, Y. S., Braban, C. F.,  
 3472 Leaver, D., Sutton, M. A., and Reis, S.: The role of long-range transport and domestic emissions in determining  
 3473 atmospheric secondary inorganic particle concentrations across the UK, *Atmos. Chem. Phys.*, 14, 8435–8447,  
 3474 <https://doi.org/10.5194/acp-14-8435-2014>, 2014.

3475 Vinken, G. C. M., Boersma, K. F., Jacob, D. J., & Meijer, E. W.: Accounting for non-linear chemistry of ship  
 3476 plumes in the GEOS-Chem global chemistry transport model. *Atmospheric Chemistry and Physics*, 11(22), 11707–  
 3477 11722. <https://doi.org/10.5194/acp-11-11707-2011>, 2011.

3478 Wang, J., Xu, J., He, Y., Chen, Y., and Meng, F.: Long range transport of nitrate in the low atmosphere over  
 3479 Northeast Asia, *Atmos. Environ.*, 144, 315–324, <https://doi.org/10.1016/j.atmosenv.2016.08.084>, 2016.

3480 Wang, R., Pan, D., Guo, X., Sun, K., Clarisse, L., Van Damme, M., Coheur, P.-F., Clerbaux, C., Puchalski, M.,  
 3481 and Zondlo, M. A.: Bridging the spatial gaps of the Ammonia Monitoring Network using satellite ammonia  
 3482 measurements, *Atmos. Chem. Phys.*, 23, 13217–13234, <https://doi.org/10.5194/acp-23-13217-2023>, 2023.

3483 Williams, J. E., van der Swaluw, E., de Vries, W. J., Sauter, F. J., van Pul, W.A.J. and Hoogerbrugge, R.:  
 3484 Modelling the future distribution of ammonium nitrate concentrations in The Netherlands for 2020: The sensitivity  
 3485 to meteorological parameters, *Atmos. Environm.*, Volume: 115, 278–285, [doi: 10.1016/j.atmosenv.2015.06.001](https://doi.org/10.1016/j.atmosenv.2015.06.001),  
 3486 2015.

3487 Williams, J. E. ., Huijnen, V., Bouarar, I., Meziane, M., Schreurs, T., Pelletier, S., Marécal, V., Josse, B., and  
 3488 Flemming, J.: Regional evaluation of the performance of the global CAMS chemical modeling system over the  
 3489 United States (IFS cycle 47R1), *Geosci. Model Dev.*, 15, 4657–4687, <https://doi.org/10.5194/gmd-15-4657-2022>,  
 3490 2022.

3491 Ye, X., Arab, P., Ahmadov, R., James, E., Grell, G. A., Pierce, B., Kumar, A., Makar, P., Chen, J., Davignon, D.,  
 3492 Carmichael, G. R., Ferrada, G., McQueen, J., Huang, J., Kumar, R., Emmons, L., Herron-Thorpe, F. L., Parrington,  
 3493 M., Engelen, R., Peuch, V.-H., da Silva, A., Soja, A., Gargulinski, E., Wiggins, E., Hair, J. W., Fenn, M., Shingler,  
 3494 T., Kondragunta, S., Lyapustin, A., Wang, Y., Holben, B., Giles, D. M., and Saide, P. E.: Evaluation and  
 3495 intercomparison of wildfire smoke forecasts from multiple modeling systems for the 2019 Williams Flats fire,  
 3496 *Atmos. Chem. Phys.*, 21, 14427–14469, <https://doi.org/10.5194/acp-21-14427-2021>, 2021

3497 Zhang, L., Jacob, D. J., Knipping, E. M., Kumar, N., Munger, J. W., Carouge, C. C., van Donkelaar, A., Wang, Y.  
 3498 X., and Chen, D.: Nitrogen deposition to the United States: distribution, sources, and processes, *Atmos. Chem.*  
 3499 *Phys.*, 12, 4539–4554, <https://doi.org/10.5194/acp-12-4539-2012>, 2012.

3500

3501

Formatted: Header

Deleted:

Deleted: 39

Formatted: Normal5, Right: 0,63 cm

Formatted: Page Number

39

Page 1: [1] Style Definition J.E. Williams 06/08/2025 12:24:00

Subtitle: (Asian) Japanese, Border: Top: (No border), Bottom: (No border), Left: (No border), Right: (No border), Between : (No border)

Page 1: [2] Style Definition J.E. Williams 06/08/2025 12:24:00

Title: Font: (Default) Calibri, (Asian) Japanese, Not Expanded by / Condensed by , Add space between paragraphs of the same style

Page 1: [3] Style Definition J.E. Williams 06/08/2025 12:24:00

Heading 6: Font colour: Black, (Asian) Japanese, Border: Top: (No border), Bottom: (No border), Left: (No border), Right: (No border), Between : (No border)

Page 1: [4] Formatted J.E. Williams 06/08/2025 12:24:00

Font: 16 pt, Not Bold, Font colour: Auto, Pattern: Clear

Page 1: [5] Formatted J.E. Williams 06/08/2025 12:24:00

Font: 16 pt, Not Bold, Font colour: Auto, Pattern: Clear

Page 3: [6] Deleted J.E. Williams 06/08/2025 12:24:00

▼

Page 3: [6] Deleted J.E. Williams 06/08/2025 12:24:00

▼

Page 3: [6] Deleted J.E. Williams 06/08/2025 12:24:00

▼

Page 3: [6] Deleted J.E. Williams 06/08/2025 12:24:00

▼

Page 3: [6] Deleted J.E. Williams 06/08/2025 12:24:00

▼

Page 3: [7] Deleted J.E. Williams 06/08/2025 12:24:00

▼

Page 3: [7] Deleted J.E. Williams 06/08/2025 12:24:00

▼

Page 3: [7] Deleted J.E. Williams 06/08/2025 12:24:00

▼

Page 3: [7] Deleted J.E. Williams 06/08/2025 12:24:00

▼

Page 3: [7] Deleted J.E. Williams 06/08/2025 12:24:00



▼.....  

Page 3: [7] Deleted	J.E. Williams	06/08/2025 12:24:00
---------------------	---------------	---------------------

▼.....  

Page 3: [7] Deleted	J.E. Williams	06/08/2025 12:24:00
---------------------	---------------	---------------------

▼.....  

Page 3: [7] Deleted	J.E. Williams	06/08/2025 12:24:00
---------------------	---------------	---------------------

▼.....  

Page 3: [7] Deleted	J.E. Williams	06/08/2025 12:24:00
---------------------	---------------	---------------------

▼.....  

Page 3: [7] Deleted	J.E. Williams	06/08/2025 12:24:00
---------------------	---------------	---------------------

▼.....  

Page 3: [7] Deleted	J.E. Williams	06/08/2025 12:24:00
---------------------	---------------	---------------------

▼.....  

Page 3: [7] Deleted	J.E. Williams	06/08/2025 12:24:00
---------------------	---------------	---------------------

▼.....  

Page 3: [8] Deleted	J.E. Williams	06/08/2025 12:24:00
---------------------	---------------	---------------------

▼.....  

Page 3: [8] Deleted	J.E. Williams	06/08/2025 12:24:00
---------------------	---------------	---------------------

▼.....  

Page 3: [8] Deleted	J.E. Williams	06/08/2025 12:24:00
---------------------	---------------	---------------------

▼.....  

Page 3: [8] Deleted	J.E. Williams	06/08/2025 12:24:00
---------------------	---------------	---------------------

▼.....  

Page 3: [8] Deleted	J.E. Williams	06/08/2025 12:24:00
---------------------	---------------	---------------------

▼.....  

Page 3: [9] Deleted	J.E. Williams	06/08/2025 12:24:00
---------------------	---------------	---------------------

▼.....  

Page 3: [9] Deleted	J.E. Williams	06/08/2025 12:24:00
---------------------	---------------	---------------------

▼.....  

Page 3: [9] Deleted	J.E. Williams	06/08/2025 12:24:00
---------------------	---------------	---------------------

Page 3: [9] Deleted	J.E. Williams	06/08/2025 12:24:00
---------------------	---------------	---------------------

▼

Page 3: [9] Deleted	J.E. Williams	06/08/2025 12:24:00
---------------------	---------------	---------------------

▼

Page 3: [9] Deleted	J.E. Williams	06/08/2025 12:24:00
---------------------	---------------	---------------------

▼

Page 3: [9] Deleted	J.E. Williams	06/08/2025 12:24:00
---------------------	---------------	---------------------

▼

Page 3: [9] Deleted	J.E. Williams	06/08/2025 12:24:00
---------------------	---------------	---------------------

▼

Page 3: [9] Deleted	J.E. Williams	06/08/2025 12:24:00
---------------------	---------------	---------------------

▼

Page 3: [9] Deleted	J.E. Williams	06/08/2025 12:24:00
---------------------	---------------	---------------------

▼

Page 3: [9] Deleted	J.E. Williams	06/08/2025 12:24:00
---------------------	---------------	---------------------

▼

Page 3: [10] Deleted	J.E. Williams	06/08/2025 12:24:00
----------------------	---------------	---------------------

▼

Page 3: [10] Deleted	J.E. Williams	06/08/2025 12:24:00
----------------------	---------------	---------------------

▼

Page 3: [10] Deleted	J.E. Williams	06/08/2025 12:24:00
----------------------	---------------	---------------------

▼

Page 3: [10] Deleted	J.E. Williams	06/08/2025 12:24:00
----------------------	---------------	---------------------

▼

Page 3: [10] Deleted	J.E. Williams	06/08/2025 12:24:00
----------------------	---------------	---------------------

▼

Page 3: [10] Deleted	J.E. Williams	06/08/2025 12:24:00
----------------------	---------------	---------------------

▼

Page 3: [10] Deleted	J.E. Williams	06/08/2025 12:24:00
----------------------	---------------	---------------------

▼

Page 3: [10] Deleted	J.E. Williams	06/08/2025 12:24:00
----------------------	---------------	---------------------

▼

Page 3: [10] Deleted	J.E. Williams	06/08/2025 12:24:00
----------------------	---------------	---------------------

▼

Page 3: [10] Deleted	J.E. Williams	06/08/2025 12:24:00
----------------------	---------------	---------------------

▼

Page 3: [11] Deleted	J.E. Williams	06/08/2025 12:24:00
----------------------	---------------	---------------------

▼

Page 3: [11] Deleted	J.E. Williams	06/08/2025 12:24:00
----------------------	---------------	---------------------

▼

Page 4: [12] Deleted	J.E. Williams	06/08/2025 12:24:00
----------------------	---------------	---------------------

▼

Page 1: [13] Formatted	J.E. Williams	06/08/2025 12:24:00
------------------------	---------------	---------------------

Header

Page 1: [14] Formatted	J.E. Williams	06/08/2025 12:24:00
------------------------	---------------	---------------------

Page Number

Page 1: [15] Formatted	J.E. Williams	06/08/2025 12:24:00
------------------------	---------------	---------------------

Normal5, Right: 0,63 cm

Page 6: [16] Deleted	J.E. Williams	06/08/2025 12:24:00
----------------------	---------------	---------------------

▼

Page 6: [17] Deleted	J.E. Williams	06/08/2025 12:24:00
----------------------	---------------	---------------------

▼

Page 6: [18] Deleted	J.E. Williams	06/08/2025 12:24:00
----------------------	---------------	---------------------

▼

Page 6: [19] Deleted	J.E. Williams	06/08/2025 12:24:00
----------------------	---------------	---------------------

▼

Page 6: [20] Deleted	J.E. Williams	06/08/2025 12:24:00
----------------------	---------------	---------------------

▼

Page 6: [21] Deleted	J.E. Williams	06/08/2025 12:24:00
----------------------	---------------	---------------------

▼

Page 6: [22] Deleted	J.E. Williams	06/08/2025 12:24:00
----------------------	---------------	---------------------

▼

Page 6: [23] Deleted	J.E. Williams	06/08/2025 12:24:00
----------------------	---------------	---------------------

▼





▼.....

Page 9: [30] Deleted	J.E. Williams	06/08/2025 12:24:00
----------------------	---------------	---------------------

▼.....

Page 1: [31] Formatted	J.E. Williams	06/08/2025 12:24:00
------------------------	---------------	---------------------

Header

Page 1: [32] Formatted	J.E. Williams	06/08/2025 12:24:00
------------------------	---------------	---------------------

Page Number

Page 1: [33] Formatted	J.E. Williams	06/08/2025 12:24:00
------------------------	---------------	---------------------

Normal5, Right: 0,63 cm

Page 15: [34] Formatted	J.E. Williams	06/08/2025 12:24:00
-------------------------	---------------	---------------------

Normal5

Page 15: [35] Deleted	J.E. Williams	06/08/2025 12:24:00
-----------------------	---------------	---------------------

▼.....

Page 15: [36] Deleted	J.E. Williams	06/08/2025 12:24:00
-----------------------	---------------	---------------------

Page 15: [37] Deleted	J.E. Williams	06/08/2025 12:24:00
-----------------------	---------------	---------------------

▼.....

Page 15: [38] Formatted	J.E. Williams	06/08/2025 12:24:00
-------------------------	---------------	---------------------

Normal5

Page 15: [39] Formatted Table	J.E. Williams	06/08/2025 12:24:00
-------------------------------	---------------	---------------------

Formatted Table

Page 15: [40] Formatted	J.E. Williams	06/08/2025 12:24:00
-------------------------	---------------	---------------------

Normal5

Page 15: [41] Formatted	J.E. Williams	06/08/2025 12:24:00
-------------------------	---------------	---------------------

Normal5

Page 15: [42] Formatted	J.E. Williams	06/08/2025 12:24:00
-------------------------	---------------	---------------------

Normal5

Page 17: [43] Deleted	J.E. Williams	06/08/2025 12:24:00
-----------------------	---------------	---------------------

▼.....

Page 17: [43] Deleted	J.E. Williams	06/08/2025 12:24:00
-----------------------	---------------	---------------------

▼.....

Page 17: [43] Deleted	J.E. Williams	06/08/2025 12:24:00
-----------------------	---------------	---------------------

▼.....

Page 17: [43] Deleted	J.E. Williams	06/08/2025 12:24:00
-----------------------	---------------	---------------------

▼.....

Page 17: [44] Deleted	J.E. Williams	06/08/2025 12:24:00
-----------------------	---------------	---------------------

▼.....

Page 17: [44] Deleted	J.E. Williams	06/08/2025 12:24:00
-----------------------	---------------	---------------------

▼.....

Page 17: [44] Deleted	J.E. Williams	06/08/2025 12:24:00
-----------------------	---------------	---------------------

▼.....

Page 17: [44] Deleted	J.E. Williams	06/08/2025 12:24:00
-----------------------	---------------	---------------------

▼.....

Page 17: [44] Deleted	J.E. Williams	06/08/2025 12:24:00
-----------------------	---------------	---------------------

▼.....

Page 17: [44] Deleted	J.E. Williams	06/08/2025 12:24:00
-----------------------	---------------	---------------------

▼.....

Page 17: [44] Deleted	J.E. Williams	06/08/2025 12:24:00
-----------------------	---------------	---------------------

▼.....

Page 20: [45] Deleted	J.E. Williams	06/08/2025 12:24:00
-----------------------	---------------	---------------------

▼.....

Page 20: [45] Deleted	J.E. Williams	06/08/2025 12:24:00
-----------------------	---------------	---------------------

▼.....

Page 20: [46] Deleted	J.E. Williams	06/08/2025 12:24:00
-----------------------	---------------	---------------------

▼.....

Page 20: [46] Deleted	J.E. Williams	06/08/2025 12:24:00
-----------------------	---------------	---------------------

▼.....

Page 20: [46] Deleted	J.E. Williams	06/08/2025 12:24:00
-----------------------	---------------	---------------------

▼.....

Page 20: [46] Deleted	J.E. Williams	06/08/2025 12:24:00
-----------------------	---------------	---------------------

▼.....

Page 20: [47] Deleted	J.E. Williams	06/08/2025 12:24:00
-----------------------	---------------	---------------------

▼.....

Page 20: [47] Deleted	J.E. Williams	06/08/2025 12:24:00
-----------------------	---------------	---------------------

Page 20: [47] Deleted	J.E. Williams	06/08/2025 12:24:00
-----------------------	---------------	---------------------

Page 20: [47] Deleted	J.E. Williams	06/08/2025 12:24:00
-----------------------	---------------	---------------------

Page 20: [47] Deleted	J.E. Williams	06/08/2025 12:24:00
-----------------------	---------------	---------------------

Page 20: [47] Deleted	J.E. Williams	06/08/2025 12:24:00
-----------------------	---------------	---------------------

Page 20: [47] Deleted	J.E. Williams	06/08/2025 12:24:00
-----------------------	---------------	---------------------

Page 20: [47] Deleted	J.E. Williams	06/08/2025 12:24:00
-----------------------	---------------	---------------------

Page 20: [47] Deleted	J.E. Williams	06/08/2025 12:24:00
-----------------------	---------------	---------------------

Page 20: [47] Deleted	J.E. Williams	06/08/2025 12:24:00
-----------------------	---------------	---------------------

Page 20: [47] Deleted	J.E. Williams	06/08/2025 12:24:00
-----------------------	---------------	---------------------

Page 20: [47] Deleted	J.E. Williams	06/08/2025 12:24:00
-----------------------	---------------	---------------------

Page 20: [47] Deleted	J.E. Williams	06/08/2025 12:24:00
-----------------------	---------------	---------------------

Page 20: [47] Deleted	J.E. Williams	06/08/2025 12:24:00
-----------------------	---------------	---------------------

Page 20: [47] Deleted	J.E. Williams	06/08/2025 12:24:00
-----------------------	---------------	---------------------

Page 20: [47] Deleted	J.E. Williams	06/08/2025 12:24:00
-----------------------	---------------	---------------------

Page 20: [47] Deleted	J.E. Williams	06/08/2025 12:24:00
-----------------------	---------------	---------------------

▼.....  

Page 20: [47] Deleted	J.E. Williams	06/08/2025 12:24:00
-----------------------	---------------	---------------------

▼.....  

Page 20: [48] Deleted	J.E. Williams	06/08/2025 12:24:00
-----------------------	---------------	---------------------

▼.....  

Page 20: [48] Deleted	J.E. Williams	06/08/2025 12:24:00
-----------------------	---------------	---------------------

▼.....  

Page 20: [48] Deleted	J.E. Williams	06/08/2025 12:24:00
-----------------------	---------------	---------------------

▼.....  

Page 20: [48] Deleted	J.E. Williams	06/08/2025 12:24:00
-----------------------	---------------	---------------------

▼.....  

Page 20: [48] Deleted	J.E. Williams	06/08/2025 12:24:00
-----------------------	---------------	---------------------

▼.....  

Page 20: [48] Deleted	J.E. Williams	06/08/2025 12:24:00
-----------------------	---------------	---------------------

▼.....  

Page 20: [48] Deleted	J.E. Williams	06/08/2025 12:24:00
-----------------------	---------------	---------------------

▼.....  

Page 20: [48] Deleted	J.E. Williams	06/08/2025 12:24:00
-----------------------	---------------	---------------------

▼.....  

Page 20: [48] Deleted	J.E. Williams	06/08/2025 12:24:00
-----------------------	---------------	---------------------

▼.....  

Page 20: [48] Deleted	J.E. Williams	06/08/2025 12:24:00
-----------------------	---------------	---------------------

▼.....  

Page 20: [48] Deleted	J.E. Williams	06/08/2025 12:24:00
-----------------------	---------------	---------------------

▼.....  

Page 20: [48] Deleted	J.E. Williams	06/08/2025 12:24:00
-----------------------	---------------	---------------------

▼.....  

Page 20: [48] Deleted	J.E. Williams	06/08/2025 12:24:00
-----------------------	---------------	---------------------

▼.....  

Page 20: [48] Deleted	J.E. Williams	06/08/2025 12:24:00
-----------------------	---------------	---------------------



Page 21: [49] Deleted	J.E. Williams	06/08/2025 12:24:00
-----------------------	---------------	---------------------

▼

Page 21: [49] Deleted	J.E. Williams	06/08/2025 12:24:00
-----------------------	---------------	---------------------

▼

Page 21: [49] Deleted	J.E. Williams	06/08/2025 12:24:00
-----------------------	---------------	---------------------

▼

Page 21: [50] Deleted	J.E. Williams	06/08/2025 12:24:00
-----------------------	---------------	---------------------

▼

Page 21: [50] Deleted	J.E. Williams	06/08/2025 12:24:00
-----------------------	---------------	---------------------

▼

Page 21: [50] Deleted	J.E. Williams	06/08/2025 12:24:00
-----------------------	---------------	---------------------

▼

Page 21: [50] Deleted	J.E. Williams	06/08/2025 12:24:00
-----------------------	---------------	---------------------

▼

Page 21: [50] Deleted	J.E. Williams	06/08/2025 12:24:00
-----------------------	---------------	---------------------

▼

Page 21: [50] Deleted	J.E. Williams	06/08/2025 12:24:00
-----------------------	---------------	---------------------

▼

Page 21: [50] Deleted	J.E. Williams	06/08/2025 12:24:00
-----------------------	---------------	---------------------

▼

Page 21: [50] Deleted	J.E. Williams	06/08/2025 12:24:00
-----------------------	---------------	---------------------

▼

Page 21: [50] Deleted	J.E. Williams	06/08/2025 12:24:00
-----------------------	---------------	---------------------

▼

Page 21: [50] Deleted	J.E. Williams	06/08/2025 12:24:00
-----------------------	---------------	---------------------

▼

Page 21: [51] Deleted	J.E. Williams	06/08/2025 12:24:00
-----------------------	---------------	---------------------

▼

Page 21: [51] Deleted	J.E. Williams	06/08/2025 12:24:00
-----------------------	---------------	---------------------

▼

Page 21: [51] Deleted	J.E. Williams	06/08/2025 12:24:00
-----------------------	---------------	---------------------

▼

Page 21: [51] Deleted	J.E. Williams	06/08/2025 12:24:00
-----------------------	---------------	---------------------

Page 21: [51] Deleted	J.E. Williams	06/08/2025 12:24:00
-----------------------	---------------	---------------------

Page 21: [51] Deleted	J.E. Williams	06/08/2025 12:24:00
-----------------------	---------------	---------------------

Page 21: [51] Deleted	J.E. Williams	06/08/2025 12:24:00
-----------------------	---------------	---------------------

Page 21: [51] Deleted	J.E. Williams	06/08/2025 12:24:00
-----------------------	---------------	---------------------

Page 21: [51] Deleted	J.E. Williams	06/08/2025 12:24:00
-----------------------	---------------	---------------------

Page 21: [51] Deleted	J.E. Williams	06/08/2025 12:24:00
-----------------------	---------------	---------------------

Page 22: [52] Deleted	J.E. Williams	06/08/2025 12:24:00
-----------------------	---------------	---------------------

Page 22: [52] Deleted	J.E. Williams	06/08/2025 12:24:00
-----------------------	---------------	---------------------

Page 22: [52] Deleted	J.E. Williams	06/08/2025 12:24:00
-----------------------	---------------	---------------------

Page 22: [53] Deleted	J.E. Williams	06/08/2025 12:24:00
-----------------------	---------------	---------------------

Page 22: [53] Deleted	J.E. Williams	06/08/2025 12:24:00
-----------------------	---------------	---------------------

Page 22: [53] Deleted	J.E. Williams	06/08/2025 12:24:00
-----------------------	---------------	---------------------

Page 22: [53] Deleted	J.E. Williams	06/08/2025 12:24:00
-----------------------	---------------	---------------------

Page 22: [53] Deleted	J.E. Williams	06/08/2025 12:24:00
-----------------------	---------------	---------------------

Page 22: [53] Deleted	J.E. Williams	06/08/2025 12:24:00
-----------------------	---------------	---------------------

▼.....

Page 1: [54] Formatted	J.E. Williams	06/08/2025 12:24:00
------------------------	---------------	---------------------

Header

Page 1: [55] Formatted	J.E. Williams	06/08/2025 12:24:00
------------------------	---------------	---------------------

Page Number

Page 1: [56] Formatted	J.E. Williams	06/08/2025 12:24:00
------------------------	---------------	---------------------

Normal5, Right: 0,63 cm

Page 23: [57] Formatted Table	J.E. Williams	06/08/2025 12:24:00
-------------------------------	---------------	---------------------

Formatted Table

Page 24: [58] Formatted	J.E. Williams	06/08/2025 12:24:00
-------------------------	---------------	---------------------

Normal5

Page 24: [59] Formatted	J.E. Williams	06/08/2025 12:24:00
-------------------------	---------------	---------------------

Normal5

Page 24: [60] Formatted	J.E. Williams	06/08/2025 12:24:00
-------------------------	---------------	---------------------

Normal5

Page 24: [61] Formatted	J.E. Williams	06/08/2025 12:24:00
-------------------------	---------------	---------------------

Normal5

Page 24: [62] Formatted	J.E. Williams	06/08/2025 12:24:00
-------------------------	---------------	---------------------

Normal5

Page 24: [63] Formatted Table	J.E. Williams	06/08/2025 12:24:00
-------------------------------	---------------	---------------------

Formatted Table

Page 24: [64] Formatted	J.E. Williams	06/08/2025 12:24:00
-------------------------	---------------	---------------------

Normal5

Page 24: [65] Formatted	J.E. Williams	06/08/2025 12:24:00
-------------------------	---------------	---------------------

Normal5

Page 24: [66] Formatted	J.E. Williams	06/08/2025 12:24:00
-------------------------	---------------	---------------------

Normal5

Page 24: [67] Formatted	J.E. Williams	06/08/2025 12:24:00
-------------------------	---------------	---------------------

Normal5

Page 24: [68] Formatted	J.E. Williams	06/08/2025 12:24:00
-------------------------	---------------	---------------------

Normal5

Page 24: [69] Formatted	J.E. Williams	06/08/2025 12:24:00
-------------------------	---------------	---------------------

Normal5

Page 24: [70] Formatted	J.E. Williams	06/08/2025 12:24:00
-------------------------	---------------	---------------------

Normal5

Page 25: [71] Deleted	J.E. Williams	06/08/2025 12:24:00
-----------------------	---------------	---------------------

▼

Page 25: [71] Deleted	J.E. Williams	06/08/2025 12:24:00
-----------------------	---------------	---------------------

▼

Page 25: [71] Deleted	J.E. Williams	06/08/2025 12:24:00
-----------------------	---------------	---------------------

▼

Page 25: [71] Deleted	J.E. Williams	06/08/2025 12:24:00
-----------------------	---------------	---------------------

▼

Page 25: [72] Deleted	J.E. Williams	06/08/2025 12:24:00
-----------------------	---------------	---------------------

▼

Page 25: [72] Deleted	J.E. Williams	06/08/2025 12:24:00
-----------------------	---------------	---------------------

▼

Page 25: [72] Deleted	J.E. Williams	06/08/2025 12:24:00
-----------------------	---------------	---------------------

▼

Page 25: [72] Deleted	J.E. Williams	06/08/2025 12:24:00
-----------------------	---------------	---------------------

▼

Page 25: [72] Deleted	J.E. Williams	06/08/2025 12:24:00
-----------------------	---------------	---------------------

▼

Page 25: [72] Deleted	J.E. Williams	06/08/2025 12:24:00
-----------------------	---------------	---------------------

▼

Page 25: [72] Deleted	J.E. Williams	06/08/2025 12:24:00
-----------------------	---------------	---------------------

▼

Page 25: [72] Deleted	J.E. Williams	06/08/2025 12:24:00
-----------------------	---------------	---------------------

▼

Page 25: [72] Deleted	J.E. Williams	06/08/2025 12:24:00
-----------------------	---------------	---------------------

▼



Page 25: [72] Deleted	J.E. Williams	06/08/2025 12:24:00
-----------------------	---------------	---------------------

▼

Page 25: [72] Deleted	J.E. Williams	06/08/2025 12:24:00
-----------------------	---------------	---------------------

▼

Page 25: [72] Deleted	J.E. Williams	06/08/2025 12:24:00
-----------------------	---------------	---------------------

▼

Page 25: [72] Deleted	J.E. Williams	06/08/2025 12:24:00
-----------------------	---------------	---------------------

▼

Page 25: [72] Deleted	J.E. Williams	06/08/2025 12:24:00
-----------------------	---------------	---------------------

▼

Page 25: [72] Deleted	J.E. Williams	06/08/2025 12:24:00
-----------------------	---------------	---------------------

▼

Page 25: [72] Deleted	J.E. Williams	06/08/2025 12:24:00
-----------------------	---------------	---------------------

▼

Page 25: [72] Deleted	J.E. Williams	06/08/2025 12:24:00
-----------------------	---------------	---------------------

▼

Page 25: [72] Deleted	J.E. Williams	06/08/2025 12:24:00
-----------------------	---------------	---------------------

▼

Page 25: [72] Deleted	J.E. Williams	06/08/2025 12:24:00
-----------------------	---------------	---------------------

▼

Page 25: [72] Deleted	J.E. Williams	06/08/2025 12:24:00
-----------------------	---------------	---------------------

▼

Page 25: [72] Deleted	J.E. Williams	06/08/2025 12:24:00
-----------------------	---------------	---------------------

▼

Page 25: [73] Deleted	J.E. Williams	06/08/2025 12:24:00
-----------------------	---------------	---------------------

▼

Page 25: [73] Deleted	J.E. Williams	06/08/2025 12:24:00
-----------------------	---------------	---------------------

▼

Page 25: [73] Deleted	J.E. Williams	06/08/2025 12:24:00
-----------------------	---------------	---------------------

▼

Page 25: [73] Deleted	J.E. Williams	06/08/2025 12:24:00
-----------------------	---------------	---------------------

▼

Page 25: [73] Deleted	J.E. Williams	06/08/2025 12:24:00
-----------------------	---------------	---------------------

Page 25: [73] Deleted	J.E. Williams	06/08/2025 12:24:00
-----------------------	---------------	---------------------

Page 25: [73] Deleted	J.E. Williams	06/08/2025 12:24:00
-----------------------	---------------	---------------------

Page 25: [73] Deleted	J.E. Williams	06/08/2025 12:24:00
-----------------------	---------------	---------------------

Page 25: [73] Deleted	J.E. Williams	06/08/2025 12:24:00
-----------------------	---------------	---------------------

Page 25: [73] Deleted	J.E. Williams	06/08/2025 12:24:00
-----------------------	---------------	---------------------

Page 25: [73] Deleted	J.E. Williams	06/08/2025 12:24:00
-----------------------	---------------	---------------------

Page 25: [73] Deleted	J.E. Williams	06/08/2025 12:24:00
-----------------------	---------------	---------------------

Page 25: [73] Deleted	J.E. Williams	06/08/2025 12:24:00
-----------------------	---------------	---------------------

Page 25: [73] Deleted	J.E. Williams	06/08/2025 12:24:00
-----------------------	---------------	---------------------

Page 25: [73] Deleted	J.E. Williams	06/08/2025 12:24:00
-----------------------	---------------	---------------------

Page 25: [73] Deleted	J.E. Williams	06/08/2025 12:24:00
-----------------------	---------------	---------------------

Page 25: [73] Deleted	J.E. Williams	06/08/2025 12:24:00
-----------------------	---------------	---------------------

Page 25: [73] Deleted	J.E. Williams	06/08/2025 12:24:00
-----------------------	---------------	---------------------

Page 25: [73] Deleted	J.E. Williams	06/08/2025 12:24:00
-----------------------	---------------	---------------------

Page 25: [73] Deleted	J.E. Williams	06/08/2025 12:24:00
-----------------------	---------------	---------------------

▼.....

Page 25: [73] Deleted	J.E. Williams	06/08/2025 12:24:00
-----------------------	---------------	---------------------

▼.....

Page 25: [73] Deleted	J.E. Williams	06/08/2025 12:24:00
-----------------------	---------------	---------------------

▼.....

Page 25: [73] Deleted	J.E. Williams	06/08/2025 12:24:00
-----------------------	---------------	---------------------

▼.....

Page 25: [74] Deleted	J.E. Williams	06/08/2025 12:24:00
-----------------------	---------------	---------------------

▼.....

Page 25: [74] Deleted	J.E. Williams	06/08/2025 12:24:00
-----------------------	---------------	---------------------

▼.....

Page 25: [74] Deleted	J.E. Williams	06/08/2025 12:24:00
-----------------------	---------------	---------------------

▼.....

Page 25: [74] Deleted	J.E. Williams	06/08/2025 12:24:00
-----------------------	---------------	---------------------

▼.....

Page 25: [74] Deleted	J.E. Williams	06/08/2025 12:24:00
-----------------------	---------------	---------------------

▼.....

Page 25: [74] Deleted	J.E. Williams	06/08/2025 12:24:00
-----------------------	---------------	---------------------

▼.....

Page 25: [74] Deleted	J.E. Williams	06/08/2025 12:24:00
-----------------------	---------------	---------------------

▼.....

Page 26: [75] Deleted	J.E. Williams	06/08/2025 12:24:00
-----------------------	---------------	---------------------

▼.....

Page 27: [76] Deleted	J.E. Williams	06/08/2025 12:24:00
-----------------------	---------------	---------------------

▼.....

Page 27: [76] Deleted	J.E. Williams	06/08/2025 12:24:00
-----------------------	---------------	---------------------

▼.....

Page 27: [76] Deleted	J.E. Williams	06/08/2025 12:24:00
-----------------------	---------------	---------------------

▼.....

Page 27: [76] Deleted	J.E. Williams	06/08/2025 12:24:00
-----------------------	---------------	---------------------

Page 27: [76] Deleted	J.E. Williams	06/08/2025 12:24:00
-----------------------	---------------	---------------------

▼

Page 27: [76] Deleted	J.E. Williams	06/08/2025 12:24:00
-----------------------	---------------	---------------------

▼

Page 27: [76] Deleted	J.E. Williams	06/08/2025 12:24:00
-----------------------	---------------	---------------------

▼

Page 27: [76] Deleted	J.E. Williams	06/08/2025 12:24:00
-----------------------	---------------	---------------------

▼

Page 27: [76] Deleted	J.E. Williams	06/08/2025 12:24:00
-----------------------	---------------	---------------------

▼

Page 27: [77] Deleted	J.E. Williams	06/08/2025 12:24:00
-----------------------	---------------	---------------------

▼

Page 27: [77] Deleted	J.E. Williams	06/08/2025 12:24:00
-----------------------	---------------	---------------------

▼

Page 27: [77] Deleted	J.E. Williams	06/08/2025 12:24:00
-----------------------	---------------	---------------------

▼

Page 27: [77] Deleted	J.E. Williams	06/08/2025 12:24:00
-----------------------	---------------	---------------------

▼

Page 27: [77] Deleted	J.E. Williams	06/08/2025 12:24:00
-----------------------	---------------	---------------------

▼

Page 27: [77] Deleted	J.E. Williams	06/08/2025 12:24:00
-----------------------	---------------	---------------------

▼

Page 27: [77] Deleted	J.E. Williams	06/08/2025 12:24:00
-----------------------	---------------	---------------------

▼

Page 27: [77] Deleted	J.E. Williams	06/08/2025 12:24:00
-----------------------	---------------	---------------------

▼

Page 27: [77] Deleted	J.E. Williams	06/08/2025 12:24:00
-----------------------	---------------	---------------------

▼

Page 27: [77] Deleted	J.E. Williams	06/08/2025 12:24:00
-----------------------	---------------	---------------------

▼

Page 27: [77] Deleted	J.E. Williams	06/08/2025 12:24:00
-----------------------	---------------	---------------------



▼.....

Page 27: [77] Deleted	J.E. Williams	06/08/2025 12:24:00
-----------------------	---------------	---------------------

▼.....

Page 27: [77] Deleted	J.E. Williams	06/08/2025 12:24:00
-----------------------	---------------	---------------------

▼.....

Page 27: [77] Deleted	J.E. Williams	06/08/2025 12:24:00
-----------------------	---------------	---------------------

▼.....

Page 27: [77] Deleted	J.E. Williams	06/08/2025 12:24:00
-----------------------	---------------	---------------------

▼.....

Page 27: [77] Deleted	J.E. Williams	06/08/2025 12:24:00
-----------------------	---------------	---------------------

▼.....

Page 27: [77] Deleted	J.E. Williams	06/08/2025 12:24:00
-----------------------	---------------	---------------------

▼.....

Page 27: [78] Deleted	J.E. Williams	06/08/2025 12:24:00
-----------------------	---------------	---------------------

▼.....

Page 27: [78] Deleted	J.E. Williams	06/08/2025 12:24:00
-----------------------	---------------	---------------------

▼.....

Page 27: [78] Deleted	J.E. Williams	06/08/2025 12:24:00
-----------------------	---------------	---------------------

▼.....

Page 27: [78] Deleted	J.E. Williams	06/08/2025 12:24:00
-----------------------	---------------	---------------------

▼.....

Page 27: [78] Deleted	J.E. Williams	06/08/2025 12:24:00
-----------------------	---------------	---------------------

▼.....

Page 27: [78] Deleted	J.E. Williams	06/08/2025 12:24:00
-----------------------	---------------	---------------------

▼.....

Page 27: [78] Deleted	J.E. Williams	06/08/2025 12:24:00
-----------------------	---------------	---------------------

▼.....

Page 27: [78] Deleted	J.E. Williams	06/08/2025 12:24:00
-----------------------	---------------	---------------------

▼.....

Page 27: [78] Deleted	J.E. Williams	06/08/2025 12:24:00
-----------------------	---------------	---------------------

Page 27: [78] Deleted	J.E. Williams	06/08/2025 12:24:00
-----------------------	---------------	---------------------

▼

Page 27: [78] Deleted	J.E. Williams	06/08/2025 12:24:00
-----------------------	---------------	---------------------

▼

Page 27: [78] Deleted	J.E. Williams	06/08/2025 12:24:00
-----------------------	---------------	---------------------

▼

Page 27: [78] Deleted	J.E. Williams	06/08/2025 12:24:00
-----------------------	---------------	---------------------

▼

Page 27: [78] Deleted	J.E. Williams	06/08/2025 12:24:00
-----------------------	---------------	---------------------

▼

Page 27: [78] Deleted	J.E. Williams	06/08/2025 12:24:00
-----------------------	---------------	---------------------

▼

Page 27: [79] Deleted	J.E. Williams	06/08/2025 12:24:00
-----------------------	---------------	---------------------

▼

Page 27: [79] Deleted	J.E. Williams	06/08/2025 12:24:00
-----------------------	---------------	---------------------

▼

Page 27: [79] Deleted	J.E. Williams	06/08/2025 12:24:00
-----------------------	---------------	---------------------

▼

Page 27: [79] Deleted	J.E. Williams	06/08/2025 12:24:00
-----------------------	---------------	---------------------

▼

Page 27: [79] Deleted	J.E. Williams	06/08/2025 12:24:00
-----------------------	---------------	---------------------

▼

Page 27: [79] Deleted	J.E. Williams	06/08/2025 12:24:00
-----------------------	---------------	---------------------

▼

Page 27: [79] Deleted	J.E. Williams	06/08/2025 12:24:00
-----------------------	---------------	---------------------

▼

Page 27: [79] Deleted	J.E. Williams	06/08/2025 12:24:00
-----------------------	---------------	---------------------

▼

Page 27: [79] Deleted	J.E. Williams	06/08/2025 12:24:00
-----------------------	---------------	---------------------

▼

Page 27: [79] Deleted	J.E. Williams	06/08/2025 12:24:00
-----------------------	---------------	---------------------

▼.....

Page 27: [79] Deleted	J.E. Williams	06/08/2025 12:24:00
-----------------------	---------------	---------------------

▼.....

Page 27: [79] Deleted	J.E. Williams	06/08/2025 12:24:00
-----------------------	---------------	---------------------

▼.....

Page 27: [79] Deleted	J.E. Williams	06/08/2025 12:24:00
-----------------------	---------------	---------------------

▼.....

Page 27: [79] Deleted	J.E. Williams	06/08/2025 12:24:00
-----------------------	---------------	---------------------

▼.....

Page 28: [80] Deleted	J.E. Williams	06/08/2025 12:24:00
-----------------------	---------------	---------------------

▼.....

Page 28: [80] Deleted	J.E. Williams	06/08/2025 12:24:00
-----------------------	---------------	---------------------

▼.....

Page 28: [80] Deleted	J.E. Williams	06/08/2025 12:24:00
-----------------------	---------------	---------------------

▼.....

Page 28: [80] Deleted	J.E. Williams	06/08/2025 12:24:00
-----------------------	---------------	---------------------

▼.....

Page 29: [81] Deleted	J.E. Williams	06/08/2025 12:24:00
-----------------------	---------------	---------------------

▼.....

Page 29: [81] Deleted	J.E. Williams	06/08/2025 12:24:00
-----------------------	---------------	---------------------

▼.....

Page 29: [81] Deleted	J.E. Williams	06/08/2025 12:24:00
-----------------------	---------------	---------------------

▼.....

Page 29: [81] Deleted	J.E. Williams	06/08/2025 12:24:00
-----------------------	---------------	---------------------

▼.....

Page 29: [82] Deleted	J.E. Williams	06/08/2025 12:24:00
-----------------------	---------------	---------------------

▼.....

Page 29: [82] Deleted	J.E. Williams	06/08/2025 12:24:00
-----------------------	---------------	---------------------

▼.....

Page 29: [82] Deleted	J.E. Williams	06/08/2025 12:24:00
-----------------------	---------------	---------------------

Page 30: [83] Deleted	J.E. Williams	06/08/2025 12:24:00
-----------------------	---------------	---------------------

▼

Page 30: [83] Deleted	J.E. Williams	06/08/2025 12:24:00
-----------------------	---------------	---------------------

▼

Page 30: [83] Deleted	J.E. Williams	06/08/2025 12:24:00
-----------------------	---------------	---------------------

▼

Page 30: [84] Deleted	J.E. Williams	06/08/2025 12:24:00
-----------------------	---------------	---------------------

▼

Page 30: [84] Deleted	J.E. Williams	06/08/2025 12:24:00
-----------------------	---------------	---------------------

▼

Page 30: [84] Deleted	J.E. Williams	06/08/2025 12:24:00
-----------------------	---------------	---------------------

▼

Page 30: [84] Deleted	J.E. Williams	06/08/2025 12:24:00
-----------------------	---------------	---------------------

▼

Page 30: [84] Deleted	J.E. Williams	06/08/2025 12:24:00
-----------------------	---------------	---------------------

▼

Page 30: [84] Deleted	J.E. Williams	06/08/2025 12:24:00
-----------------------	---------------	---------------------

▼

Page 30: [84] Deleted	J.E. Williams	06/08/2025 12:24:00
-----------------------	---------------	---------------------

▼

Page 30: [84] Deleted	J.E. Williams	06/08/2025 12:24:00
-----------------------	---------------	---------------------

▼

Page 30: [84] Deleted	J.E. Williams	06/08/2025 12:24:00
-----------------------	---------------	---------------------

▼

Page 30: [84] Deleted	J.E. Williams	06/08/2025 12:24:00
-----------------------	---------------	---------------------

▼

Page 30: [84] Deleted	J.E. Williams	06/08/2025 12:24:00
-----------------------	---------------	---------------------

▼

Page 30: [84] Deleted	J.E. Williams	06/08/2025 12:24:00
-----------------------	---------------	---------------------

▼

Page 30: [84] Deleted	J.E. Williams	06/08/2025 12:24:00
-----------------------	---------------	---------------------

▼.....  

Page 30: [84] Deleted	J.E. Williams	06/08/2025 12:24:00
-----------------------	---------------	---------------------

▼.....  

Page 30: [84] Deleted	J.E. Williams	06/08/2025 12:24:00
-----------------------	---------------	---------------------

▼.....  

Page 30: [84] Deleted	J.E. Williams	06/08/2025 12:24:00
-----------------------	---------------	---------------------

▼.....  

Page 30: [84] Deleted	J.E. Williams	06/08/2025 12:24:00
-----------------------	---------------	---------------------

▼.....  

Page 30: [84] Deleted	J.E. Williams	06/08/2025 12:24:00
-----------------------	---------------	---------------------

▼.....  

Page 30: [84] Deleted	J.E. Williams	06/08/2025 12:24:00
-----------------------	---------------	---------------------

▼.....  

Page 30: [84] Deleted	J.E. Williams	06/08/2025 12:24:00
-----------------------	---------------	---------------------

▼.....  

Page 30: [84] Deleted	J.E. Williams	06/08/2025 12:24:00
-----------------------	---------------	---------------------

▼.....  

Page 30: [84] Deleted	J.E. Williams	06/08/2025 12:24:00
-----------------------	---------------	---------------------

▼.....  

Page 30: [84] Deleted	J.E. Williams	06/08/2025 12:24:00
-----------------------	---------------	---------------------

▼.....  

Page 30: [84] Deleted	J.E. Williams	06/08/2025 12:24:00
-----------------------	---------------	---------------------

▼.....  

Page 30: [84] Deleted	J.E. Williams	06/08/2025 12:24:00
-----------------------	---------------	---------------------

▼.....  

Page 30: [84] Deleted	J.E. Williams	06/08/2025 12:24:00
-----------------------	---------------	---------------------

▼.....  

Page 30: [85] Deleted	J.E. Williams	06/08/2025 12:24:00
-----------------------	---------------	---------------------

▼.....  

Page 30: [85] Deleted	J.E. Williams	06/08/2025 12:24:00
-----------------------	---------------	---------------------



Page 30: [85] Deleted	J.E. Williams	06/08/2025 12:24:00
-----------------------	---------------	---------------------

▼

Page 30: [85] Deleted	J.E. Williams	06/08/2025 12:24:00
-----------------------	---------------	---------------------

▼

Page 30: [85] Deleted	J.E. Williams	06/08/2025 12:24:00
-----------------------	---------------	---------------------

▼

Page 30: [85] Deleted	J.E. Williams	06/08/2025 12:24:00
-----------------------	---------------	---------------------

▼

Page 30: [85] Deleted	J.E. Williams	06/08/2025 12:24:00
-----------------------	---------------	---------------------

▼

Page 30: [85] Deleted	J.E. Williams	06/08/2025 12:24:00
-----------------------	---------------	---------------------

▼

Page 30: [86] Deleted	J.E. Williams	06/08/2025 12:24:00
-----------------------	---------------	---------------------

▼

Page 30: [86] Deleted	J.E. Williams	06/08/2025 12:24:00
-----------------------	---------------	---------------------

▼

Page 30: [86] Deleted	J.E. Williams	06/08/2025 12:24:00
-----------------------	---------------	---------------------

▼

Page 30: [86] Deleted	J.E. Williams	06/08/2025 12:24:00
-----------------------	---------------	---------------------

▼

Page 30: [87] Deleted	J.E. Williams	06/08/2025 12:24:00
-----------------------	---------------	---------------------

▼

Page 30: [87] Deleted	J.E. Williams	06/08/2025 12:24:00
-----------------------	---------------	---------------------

▼

Page 30: [87] Deleted	J.E. Williams	06/08/2025 12:24:00
-----------------------	---------------	---------------------

▼

Page 30: [87] Deleted	J.E. Williams	06/08/2025 12:24:00
-----------------------	---------------	---------------------

▼

Page 30: [87] Deleted	J.E. Williams	06/08/2025 12:24:00
-----------------------	---------------	---------------------

▼

Page 30: [87] Deleted	J.E. Williams	06/08/2025 12:24:00
-----------------------	---------------	---------------------

▼.....  

Page 30: [87] Deleted	J.E. Williams	06/08/2025 12:24:00
-----------------------	---------------	---------------------

▼.....  

Page 30: [87] Deleted	J.E. Williams	06/08/2025 12:24:00
-----------------------	---------------	---------------------

▼.....  

Page 30: [87] Deleted	J.E. Williams	06/08/2025 12:24:00
-----------------------	---------------	---------------------

▼.....  

Page 30: [88] Formatted	J.E. Williams	06/08/2025 12:24:00
-------------------------	---------------	---------------------

Subscript

Page 30: [88] Formatted	J.E. Williams	06/08/2025 12:24:00
-------------------------	---------------	---------------------

Subscript

Page 30: [88] Formatted	J.E. Williams	06/08/2025 12:24:00
-------------------------	---------------	---------------------

Subscript

Page 1: [89] Formatted	J.E. Williams	06/08/2025 12:24:00
------------------------	---------------	---------------------

Page Number

Page 1: [90] Formatted	J.E. Williams	06/08/2025 12:24:00
------------------------	---------------	---------------------

Normal5, Right: 0,63 cm

Page 31: [91] Deleted	J.E. Williams	06/08/2025 12:24:00
-----------------------	---------------	---------------------

▼.....  

Page 31: [92] Deleted	J.E. Williams	06/08/2025 12:24:00
-----------------------	---------------	---------------------

▼.....  

Page 31: [93] Deleted	J.E. Williams	06/08/2025 12:24:00
-----------------------	---------------	---------------------

▼.....  

Page 31: [94] Formatted	J.E. Williams	06/08/2025 12:24:00
-------------------------	---------------	---------------------

Subscript

Page 31: [95] Formatted	J.E. Williams	06/08/2025 12:24:00
-------------------------	---------------	---------------------

Subscript

Page 31: [96] Formatted	J.E. Williams	06/08/2025 12:24:00
-------------------------	---------------	---------------------

Subscript

Page 31: [97] Deleted	J.E. Williams	06/08/2025 12:24:00
-----------------------	---------------	---------------------

▼.....

Page 31: [98] Formatted	J.E. Williams	06/08/2025 12:24:00
-------------------------	---------------	---------------------

Font: Not Italic

Page 31: [99] Deleted	J.E. Williams	06/08/2025 12:24:00
-----------------------	---------------	---------------------

▼.....

Page 31: [100] Formatted	J.E. Williams	06/08/2025 12:24:00
--------------------------	---------------	---------------------

Font: 10 pt, Not Italic